77-12,747

LINDSAY, Edward Williams, Jr., 1950-
HYGROMETRIC SODAR.

The University of Oklahoma, Ph.D., 1976
Physics, atmospheric science

Xerox University Microfilms, Ann Arbor, Michigan 48106

THE UNIVERSITY OF OKLAHOMA

GRADUATE COLLEGE

HYGROMETRIC SODAR

A DISSERTATION

SUBMITTED TO THE GRADUATE FACULTY

in partial fulfillment of the requirements for the

degree of

DOCTOR OF PHILOSOPHY

BY

EDWARD WILLIAMS LINDSAY

Norman, Oklahoma

1976

HYGROMETRIC SODAR

APPROVED BY

DISSERTATION COMMITTEE

DEDICATION

This work is dedicated to my family, who encouraged me to continue my technical education; and especially to the late Winston S. Lindsay, Sr., a lawyer by profession and my grandfather, who encouraged my development in those skills, other than technical expertise, which were vitally necessary for the completion of this dissertation.

TABLE OF CONTENTS

Chapter		Page
I.	INTRODUCTION	1
II.	THE METEOROLOGICAL ATMOSPHERE	6
III.	REMOTE SENSING	13
IV.	ATMOSPHERIC ACOUSTICS	20
V.	HYGROMETRIC SODARS	37
VI.	RELAXATION FREQUENCY METHOD	42
VII.	STATISTIC ANALYSIS	53
VIII.	DESIGN CONSIDERATIONS	72
IX.	SUGGESTIONS FOR FUTURE STUDY	90
X.	CONCLUSION	95
	NOTES	98
	FIGURES	107
	NOTES FOR FIGURES	124
	BIBLIOGRAPHY	125

CHAPTER I

INTRODUCTION

Presented in this dissertation is a new technique to remotely sense water vapor in the atmosphere. The principal concept involved is that, for a given location, knowledge of just the derivative of the acoustical absorption spectrum for audible-frequencies is sufficient to determine water vapor content and temperature at that location.

The balance of the dissertation concerns the questions of whether the technique is superior to others that have been tried or proposed, whether the technique can be practically and economically implemented, and whether the range of a practical device would be sufficient for most meteorological purposes.

Chapters II and IV provide background information on the atmosphere and acoustics. Chapter III describes the field of remote sensing of meteorological variables, while Chapter V presents previous proposals and possible improvements for hygrometric sodars. The new technique is described and analyzed in Chapters VI, VII, and VIII; analytical expressions are derived for the probability distributions for variables involved in the measuring process. Chapter IX presents related information with suggestions for future study, and Chapter X summarizes and lists the conclusions of the dissertation research.

A condensed description of the dissertation follows:

Although water vapor comprises only a small fraction of the atmosphere, it is meteorologically the most important constituent; it acts as a main energy storage and transportation element in the atmosphere. Water vapor is further distinguished as the sole major atmospheric component whose concentration is widely variable.

Environmental protection programs and the economic need for more accurate and longer range weather forecasts have spurred the development of data systems capable of furnishing the requisitely detailed, three-dimensional picture of the atmosphere (mainly the first one or two kilometers above the surface, where short- and intermediate-term weather patterns are determined). Knowledge of water vapor concentration is a necessary part of this description. To furnish such a picture, mere extension of the present, three-dimensional monitoring system (radiosondes at roughly 500 km spacings, twice daily), is definitely not economically feasible. Hence, interest has been shifted from *in situ* sensors to systems capable of remotely monitoring the desired meteorological variables (mainly wind, temperature, humidity, and turbulence).

Systems based on electromagnetic (including optical) and acoustic interactions with the atmospheric variables have been proposed and many working systems have been built. Acoustic devices enjoy the advantages, in most cases, of a much stronger interaction with the atmosphere and of costing far less. These devices suffer the disadvantages, among others, of vastly decreased range and directivity and of greatly increased sampling time, on the order of the time constants characterizing substantial atmospheric change.

All proposals to date for a humidity-sensing system have been unsuccessful either practically or economically. Two proposals have been made for an acoustic radar (sodar) capable of measuring water-vapor; the proposal of Gething and Jenssen was a considerably more refined version of the earliest one, made by Little. Gething tested his proposal and found that the received acoustic intensity could not be measured with enough accuracy in practice.

As indicated in figure (1:1), the Jenssen and Gething Method (JGM) consisted of transmitting pulses at four different frequencies. Since the absorption of acoustic energy is dependent on the humidity, temperature, and turbulence of the atmosphere, and that dependence is in turn dependent on the frequency of the propagating wave (as shown in figures (4:1) through (4:9)), then each frequency pulse will be attenuated differently, depending on the atmospheric variables. As the pulses propagate, some of their energy is scattered back to the sodar by the inhomogeneities of the temperature field. The relative intensities of the received signals indicate the integrated effect of the atmospheric variables between the source and scattering volume (the altitude of this volume is obviously determined by the time interval between transmitted and received pulses). Four frequencies were required to analytically eliminate the effects of temperature and turbulence.

The effects of temperature and turbulence were not well understood at the time of the JGM proposal, and, most importantly, the random nature of the returning pulse intensities was not fully appreciated. The JGM would have required many hours to obtain even marginally useful data (for a range of 17 meters), but, of course, the atmospheric turbulence changes much faster.

The proposal of a new technique, the Relaxation Frequency Method (RFM) is now possible because of the detailed knowledge of the acoustic attenuation process which has only recently become available. As illustrated in figure (1:2), the RFM involves transmitting a single frequency at any particular time but receiving the returning signal from scattering volumes at two different heights. Comparing returns from the same transmitted wave eliminates a great deal of error inherent in the JGM. In addition, a continuous wave, rather than a pulse, is transmitted with a constantly changing frequency (FM-CW), which furnishes more data while still avoiding ambiguous returns. Sweeping the frequency naturally produces an attenuation spectrum. The heart of the RFM is that the spectrum has a very definite shape (see, e.g. fig. (4:2)) which is strongly dependent on the humidity. Therefore, the humidity can be determined without relying on the magnitude of the spectrum, which is very error-prone. The mechanism of the RFM also allows independent data to be gathered simultaneously by suitably separated receivers, which is important because the time necessary to collect a given amount of data is decreased and time is the "Achilles' heel" of acoustic radar systems.

A statistical analysis has shown that the RFM is clearly superior to the JGM. Typical uncertainties in wind, temperature, pressure, and turbulence have little effect on the relaxation frequency of the absorption process.

The question of whether a system using the RFM can furnish most of the required meteorological data economically cannot be fully answered without more information on the practical limitations and cost of various sodar designs.

The trade-off involves sampling distance, frequency range, resolution, sampling time, cost, and the percentage of time when meteorological conditions are "favorable".

It can be concluded on the basis of present information that a sodar with modest improvements over existing (low-cost) sodars can provide some information under most conditions and most of the required information under some conditions. If the ultimate system described by Little is achievable, then it should be possible to obtain the necessary information (within the first one or two kilometers of the surface) for all but extreme weather conditions.

CHAPTER 2

THE METEOROLOGICAL ATMOSPHERE

Structure

The atmospheric weather processes are driven by two kinds of forces. First are thermal gradients caused by differential solar heating. Second are frictional forces caused by the "drag" between the atmosphere and the rotating earth. These forces can be used to differentiate various regions of the atmosphere.[1]

Virtually all of determinants and manifestations of weather are contained in the troposphere, which extends from the earth's surface to a height of 10 to 15 km. at mid-latitudes. The troposphere is characterized by a negative vertical temperature gradient which vanishes or changes sign at the tropopause, the upper boundary of the troposphere.

The troposphere can be further subdivided into the Ekman layer, or planetary boundary layer, and a surface layer which is contained in the boundary layer. The surface layer extends the first few tens of meters above the earth's surface, and is typically a layer of laminar flow (with constant shearing stress) which "matches" the motion of rest of the atmosphere to that of the earth. Weather conditions within this layer are extremely variable; very large gradients of temperature and wind speed can occur.

The boundary layer is defined as that lower portion of the troposphere which is effected by the surface friction force. About half the atmosphere's loss (or gain depending on the accounting procedure) of kinetic energy takes place in this region (most of the remaining energy is dissipated near the tropopause). The boundary layer is usually about one kilometer thick, but this figure can easily vary from a hundred meters to 2 or 3 km. That portion of the boundary layer above the surface layer is characterized by a great deal of turbulence (compared to the higher atmosphere) and is called the mixed layer. The end of the turbulence, which corresponds to top of the boundary layer, is termed "subsidence"; a temperature inversion usually accompanies this subsidence. Most clouds form at this level, where rising water vapor contacts colder, calmer air.

Surface layer winds are primarily caused by the surface friction force. At the top of the surface layer, air is far enough away from a rigid boundary that it can no longer support the shearing stress of the laminar flow; large diameter (on the order of 100 meters) vortices "spin off" the top of the surface layer. These vortices have horizontal axes which are approximately parallel to the wind direction. The mechanism of a vortex is such that it gives up energy to form smaller vortices which continue the process until a lower limit on the diameter of the vortices is reached. This lower limit is called the "Kolmogorov microscale", which has a value of about one millimeter. The limit is the result of the viscosity of the air; so that energy lost by the smallest vortices is dissipated as heat energy (the ordered kinetic energy of wind is traded for random kinetic, or thermal, energy). The phenomenon is sometimes described as an "energy cascade".

Composition

The principal components of dry air are nitrogen (78.08%, by volume) and oxygen (20.95%). The remaining 1% is composed chiefly of argon (0.93%) and carbon dioxide (0.03%, varying at different places and times). The amount of water vapor in air is quite variable; an average figure would be 0.5% by molar concentration (or, equivalently, by volume). The concentration is almost always below 3%.

Water vapor is, meteorologically, the most important atmospheric constituent and also the most widely variable. It can be considered the main short-term energy-storage mechanism of the atmospheric weather machinery since water vapor can undergo both of its phase changes within the normal temperature range of the atmosphere. Because of its tremendous heat capacity, atmospheric water has a moderating effect on temperature; regions of temperature extremes and the very dry areas of the world coincide. Virtually all the water vapor in the atmosphere is contained in the troposphere and most is found within the boundary layer.

Water vapor also affects weather because moist air is more buoyant than dry air at the same temperature and pressure; for a volume concentration of 2% water vapor, the mixture is about 1% lighter than dry air. This effect can easily be more important than the existing thermal gradient for the vertical transportation of the moist air.

Atmospheric Variables

Principal measures of the atmospheric state include temperature, pressure, wind speed, and humidity. Also of interest are the structure constants which characterize the turbulence of both the temperature and velocity fields.

The temperature will be denoted by "T", and will be expressed in units of degrees Kelvin in all formulae and otherwise unless indicated. Celsius readings are converted to Kelvin by adding 273., approximately. A normal range for T is $-30°C < T < 40°C$, with $-60°C$ and $+60°C$ being extremes. At mid-latitudes, the average summer temperatures for 0 and 2 km altitudes are about 15°C and 0°C, respectively. As previously mentioned, T decreases with altitude within the troposphere about 6.5°C/km. For winter, the average temperature at sea level drops to 0°C.

The pressure, designated by "P", will be expressed in atmospheres; one atmosphere is the typical pressure at sea level, while $P = 0.8$ atm. at 2 km, and $P = 0.47$ at 6 km altitude. The pressure at a given location normally varies by less than 5% from its mean value. The equation below, after the Hydrostatic Equation, gives the pressure, P, as a function of altitude, x :

$$P[x] = P_0 * \mathrm{EXP}[-0.0341 \int_0^x T[z]^{-1}\, dz] \qquad (2\text{-}1)$$

where square brackets enclose the argument of a function,
$P[x]$ is the pressure, in atmospheres, at height x,
x is the height in meters,
P_0 is the pressure, in atmospheres, at $x = 0$,
EXP[ ] is the exponential function,
the asterisk denotes multiplication and is used where the meaning might not otherwise be clear,
$T[z]^{-1}$ is the reciprocal of the absolute temperature, in degrees Kelvin, at height z, and z is a dummy integration variable.

This equation neglects the buoyancy of moist air. An approximate correction can be made, although it is small, by replacing T by T_V, the virtual temperature:

$$T_V[x] = T[x]\ (1 + H[x]/100.) \quad , \qquad (2\text{-}2)$$

where H[x] is the percent molar concentration of water vapor at altitude x.

The horizontal and vertical wind speeds will be denoted by V_h and V_v, respectively, and will have units of meters per second. Mean values for V_h differ widely with locality and time, but an average figure of 5 to 10 m/s is useful. Values for V_v are, roughly, one-tenth of those for V_h.

The water vapor will be represented by H, and will be measured as the percent molar concentration, which is the same as the percent concentration by volume. The percent concentration is related to the relative humidity, H_R (in percent), as follows:

$$H = H_R \, P_{SAT}/P \quad , \tag{2-3}$$

where P is the total pressure in atm, and
P_{SAT} is the saturation partial pressure of water vapor, in atm.

The saturation pressure is a function of temperature only, and can be approximated within 0.1% for -40°C < T < 60°C, as follows:

$$P_{SAT} = 10^{(20.53 - (2939./T) - 4.922*LOG_{10} [T])} \tag{2-4}$$

where P_{SAT} is expressed in atmospheres and
T is the temperature in degrees Kelvin.[2]

Figure (2:1) is a plot of the maximum H, which corresponds to P_{SAT} and to H_R = 100%, versus T; it can be used to convert between H and H_R, if T is known.

Average annual, mid-latitude values for H are: H = 1% at 0 km; H = 0.5% at 2 km; H = 0.1% at 6 km; and H = .003% at 8 km.

Turbulence can be measured by the change in field values over a specified distance. The variables C_T and C_V have been chosen to represent turbulence in the temperature and velocity fields, and are called structure constants.

$$C_T[\vec{x}] = \{<(T[\vec{x}] + T[\vec{x} + \vec{\rho}])^2>/\rho^{2/3}\}^{1/2} \tag{2-5}$$

where $C_T[\vec{x}]$ is measured at the point defined by the location vector, $\vec{x}$, and has units of °K $m^{-1/3}$,
ρ, with magnitude $\rho=|\vec{\rho}|$, is the separation length over which the averaging indicated by the bent brackets, < >, is to take place, and has units of meters, as does $\vec{x}$, and
$T[\vec{x}]$ is the absolute temperature, °K, at $\vec{x}$.

The analogous expression applies for C_V, which has the units of $m^{2/3}$/sec. The divider, $\rho^{2/3}$, was chosen so that C_T would be constant with respect to $\vec{\rho}$ over a wide range, provided that, as is usually assumed, the turbulence corresponds to the Kolmogorov spectrum.[3]

Brown and Clifford[4] have concluded that C_T ranges typically between 0.03 and 0.07 °$Km^{-1/3}$, with extreme values of 0.001 and 0.3 °$Km^{-1/3}$. Typical values for C_V would be 0.2 to 1.0 $m^{2/3}$/sec. Empirical studies have produced the forms of equations of the variation of C_T^2 and C_V^2 with altitude:

$$\begin{aligned} C_V^2 &= A + B(r/r_i)^{-2/3} \\ C_T^2 &= C(r/r_i)^{-4/3} \end{aligned} \tag{2-6}$$

where A, B, and C are empirical constants,
r_i is the height of the boundary layer inversion, in meters, and
r is the altitude, in meters.

For typical values of A, B, and C, and r_i = 1.25 km, equations (2-6) become:

$$\begin{aligned} C_V^2 &= 0.04 + 0.33\ r^{-2/3} \\ C_T &= 1.7\ r^{-2/3} \end{aligned} \tag{2-7}$$

Equations (2-6) and (2-7) are intended to apply only when $r \leq r_i$.

Autocorrelation of Variables

Normally, the variables P and H change very slowly -- on the scale of hours. The means of T, V_h, V_v, C_T, and C_V, if averaged over several meters and minutes, require times on the order of 15 minutes to change. Instantaneous values for these last five variables, averaged over a few meters, can change significantly every one to ten seconds.

Changes in the general canonical variables of the troposphere (e.g., total moisture, energy, latent-heat) require from one day to a week.[5]

CHAPTER III

REMOTE SENSING

The relatively recent, strong interest in remotely sensing meteorological variables is the result of a multifaceted need for more temporally and spacially frequent meteorological data and of the related need to sense new "dynamic parameters" of the atmosphere such as wind and temperature turbulence which cannot be well-characterized by single-point measurement. Air pollution control activities, the economic desirability of more accurate, short-term, and local weather forecasts, and the aeronautical interest in predicting aircraft-noise propagation and in monitoring potentially dangerous atmospheric phenomena in and around airports constitute the main motivating factors behind the investigation of remote sensing.

Air pollution control activities especially require the sensing of the dynamic parameters of the atmosphere so that the flow and mixing of pollutants may be analyzed. Beran and Hall write that: "Intelligent air quality control decisions can only come about through effective real-time monitoring and accurate short-term prediction..." of such factors as low level stability, mesoscale flow patterns, and inversion topography and depth.[6]

The vortex-wakes of large aircraft and sudden wind-shears during aircraft landing or take-off are two potentially dangerous conditions which can only be remotely sensed. Considerable work has been done in this area.[7] The problems of aircraft noise are well-known; unfortunately, the measurement of such noise at a distance, for engineering design and comparison purposes, is extremely dependent on local geography and weather conditions (hence the need for remote sensing).

The economically most important consideration is improvement in weather forecasting. Little has stated that "recent analyses of national needs for improved weather services show that these needs lie primarily in the area of short-term <u>local</u> weather forecasts, <u>e.g.</u>, forecasts for a local area 1 to 100 km in size, for time periods ranging from 0 to 6 hours." Little estimates that such forecasts will require "at least four orders of magnitude" more data than is provided by the current radiosonde observation system (which is employed twice per day at about 500 km horizontal intervals); estimates of the cost of extending the present system to provide the requisite data show that such action is completely impractical.[8]

Remote sensing systems have several possible advantages over <u>in situ</u> devices, including: 1) the providing of a truly three-dimensional picture of the measured atmospheric variable; 2) the sensing of variables remotely, (the apparatus does not have to be transported to the region of concern); 3) virtually no modification of the quantity being measured; and 4) the capacity of measuring new parameters describing the dynamic nature of the atmosphere, and of discerning features of the atmospheric structure such as subsidence, which essentially represent highly processed data of fundamental variables. The possible problems with remote sensing systems include: 1) the interpretation of received data; 2) the initial calibration of a system; 3) the limitations on use caused by various weather conditions; and 4) higher operational costs resulting from the required maintenance of more complex equipment, and from the possible requirement of having a highly skilled operator. These advantages and problems are not universal. Whether *in situ* or remote sensing equipment is used for routine meteorological purposes will probably be determined by the cost of measuring the fundamental atmospheric variables. Remote sensing will always have a place in atmospheric physics research since it alone can provide the required, three-dimensional picture of atmospheric processes.

The advantages listed above apply principally to monostatic systems which operate in the same way as the most famous remote sensor, radar, *i.e.*, by receiving energy reflected back to the sensor. The line-of-sight[9] and passive devices give integrated measurements of a variable; for three-dimensional pictures such devices usually require gross physical movement.

Remote Sensing System Requirements

For the purposes mentioned above, a remote sensing system should be able to completely probe the boundary layer; as discussed in Chapter II, this layer extends to roughly 1 km, and contains most of the short- and intermediate-term weather-determining factors (so that a system should have a vertical range of about 2 km). Also, the data gathering process should not take longer than for substantial change in the quantities being measured; this time would be approximately fifteen minutes for the fundamental variables, temperature, humidity, pressure, and mean wind. The system should be able to take data under most meteorological conditions; in addition to the usual ranges of the fundamental variables given in Chapter II, these conditions also include, e.g., night and day, fog, cloud cover, and precipitation.

Ideally, a remote system should be based on just one device which is capable of measuring at least the fundamental variables mentioned above, and which is portable and also easy to operate (or automate) and to maintain. Of course, the per-unit cost and necessary grid spacing should be such as to minimize total cost. A resolution cell of about 10 meters high by 100 meters square should be sufficient for the purposes noted above, although much finer resolution may be required for research purposes.

Remote Sensing Schemes

Methods for remote sensing are based on the interaction with atmospheric variables of either electromagnetic waves (mainly radio and optical) or acoustic waves (mainly audible sound). The cost of active, monostatic devices built to date which utilize these interactions can be estimated as follows (in order of magnitude of dollars):[10] acoustic (called sodar or acoustic radar) $\$10^3$ to 10^4; optical (lidar) $\$10^4$ to 10^5; and radio (radar) $\$10^5$ to 10^6. A combination, called RASS or EMAC, which uses radar to follow acoustic waves has also been studied.[11]

Lidar, which may be the ultimate choice for remote sensing, because of its high resolution and ability to identify molecular species, currently has several major disadvantages: 1) there exists a possibility of eye damage by the lidar beam during its sweep; 2) the noise of sunlight effectively restricts lidar to night use; 3) the expense and complexity of equipment is quite high; and 4) sensing is blocked by clouds and fog.

Acoustic devices benefit from much stronger interactions with atmospheric variables, and from costing far less to construct. Little[12] has examined the relative interactions of the methods and finds that the relative backscattered energy is about one million times greater for sodar and that the change in refractive index caused by temperature changes is 1,700 times stronger. For humidity changes, this last figure is 35 for radar and 3500 for lidar. Acoustic waves are strongly affected by wind changes, whereas electromagnetic radiation is essentially unaffected. The attenuation of acoustic waves is also much more strongly dependent on temperature and humidity. Sodars suffer the disadvantages of vastly decreased range and resolution and of much longer sampling times. However, these disadvantageous features do not necessarily prohibit the sodar from meeting the requirements of the previous section, but they do demand a great deal of design consideration. When acoustic interactions can be utilized, sodar is the favored choice because of its lower construction and maintenance costs. However, in order to use sodar fully, it is necessary to predict the absorption of sound by the atmosphere, which requires a good estimate of humidity and rough estimates of temperature and pressure. The last two estimates are fairly easily attained, but the lack of a good humidity estimate has been a major obstruction to sodar improvement.

Devices

Many proposals have been made and working systems built using the above methods to monitor various atmospheric variables; Little and Derr[13] have compiled and evaluated the numerous papers on these proposals and devices, and have concluded that, taken as a whole, they will be able to provide a nearly complete, three-dimensional picture of the boundary layer in the near future. The one weak area has been the detection of the fundamental variable, water vapor concentration. No radar methods exist for the detection of water vapor, although detection of water in liquid form by radar is in wide-spread use. A passive microwave technique sensing the 20 GHz emissions of water vapor molecules has been successfully tested by Westwater, et al.[14], but it is sensitive to haze and provides directly only an integrated measure of water vapor. An infrared, satellite-based system which yields integrated water vapor data but which cannot sense accurately below two kilometers above the earth's surface (the region of greatest importance) has also been described.[15] A lidar technique, based on Raman-scattering by water vapor molecules, has been tested against a tower-based measurement device at a height of 30 meters and was found to be very accurate. On the basis of this test, Strauch, et al.[16], have estimated that an improved version of their lidar (100 kilowatt, 10 nanosecond pulselength, 100 pulses per second) could measure water vapor to a height of 4 kilometers with an SNR of 10 (at night) with a fifty meter range resolution and a five-minute observation time for 50% relative humidity at 20°C. Unfortunately, this lidar used expensive, near state-of-the-art laser equipment which required great care in construction, maintenance, and operation. This lidar suffers from all the disadvantages of lidar systems listed above. Especially objectionable is the night-only restriction; a chart prepared by McNice[17] indicates that even moonlight will restrict the ultimate range to less than 800 meters, and that twilight will reduce it to 20 meters or so. This technique will have to await the development of better lasers, especially lasers that operate at frequencies at which the atmosphere is opaque to solar radiation.

The sodar designs which have been proposed have been unsuccessful, as discussed in Chapter V. In 1973, Little[16] concluded that "the ability to sense the three-dimensional humidity field remotely ... seems to be many years away."

CHAPTER IV

ATMOSPHERIC ACOUSTICS

Essential to the design of a hygrometric sodar is circumspect knowledge of the interaction of the atmosphere with acoustic waves. A sufficiently detailed knowledge did not exist as recently as 1974, so that previous sodar designs were based upon empirical data, usually taken in calm, laboratory conditions, and extrapolations of such data. Much work remains to be done in this area of physical acoustics, but the information now available provides a solid theoretical foundation in the major areas of interest to the sodar designer. Most importantly, the experimental data, which in many cases seemed to be in conflict, can be reasonably ordered by the present theoretical framework.

Attenuation

In calm, homogeneous air, the propagation of sound is affected by the air's temperature, pressure, and humidity, and by the frequency, shape, and intensity of the propagating wave. In the actual atmosphere, the additional variables of wind speed and turbulence, of pressure, and of temperature turbulence must be considered. Inhomogeneities in the atmosphere cause changes in the acoustic refractive index with the consequence that acoustic energy is scattered from the main wave direction and is distorted in frequency.

The acoustic waves normally encountered in the atmosphere are generally spherical in shape and so are subject to geometric spreading. Taking into account physical attenuations which are proportional to the amplitude of the wave (provided the amplitude is not too great), the amplitude, A, of a spherically propagating wave can be described by the following equation:[17,18]

$$A[R] = A_0 * \frac{R_0}{R} * \mathrm{EXP}[-\int_{R_0}^{R} \alpha[x]\, dx] \quad , \tag{4-1}$$

where R is distance from the wave source, in meters,
A_0 is the amplitude at $R=R_0$, in atmospheres,
x is a dummy variable for the integration, and
α is the attenuation coefficient, in nepers per meter.

The problem is to express the atmospheric parameters as functions of distance and to express α as a function of the parameters. Furthermore, α may be affected by the frequency and amplitude of the acoustic wave. These effects are best handled separately from equation (4-1); they arise from the nonlinear characteristics of the propagation medium, and are discussed later in this chapter.

The attenuation has traditionally been studied in the form:[19] $\alpha = \alpha_{cl} + \alpha_m + \alpha_s$, where the subscripts refer to classical absorption, molecular absorption, and excess attenuation, respectively. The classical absorption of acoustic energy is that which would be expected if the air molecules were treated as "billiard balls" having only translational energy states; the theory for classical absorption has been known for many years. Molecular absorption is the absorption of acoustic energy by the internal energy states of the molecules; good data for this absorption has been available for many years, but no theoretically based equations were available for it until the last couple of years.[20]

Historically, the excess attenuation has been that attenuation which was not covered by the other two terms, although it was generally attributed to atmospheric turbulence. No consistent data seemed to exist for this attenuation, which would occasionally even be measured as an amplification; and until a few months ago, no generally satisfactory theory had been constructed. The work of Brown and Clifford (1976), seems to have clarified this area.

It is more convenient to study α as:

$$\alpha = \alpha_{cr} + \alpha_{v,O} + \alpha_{v,N} + \alpha_s \quad , \tag{4-2}$$

where

$$\alpha_v = \alpha_{v,O} + \alpha_{v,N} \quad , \text{ and}$$
$$\alpha_{cr} = \alpha_{cl} + \alpha_r \quad .$$

The subscripts r and v signify those portions of the molecular absorption due to rotational and vibrational internal energy modes. The additional subscripts O and N designate the vibrational absorption associated primarily with oxygen and nitrogen molecules. As the last equation suggests, "cr" signifies "classical plus rotational".

Equation (4-2) is convenient because the vibrational absorption terms are the only ones effected by H, and because each term has a particular frequency dependence: α_{cr} is proportional to f^2; $\alpha_{v,O}$ and $\alpha_{v,N}$ depend as $f_r f^2/(f^2+f_r^2)$, where f_r is a constant defined below; and α_S is generally considered to be proportional to the cubic root of the frequency.

It should be noted that absorption is a subcase of attenuation in which acoustic energy is actually absorbed in the volume through which the wave is passing, whereas the term "attenuation" includes any loss such as refractive scattering in which energy is removed from the wave, but not absorbed.

Classical and Rotational Absorption

Classical absorption is almost completely the result of friction due to the viscosity of the air and to thermal conduction from the converging velocity regions of the acoustic wave. (The local-velocity is "ninety degrees out of phase" with the local pressure.) The net effect of classical absorption is to randomize the ordered translational motion of the air molecules. A decrease in ordered motion constitutes a decrease in the acoustic wave's amplitude, while an increase in random translational motion is simply an increase in average temperature. Therefore, classical absorption converts acoustic energy into heat.

Rotational absorption is actually a relaxation process (described below), with an extremely high relaxation frequency, f_r > 10 MHz. Thus, the $f^2/(f^2+ f_r^2)$ dependence observed for relaxation processes appears as an f^2 dependence in the audible frequency range. For all atmospheric conditions, and for frequencies less than 10 MHz, the rotational absorption is about one-third the magnitude of classical absorption.

The following equation for the classical and rotational attenuation is accurate to within 2% for 213°K < T < 373°K:

$$\alpha_{cr} = 1.075 * 10^{-12} f^2 * T^{1/2}/P \quad , \quad N_p/m \quad , \tag{4-3}$$

where f is the frequency in hertz.[22] Relative to vibrational absorption, the effect of α_{cr} is small (less than 10%) for temperate atmospheric conditions and for frequencies between 50 and 100,000 hertz.

The Relaxation Process

The equipartion principle states that for a molecular to be in equilibrium, its total energy must be divided among the translational, rotational, and vibrational energy forms in proportion to the number of degrees of freedom associated with each form. Consequently, if energy is added to a molecule in one form, it will be redistributed to the other forms as well when the equilibrium state is reached. Exchange of energy between forms of energy storage can occur only during molecular collisions, so that there will be a time lag between a change in energy and the redistribution of energy according to the equipartion principle.

An acoustic wave represents an oscillation of energy between a potential energy field (pressure) and a kinetic energy field (velocity, i.e. temperature). As the local temperature increases during the passage of a wave, energy will be transferred from molecular translation to molecular rotation; the energy will be returned to ordered, acoustic translational motion as the local temperature decreases, provided that the duration of the change in temperature is long compared to the time constants characterizing the interchange of translational energy with rotational and vibrational energy levels. If the period of the change in temperature is too short, the energy transferred to vibration and rotation will be returned out of phase with the wave causing attenuation, or relaxation.

The time constant for energy interchange can be expressed as a frequency, f_r, the relaxation frequency. There will be one relaxation frequency for each possible energy interchange mechanism. Fortunately, the frequencies for translation-rotation exchanges for air are closely grouped and can be replaced by one $f_{r,rot}$, which has been given above. Translation-vibration exchanges require two frequencies for air.[23] The frequency dependence of absorption associated with a relaxation frequency, f_r, can be expressed[24] as $2\, f\, f_r/(f^2 + f_r^2)$, which equals one when $f = f_r$.

It should be emphasized that a relaxation process is not a resonance phenomenon. Most significantly, for example, the sum of two acoustic waves with similar frequencies f_1 and f_2, such[25] that $(f_2-f_1)^2<<f_1^2$, will be attenuated at the same rate as a wave of frequency $f = (f_1+ f_2)/2$, rather than as separate waves as would be the case if $(f_2- f_1)^2>> f_1^2$. The following trigonometric identity demonstrates the concept:

$$COS[A] + COS[B] = \frac{1}{2} COS[(A-B)/2] * SIN[(A+B)/2]$$

so that if f_1 and f_2 are close, the sum of the two waves appears as a wave of frequency $(f_1+ f_2)/2$ with a slowly modulated amplitude. Since the relaxation process is concerned mainly with the duration of the change in local temperature, the wave sum will be attenuated as though it were a wave of the single frequency $(f_1+ f_2)/2$.

Vibrational Absorption

The two relaxation frequencies mentioned above which are needed to characterize vibrational absorption can be roughly associated with oxygen and nitrogen. A third relaxation frequency actually exists which is associated with carbon dioxide; its omission causes less than 1% error.[26]

The addition of water vapor greatly increases these vibrational relaxation frequencies ($f_{r,rot}$ is already extremely high so that water vapor below saturation in the atmosphere has no effect). Water molecules, because of their non-linear structure, have many times the number of internal degrees of freedom possessed by oxygen and nitrogen molecules; therefore, they can absorb much more energy. More importantly, external-internal energy exchanges are much more probable for air-water collisions than for air-air collisions; the frequencies associated with air-water reactions are from one hundred thousand to a billion times greater than for air-air reactions. As water content is increased more energy is transferred per collision and more effective collisions occur (the exchange is faster). Consequently, for $f < f_r$, addition of water vapor decreases absorption; for $f > f_r$, absorption is increased.

Bass et al. have derived a theoretical expression for α_v which is in agreement with the experimental data. It is more convenient and accurate to evaluate constants in the expression empirically; the following expression is believed to be accurate to within 5% for 273°K < T < 313°K and for 50 Hz < f < 10 MHz:[27]

$$\alpha_v = \alpha_{v,O} + \alpha_{v,N} \quad \text{where}$$

$$\alpha_{v,i} = (\alpha\lambda)_{max,i} * \frac{f}{c}\,(2ff_{r,i}/(f^2 + f_{r,i}^{\ 2})) \tag{4-4}$$

$$(\alpha\lambda)_{max,i} = 0.179\ M_i \left(\frac{\theta_i}{T}\right)^2 * \frac{EXP[-\theta_i/T]}{(1-EXP[-\theta_i/T])^2}\ ,\ \text{nepers} \tag{4-5}$$

$$c \cong 20.06 * T^{1/2}\ ,\ m/s\ , \tag{4-6}$$

$$f_{r,O} = P * (24. + 44100. * H * (0.05+H)/(0.391+H), \tag{4-7}$$

$$f_{r,N} = P*(293./T)^{1/2} * (9.+350.*H*EXP[-6.142((293./T)^{1/3}-1)]). \tag{4-8}$$

where the subscript i can denote either O or N,

$(\alpha\lambda)_{max,i}$ is the maximum absorption per wavelength, nepers,

$f_{r,i}$ is the vibrational relaxation frequency, hertz

M_i is the fractional molar concentration of gas i in dry air,

θ_i is the vibrational temperature for gas i, in °K, and

c is the speed of sound, m/s.

The values of M_i and θ_i are given in table 4-1.

Table 4-1

i	M_i	θ_i, °K
oxygen	0.2095	2239.
nitrogen	0.7808	3352.

Equations (4-4) through (4-5) can be condensed (with slight loss of accuracy) as:

$$\alpha_{v,O} = 1.88*10^4*T^{-5/2}* \text{EXP}[-2239./T]*f^2f_{r,O}/\left(f^2+f_{r,O}^2\right) , \tag{4-7}$$

$$\alpha_{v,N} = 4.22*10^4*T^{-5/2}* \text{EXP}[-3352./T]*f^2f_{r,N}/\left(f^2+f_{r,N}^2\right) , \tag{4-8}$$

The relaxation frequencies can be very roughly estimated as: $f_{r,O} = P * 3.3 * 10^4 * H^{1.8}$, and $f_{r,N} = P * 350. * H$. The oxygen relaxation frequency is more strongly dependent on H because there exists a vibrational to vibrational energy exchange reaction for water and oxygen involving very nearly equal vibrational energy states so that the reaction is near resonance. Another consequence of this dominant reaction is that $f_{r,O}$ is not affected by temperature; in contrast, $f_{r,N}$ has a mild temperature dependence because vibrational-translational energy exchanges play a more important role in the overall relaxation process for nitrogen.

For H=0%, $f_{r,O}$= 24 hertz and $f_{r,N}$= 9 hertz, while for H = 1%, $f_{r,O} \cong 30$ kHz and $f_{r,N} \approx 350$ Hz; these figures highlight the strong effect of water vapor on the vibrational relaxation frequencies.

The absorption per wavelength, $(\alpha\lambda)$, is a convenient means of expressing the total absorption since $(\alpha\lambda)$ will vary only by one or two orders of magnitude over the audio frequency range, and since the maximum value of the variable, $(\alpha\lambda)_{max}$, which occurs at $f=f_r$, is a constant for a given temperature.

Equations (4-9) and (4-10) are useful for the real atmosphere, but equations (4-4) are valid only for still air. The problem with (4-4) is that "c" has been used to produce the factor $(\alpha\lambda)_{max,i}*f/c$, which is correct for moving air only if (4-6) is used for "c" rather than the more general expression:

$$c = 20.05*T^{1/2}\left(1 + H/(100.*P)\right)+ v \cos \theta , \tag{4-11}$$

where v is the magnitude of the wind vector, m/s, and
θ is the angle between the wind and the direction of propagation.

A more physically-based expression, as can be anticipated from the above discussion of the relaxation frequency process, would be:

$$(\alpha/f) \equiv (\alpha\lambda)/c \quad \text{, neper-sec/meter,} \tag{4-12}$$

where c is that given by (4-6), and (α/f) will be called the attenuation per cycle.[28] Therefore, e.g., from (4-9):

$$(\alpha/f)_{max,0} = 9.4*10^3 * T^{-5/2} * \mathrm{EXP}[-2239./T] \quad . \tag{4-13}$$

Excess Attenuation

Unlike the other sources of attenuation, excess attenuation is a stochastic process and can even result in an amplification of a received signal over what would be expected considering classical and molecular absorption alone. Also unlike the previously discussed mechanisms of attenuation, α_s is not an absorption process, but represents a loss of energy through scattering of energy out of the beam or by shifting some of the energy to higher frequencies. Excess attenuation does not occur in calm, homogeneous air, but it is present in the atmosphere even under zero-wind conditions. In the discussion that follows, it will be assumed that reflectors and ground effects (which are unimportant if the acoustic wave is propagating at an angle to the ground of greater than 10°) are not involved; therefore, excess attenuation can be attributed to scattering by temperature and velocity turbulence.[29]

De Loach[30] made a study of the experimental observations and theories concerning excess attenuation reported prior to March, 1975. His summary included the following observations: 1) The excess attenuation can be of the same magnitude as the molecular absorption. 2) The ratio $\alpha_s/(\alpha_{cr}+\alpha_r)$, can change by an order of magnitude within a few minutes. 3) Excess attenuation is greater near the earth's surface than at higher altitudes.[31] 4) Larger values of α_s are generally observed in the early morning than in the late afternoon.

Since α_s does not occur in calm, homogeneous air, it cannot be an intrinsic quality of air; neither can it depend solely on the turbulence of the air for the following reasoning: If α_s is caused solely by turbulence scattering acoustic energy out of a propagating wave, as suggested by the theories of De Loach and others, then excess attenuation cannot occur for a plane wave in an absorptionless medium. (The theory of De Loach misses this point because it makes no provision for energy returned to the wave by other scatterings.) This point can be justified by considering an ideal acoustic source (the "pulsating sphere" of infinitesimally small radius) radiating uniformly in a perfectly homogeneous and absorption-free medium. Once steady state has been achieved, the total acoustic energy flux across any closed, three-dimensional surface enclosing the source will be the same; otherwise, energy would build up in some region (since there is no absorption), and the steady-state condition would be violated. This argument also holds for a turbulent medium and can be extended to plane waves which are the limiting case of spherical waves. Turbulence-induced scattering can lengthen the average path traversed by a wave which has travelled to a surface a fixed distance from the source, so that in an absorptive medium additional absorption can occur. But this attenuation would appear as simply a factor multiplying the absorption. Also, for normal atmospheric conditions, the increase in average path length would be quite small. Therefore, excess attenuation must depend critically on the geometry of the source, as well as on the turbulence. For example, if the source were highly directional, turbulence could scatter energy out of the beam without compensating energy being returned; the beam will "spread". This effect would indeed decrease with distance and increase with frequency. It would also be much more sensitive to turbulence located in the beam near the source. Ingard[32], for example, has pointed out that the temperature gradient below approximately 5 meters from the surface varies greatly with time of day; this would explain the fourth observation of De Loach mentioned above.

Brown and Clifford (1976) have recently formulated a new theory based on a forward-propagation-through-turbulence theory (developed for optics) rather than based on subtracting out the energy scattered from the beam according to the scattering cross-section equation given below, as was done by earlier theories. The results of the theory are in agreement with the points mentioned above and with the observations given by De Loach. It is further concluded that excess attenuation is primarily determined by the phase fluctuations caused by changes in the acoustic refractive index, rather than amplitude fluctuations.

Brown and Clifford derive the following formula for the total excess attenuation, A_s, in nepers,[33] encountered along a path of length L, in meters:

$$A_s = \frac{1}{2} * LN\left[1. + 1.56k^{12/5}\ D_0^2 * INT\left[C_n^2[s] * \left(\frac{L-s}{L}\right)^{5/3};\ s:0,L\right]^{6/5}\right] \quad , (4\text{-}14)$$

Where LN is the natural logarithm,
k is the wave number, $k \equiv 2\pi f/c$,
D_0 is the diameter of the source, in meters,
C_n is the structure parameter for refractivity fluctuations, with:

$$C_n^2[s] = (C_T^2[s]/4*T^2) + (C_V^2[s]/c^2) \qquad (4\text{-}15)$$

INT is the integral operator:

$INT[f(x); x:a,b] \equiv \int_a^b f(x)dx$, and

s is the dummy variable of integration.

For constant C_n, equation (4-14) has been reduced to:

$$A_s = \frac{1}{2} * LN\left[1 + 0.59\ D_0^2\left(k^2 L\ C_n^2\right)^{6/5}\right] , \tag{4-16}$$

It appears that the far field diameter, D[r] in meters, of the beam is related to the beam diameter, $D_f[r]$ in meters, expected on the basis of only Fraunhafer and Fresnel diffraction, as follows:

$$D[r] = D_f[r] * EXP[2A_s] \quad . \tag{4-17}$$

The factor, $\left(\frac{L-s}{L}\right)^{5/3}$, in equation (4-14) "weights" the near-field turbulence more heavily. The attenuation per meter, α_s, can be evaluated by taking the derivative of (4-14).

Brown and Clifford, using equations (2-7), have produced typical mean values for α_s over a 600 meter vertical path with f = 4KHz and D_0 = 1m: for a ground-based source, $\alpha_s \approx 8.0$ dB/km, but for an elevated source, $\alpha_s \approx 1.5$ dB/km.[34] Equation (4-14) appears to be in agreement with the available data on excess attenuation.

Curves

Figures (4:1) and (4:2) demonstrate the relative contributions of α_{cr}, α_v, and a possible realization of α_s, upon the total attenuation and the total attenuation per wavelength, for specific values of T and H. Figures (4:3) and (4:4) demonstrate the effect of changes in relative humidity on α and $(\alpha\lambda)$ for fixed T.

The influences of T and H on attenuation can be separated, except for a slight dependence of $f_{r,N}$ on T. The influence of T is displayed in figures (4:5) and (4:6), in which the maximum values of the attenuation per cycle, $(\alpha/f)_{max}$, are shown for the oxygen and the nitrogen vibrational relaxation processes. The influence of H is evidenced by its effect on f_r; $(f_{r,O}/P)$ and $(f_{r,N}/P)$ and corresponding values of H are given in figures (4:7), (4:8), and (4:9). The pressure, P, simply scales the relaxation frequencies.

For given values of f, H(or H_R), T, and P, the vibrational absorption can be determined from the aforementioned figures by the following procedure (H_R can be converted to H using figure (2:1)): For $\alpha_{v,O}$, enter (4:5) with T to find $(\alpha/f)_{max,O}$, and multiply by the frequency, f, to give $\alpha_{max,O}$(which is α if $f=f_{r,O}$). Then find$(f_{r,O}/P)$ from (4:5) and multiply by P to give $f_{r,O}$. Next form the quotient, $\rho = f/f_{r,O}$. Then $\alpha = \alpha_{max,O}*$ $2\rho/(\rho^2+1)$. A similar procedure holds for finding $\alpha_{v,N}$ and then $\alpha_v = \alpha_{v,N} + \alpha_{v,O}$. Normally $\alpha \simeq \alpha_v$.

Nonlinearity

The nature of air is such that the acoustic energy of a pure, single frequency wave will be partially transferred to harmonics of the original frequency, even if the wave is of very small amplitude relative to the maximum amplitude which can be propagated. (The maximum amplitude is naturally just somewhat less than the atmospheric pressure.) The wavefront becomes progressively steeper because the more highly compressed areas of the wave propagate faster. This process continues until balanced by viscous forces[35] limiting the steepness of the wave-front. A sawtooth wave-shape is the result; in air, for audible frequencies, this waveform is fully developed within a few meters of the source. The exact shape of the wave is determined by the energy-transfer equilibrium. The rate at which energy is transferred to higher harmonics is very dependent on the amplitude of the wave; the rate at which energy is lost from a higher harmonic is primarily determined by the attenuation of the air. Energy attenuation is very roughly proportional to f, so that only the second (or possible, third) harmonic is of any consequence. The upper limit to the energy carried into the nth harmonic can be estimated at $100/m^2$ percent of the energy currently carried at the original frequency by forming the Fourier series of the limiting sawtooth wave-shape. For spherical waves in a dissipative medium, nonlinear effects are much less important than for plane waves in a lossless medium, because of the rapid decrease in amplitude caused by spherical spreading and attenuation.

This subject is reviewed in a treatise by Beyer.[36] For the purpose of sodar design, it seems that nonlinear effects can be neglected, except that they place an upper limit on source strength and that there can be a measurable second harmonic.

Fluctuations

Another aspect of excess attenuation is the amplitude fluctuations in the propagating wave caused primarily by turbulence-induced phase changes along each wave-front.

Brown and Keeler[37] have observed phase fluctuations of up to 10 cycles and amplitude fluctuations of up to 30 dB, for "high-frequency, high-turbulence, long-range" conditions (f=4000 Hz, $C_n^2 \approx 10^{-6} m^{-2/3}$, r=333m). These extreme fluctuations had time constants of several tenths of a second, while fluctuation time constants for a wide range of conditions varied from five hundredths of a second to several seconds.

Kasper *et al.*,[38] find that virtually all of the fluctuation power spectra measured by them (under similar conditions to above) show that most of the fluctuation energy occurs at frequencies of less than 10 Hz (usually less than 5 Hz). In terms of rms error in the received sound pressure level (measured in decibels), the fluctuations were from 2% for 550 Hz, to 25% for 8000 Hz, for a distance of 150 meters. The error was roughly proportional to the frequency and to the square root of the distance. Signal oscillograms indicating instantaneous pressure displayed some slow fluctuations with time constants of several seconds, but essentially no fluctuations for times less than a tenth of a second.

Tatarskii[39], among others, has obtained a theoretical formula for these fluctuations which can be expressed as follows:

$$<\chi^2> \equiv <LN[A/<A>]^2> \approx \ 0.124\ k^{7/6}L^{11/6}<C_n^2>\ , \qquad (4\text{-}18)$$

where $$<C_n^2> \ = (5.544/L^2)*INT\left[\left(s*\frac{L-s}{L}\right)^{5/6} C_n[s]^2;\ s:0,L\right]\ , \qquad (4\text{-}19)$$

and where χ is the root mean square average of LN[a/<A>] which
is a measure of the fluctuations,
< > brackets denote "average", and
L is the path length from source, in meters.

The quantity χ is essentially the log-amplitude variance for small fluctuations. A formula for the spacially-dependent log-amplitude covariance has also been derived and has been evaluated by Brown and Keeler for L = 1 km and high turbulence $\left(C_n^2 = 10^{-6}, m^{-2/3}\right)$, for several frequencies. The phase coherence length, ρ, is proportional to $(L/f^6)^{1/5}$; ρ= 1052 meters for f = 5000 Hz and ρ= 87 meters for f = 400 Hz.

The phase fluctuations constitute a limiting factor on how far a coherent wave can propagate (the exact meaning of the term "coherent" depends on the size of the receiver). As pointed out by Brown and Keeler, phase fluctuations will not be a serious limitation for remote sensing in the boundary layer, for audible frequencies.

Scattering

Monin[40], among others, has helped develop a theoretical expression for the amount of acoustic energy scattered out of a propagating wave by turbulence. The effect of turbulence is conveniently represented as a partial reflection, and is measured in terms of the scattering cross-section per unit area for a unit solid angle making a plane angle of θ degrees with the original direction of propagation:

$$\sigma = 0.055\left(f/c\right)^{1/3} V * \cos[\theta]^2 \left(\cos[\theta/2]^2 * C_V^2/c^2 + 0.13 * C_T^2/T^2\right) \sin[\theta/2]^{-11/3}, \tag{4-20}$$

where σ is the ratio of power scattered (in the direction determined by θ) per unit solid angle to the power incident on the scattering volume
V is the volume of the scattering volume in cubic meters,
θ is the angle between the scattered beam (one steradian in size) and the original direction of propagation, in degrees or radians, and
c is the speed of sound in still air as given by equation (4-6).

For the backscatter (θ=180°), equation (4-20) reduces to:

$$\sigma = .004\ k^{1/3} V * C_T^2/T^2 \tag{4-21}$$

There are many tacit assumptions involved in (4-20), but the equation is in good agreement with available data except for the case of a transverse wind.[41] This exception does not apply to the backscatter equation, (4-21).

Typically, the backscattered signal intensity is 85 to 90 dB below the intensity of the original wave.[42] According to equation (4-20), wind variations have no effect on the intensity of the backscattered wave; however, a transverse wind can cause a "non-negligible" frequency shift, <u>i.e.</u> spectrum broadening,[43] for a sufficiently broad acoustic beam.

Speed of Sound

The speed of sound as a function of H and T has already been presented as equation (4-11). However, c is also dependent (very weakly) on the frequency of the wave:[44]

$$c^2 = (f^2 c_\infty^2 + f_r^2 c_0^2)/(f^2 + f_r^2) \tag{4-22}$$

Here f_r is the relaxation frequency important in the range of f being used, and c_0 and c_∞ are the speed of sound for $f \ll f_r$, and $f \gg f_r$, respectively. Furthermore, the difference between c_∞ and c_0 for the oxygen relaxation in air is only 0.12 meters per second.

CHAPTER V

HYGROMETRIC SODARS

The concept of remotely measuring atmospheric water vapor concentration by observing the relative attenuation for acoustic waves of different frequencies was first mentioned (in 1969) by Little[45], who cited the work of Harris.[46] Harris had published a paper which contained graphs showing acoustic vibrational absorption versus relative humidity for several discrete frequencies and discrete temperatures at a pressure of one atmosphere; but Harris' analysis overlooked the nitrogen component[47] (although its effect was clearly contained in his raw data) so that the graphs were only "best fits" of an equation of the form: $\alpha_v = K * f^2 f_r / (f^2 + f_r^2)$, where K is a constant with respect to frequency.

Little suggested that three identical sodars be used successively to obtain echoes from the same volume of space at three different frequencies (the third sodar was not necessary under certain conditions). The suggested frequencies were 2, 4, and 8 kHz. Little supplied a graph showing (for T=20°C only) the decibel change per hundred meters of the ratio of received signal intensities for 2 kHz and 4 kHz, and for 4 kHz and 8 kHz, after correction for the change in backscattering cross-section (which is proportional to the cube root of the frequency, for a Kolmogorov spectrum of turbulence). Presumably, the graph could be used to predict relative humidity (integrated over the path length) based on the returned signal intensities.

Little stated that, "One obvious weakness of this method is the assumption of an isotropic, homogeneous Kolmogorov spectrum of turbulence." He suggested that bistatic acoustic echo-sounding be used to identify atmospheric regions which should be avoided. But Little also assumed that identical transducers could be constructed which, at different frequencies, would radiate the same peak power with the same antenna pattern and transducer efficiency. Also, Little did not make provisions for pressure or temperature changes and did not consider the very serious effects of excess attenuation. There was also a tacit assumption that the scattering volume would appear the same at each frequency, i.e., that except for the $f^{1/3}$ dependence the backscattered, received signal power would be the same fraction of incident power for each frequency at any given time; this is definitely not the case unless the frequencies are very nearly the same and the thickness of the scattering volume is very small.[48] Normally the received-, backscattered-signal amplitudes will have a Rayleigh or Rice-Nakagami[49] distribution and will be independent after a few seconds or with relatively small change in frequency.

Little's suggestions were partly revised by Parry and Sanders.[50] Apparently mindful of the problems (mentioned directly above) in assuming that any random fluctuations induced by the backscattering process would be the same for each frequency, Parry and Sanders specified that the frequencies be transmitted simultaneously and that the frequencies be "near each other". Unfortunately, the closer the signals get the less will be the difference in absorption which,is the desired quantity. More importantly, as indicated in Chapter IV in the discussion of the relaxation process, signals whose frequencies are too close (i.e., $\frac{1}{3} \leq f_1/f_2 < 3$) appear as one signal and will be attenuated at exactly the same rate. This condition will exist whenever the frequencies are close enough that the fluctuations of the backscattered signals are even weakly correlated.[51] Parry and Sanders do address the question of temperature change; they present a graph[52] for two different temperatures for frequencies so close together (the only frequency specified is 1000 Hz) that the detected change for most values of relative humidity is less than 0.2% of the received signal.

Gething and Jenssen[53] authored the first paper devoted completely to hygrometric sodar. They cited Little's suggestions as the basis for their study, but they did treat the effect of excess attenuation. Although unsure of the frequency dependence of α_s, they assumed that it was proportional to the cube root of the frequency[54]; they stated that their method of determining water vapor concentration would still be applicable provided that α_s was directly proportional to some power of the frequency (which it is not, as is described in Chapter IV).

The Jenssen-Gething Methods (JGM) assumed that the attenuation depended on the sum of three terms a_c, a_m, and a_s, whose functional form was assumed to be as follows:

$$a_c = C*f^2 \tag{5-1}$$

$$a_m = M*f^2 f_r/(f^2 + f_r^2) \tag{5-2}$$

$$a_s = S*f^{1/3} \tag{5-3}$$

where C, M and S are constants with respect to frequency. Relation (5-2) also suffers from Harris' neglect of nitrogen relaxation. The JGM required that four different frequencies be used. The received signal intensities were then used to mathematically eliminate the unknowns C, M, and S from equations (5-1), (5-2), and (5-3). The JGM yields both the temperature and the relative humidity.

Jenssen and Gething simulated their method on a computer and found that, for even marginally useful results from one measurement set, the JGM required that the received intensities be measured with a standard deviation of less than 0.1% of the mean intensity. But if the amplitudes of the received signals are approximately Rayleigh distributed, then the per cent standard deviation will be about 90%. Therefore, the number of observations required to reduce the error to 0.1% would be $(90)^2/(0.1)^2 \cong 8 \times 10^5$. Assuming that the scattering volume is at a height of 17 meters, which is close to the minimum altitude of interest) the time per observation is about 0.1 seconds, so that the total time required for a standard deviation of 0.1% is 8×10^4 seconds, or about 22 hours. This time is much too long considering that, as stated in Chapter II, even the major atmospheric variables T, P, and H can change significantly within 15 minutes.

The bad prognosis yielded by these figures was apparently borne out by subsequent experiments performed by Gething to test the JGM; the results were, "... if not entirely negative, so at least unhelpful as far as practical applications are concerned."[55]

Regarding the JGM, Little has written that[56], "This multi-frequency approach requires accurate measurements of the changing ratio of echo strengths on the different frequencies as a function of height, and makes a number of critical assumptions as to the propagation conditions and the nature and constancy of the scattering process. The author [Little], therefore remains doubtful that these techniques will in fact prove useful in practice." In another paper, Little analyzed the existing (1973) proposals for remotely sensing water vapor (including the Raman scattering lidar) and concluded that, "... the ability to sense the three-dimensional humidity field remotely ... seems to be many years away." (The same conclusion was reached for temperature.)

The major problems with the techniques presented in this chapter are: 1) the limit on the number of data per unit time for a pulsed radar, which is imposed by the long period of transmission silence necessary for unambiguous returns (which sets the minimum time between pulses) and by the desired resolution of the sodar (which sets the maximum length of the pulse); 2) the limitation on the total length of time available for observations, which is required because of the possibility of significant changes in the meteorological variables; 3) the random fluctuations caused by the backscatter process which differ with frequency; 4) the random fluctuations caused by rapid changes in the excess attenuation; 5) the problem of building a transducer having identical characteristics for widely varying frequencies; and 6) a lack of precise knowledge of the effects on attenuation caused by changing temperature and pressure.

Problem (6) is solved by the new information on attenuation presented in Chapter IV. Problems (2) and (3) are ineluctable for a sodar system. However, the new proposal for a hygrometric sodar, which is presented in the next chapter, eliminates or mitigates the remaining problems so that the problems of backscatter fluctuations and of limited observation time can be tolerated.

CHAPTER VI

RELAXATION FREQUENCY METHOD

This chapter presents a collection of improvements for the hygrometric sodar proposals discussed in Chapter V. The resulting sensing plan will be referred to as the Relaxation Frequency Method (RFM). This method, which ameliorates the problems listed in Chapter V, will be statistically analyzed in Chapter VII, and the limitations on its use will be treated in Chapter VIII. This chapter includes a preliminary "propagation-of-error" analysis to demonstrate that the RFM is superior to the JGM; intuitive reasons for this superiority are also presented.

Development of the RFM

One very effective way to achieve more data per unit time from a sodar is to sweep the frequency, as in the manner of FM-CW radars so that the sodar can be transmitting continuously without producing ambiguous returns, (the frequency would have to be constantly increasing in order to avoid possible harmonic interference). The receiver would correspondingly have the center frequency of its band-pass filter swept at the same rate as the transmitter so that the passed signal would be from the same scattering volume. Although this technique could conceivably yield a hundred times[57] the data available from a pulsed radar, it would not be enough to make the JGM feasible.[58]

The errors and random fluctuations of excess attenuation can be virtually eliminated as a problem by transmitting just one frequency and forming the amplitude ratio for received signals which have been backscattered from two different heights (as seen in figure (1:2)) rather than forming the ratios of pairs of many frequencies backscattered from the same scattering volume (as with the JGM). Of course, this requires that the receiver have two band-pass filters, one for each height. By using the same transmitted frequency, the excess attenuation along with induced random fluctuations incurred between the transmitter and the first scattering volume will exactly cancel when the ratio of the two backscattered signals is formed. Since, as discussed in Chapter IV, most of the excess attenuation is due to the turbulence located directly in front of the transmitter, and since, as discussed in Chapter II, the turbulence as measured by C_V and by C_T, decreases rapidly with increasing altitude, then it follows that most of the excess attenuation is cancelled.[59] In addition, any excess attenuation incurred by the signals on the return trip from the height of the first scattering volume to the receiver will also cancel, provided that the time delay between the two signals is not too great (roughly less than two seconds, corresponding to a separation distance of less than 340 meters) since the turbulence field which causes attenuation will appear stationary over a time span of a few seconds.[60] Therefore, the only effect of turbulence induced fluctuations is found in the transmitted signal as it propagates from the first scattering volume to the second volume and the second signal as it propagates from the second scattering volume back to the first; but this occurs at the highest altitudes involved in the process where

C_T and C_V will usually be minimized. Also the time or distance traversed will probably be relatively short so that the effect of excess attenuation will be very small compared to that experienced with the JGM. Because of the virtual absence of excess attenuation with the RFM, there is no need to correct for the $f^{1/3}$ dependence as with the JGM. In addition, because the same transmitted signal is used for both returning signals, no correction is needed for transducer characteristics.

As a bonus for using the FM-CW transmission scheme, an attenuation spectrum is produced which not only provides amplitude information for each frequency but also derivative information, which is very significant since the amplitude information[61] is very "error-prone", whereas the derivative, because of the strong frequency dependence of the relaxation process compared to the frequency dependence of possible error processes, is not very sensitive to errors in amplitude. For example, if the absorption per cycle is plotted versus frequency such that peaks appear as in figures (4:2) or (4:4), then systematic errors can be detected by examining the shape of the curve; if the peaks are too "broad", the separation distance between the two scattering volumes is too great (e.g., H varies significantly over this distance), or if the peaks are "skewed" then a frequency-dependent error is present (such as might occur if the scattering volume's mean value of C_T were to significantly change as the frequency changed at one scattering volume but not the other). Hopefully, once the error is detected, corrective action can be taken; with the JGM, there would be no direct indication of an error.

The humidity, H, can be determined directly from the attenuation spectrum by estimating one or both of the relaxation frequencies or the frequency of the minimum or "valley" between peaks, if it exists for the current combination of H and T. The frequencies divided by the pressure in the region between the scattering volumes can be related directly to the humidity[62] (except for a very slight dependence on temperature displayed by the nitrogen peak and the "valley"). The pressure can be estimated with negligibly small resultant error in humidity from the Hydrostatic Equation, (2-1), and ground-based measurements of temperature and pressure. Alternatively, the humidity (and temperature) can be determined by fitting the relevant equations of Chapter IV to the attenuation curve. The fitting can be accomplished with greater confidence if one of the relaxation frequency peaks or the valley is contained within the range of frequencies swept by the sodar.

Another method of increasing the amount of data per unit time is available if two scattering volumes are used; independent data can be collected at the same time from receivers separated by a sufficient distance (usually over a wavelength). The topic of independence of backscattered signals in space, time, and the frequency-domain has been treated by Tatarskii.[63] For four receivers (which might be a reasonable compromise between cost and statistics), the resultant error in H would be reduced by half, as an example. This technique is not available to the JGM where frequencies close enough to one another to be identically backscattered from the same scattering volume are used, because a change in receiver location which results in a change of the "aspect" of the scattering volume[64] for one frequency will result in nearly the same change for the other frequencies; thus the ratios formed from the signals received by two separated receivers would not be independent.

Statement of the RFM

First, a continuous wave of increasing frequency is transmitted for the length of time necessary for sound to travel to the top of the atmospheric region which is to be sampled and to return to the transmitter (the transmission is then repeated). The signal is, of course, partially backscattered continuously as it propagates. A number of receivers are equipped with two or more[65] band-pass filters whose center frequency is swept at the same rate as the transmitted signal's frequency but whose sweep starting-times are delayed after the start of the transmission sweep by different amounts so that the returns from scattering volumes at two selected heights are continuously monitored. The ratio of the two amplitude signals received at each speaker at each frequency is then continuously formed and its logarithm continuously taken (correction for additional spherical spreading of the second signal can be made). The resultant signals from all of the receivers are then averaged[66] to form a function of frequency or, equivalently, of time (this function should differ from the attenuation spectrum by only a constant). The humidity, H, (and other variables)[67] is then estimated from this function; methods of estimation are discussed below. In an advanced system, the estimated variable values can be used as feedback, allowing system parameters to be changed in order to give a better estimate of H (and the other variables).[68] The sweep is repeated as many times as desired or permitted by changing meteorological conditions, and the estimates of H are then averaged.

There are many ways of estimating H from the function mentioned above. The best way is to fit the frequency-derivative of the function with the sum of the derivatives of equations (4-4), (4-9), and (4-10), where T and H are the independent variables. A simpler method (the "eye-ball" method) would be to estimate the values of $f_{r,N}$ and $f_{r,0}$ from the function and then use figures (4:7) and (4:9) to find H. Both of these methods require that P be known accurately. An estimate of the necessary accuracy can be obtained from ground-based[69] measurements and the Hydrostatic Equation, (2-1); and the accuracy can be increased by using the estimates of T resulting from the curve-fitting procedure mentioned above.

This procedure gives the average concentration of water vapor existing between the two scattering volumes. A three dimensional picture of H can be obtained by varying the heights of the two scattering volumes[70], and by varying the angle at which the original acoustic wave is transmitted.

Sources of Error

Uncertainties in the values of P, T, and the wind (which affects the estimated height of the scattering volume) can cause errors in the estimation of H. As will be demonstrated in the next chapter, the resultant error in H when the RFM is used can be held to less than 1% for each variable.

Also, there is a slight error due to the excess attenuation occurring between the two scattering volumes. As mentioned above, this attenuation should be relatively small,[71] and if of a significant magnitude, it can be detected from the attenuation spectrum, and compensation can be made. In addition, the magnitude of this excess attenuation can be estimated from equations (4-16) and (4-18).

Because the values of C_T can be different at the two scattering volumes, a constant, the logarithm of the ratio of the two values of C_T, will be added to the attenuation spectrum (along with a constant representing the additional spherical spreading of the second signal, if compensation has not already been made) to get the ratio function mentioned above. But the addition of a constant does not affect either of the two estimation methods mentioned above.

As the frequency of the transmitted signal increases, the acoustic beam width should decrease, meaning that the diameters of the scattering volumes decrease. In a homogeneous turbulence spectrum (such as Kolmogorov's) no difference would be noticed; but for the nonhomogeneous case, the average value of C_T for each volume may change significantly (especially if the diameter of the beam approaches the diameter of the regions of relatively constant C_T). The magnitude of this effect is not known; however, its frequency dependence is mild. Examining the attenuation spectrum should reveal the error and permit compensation for it. Other methods of reducing any effect from this source will be discussed in Chapter VIII.

The major source of error, then, is the randomness of the Rayleigh-distributed backscattered signals. Although the percent rms error[72] in received amplitude signal for this source is very high (about 50%), it is well characterized and fixed, so that a good maximum likelihood estimator of the backscatter can be derived. Hopefully, enough data can be taken in a reasonable period of time so that the resultant error in H can be reduced to a few per cent; this is the topic of the next section.

Propagation of Error

The propagation of error[73] analysis for the RFM, which is presented below, is a quick and simple way to estimate the usefulness of the RFM; the results are in fair agreement with the formal statistical analysis presented in the next chapter. For convenience, the per cent root-mean-square error, designated by an "S" subscripted by the symbol of the variable concerned, will be used as the indication of error in this analysis. It is assumed in the analysis that the only source of error[74] in the received signal is caused by the random phase fluctuations of the backscattered waves.

Let Q be defined as ratio of the amplitude signal received from the second scattering volume, A_2, to that received from the first, A_1, then:

$$Q \equiv A_2/A_1 = (\sigma\,[r+x]/\sigma\,[r])^{1/2}(r/(r+x))*\mathrm{EXP}[-2x\alpha] \qquad (6\text{-}1)$$

where $\sigma\,[r]$ is the backscattering cross-section from height r,
r is the distance from the transmitter to the first scattering volume,
x is the distance between scattering volumes, and
α is the average attenuation between the scattering volumes.

Since the amplitudes are Rayleigh distributed, $S_{A_1} = S_{A_2} = 52\%$, and $S_Q \le \sqrt{S_{A_1}^2 + S_{A_2}^2} \cong 52*(1.414) \cong 73\%$. Now S_α is related to S_Q by:

$$S_\alpha/S_Q = \left|\frac{d\alpha/\alpha}{dQ/Q}\right| = \frac{Q}{\alpha} * \left|\frac{d\alpha}{dQ}\right| = \frac{1}{2x\alpha} \qquad (6\text{-}2)$$

So that[75] $S_\alpha \cong 36/(x\alpha)\ \%$ (6-3)

Assume that the "eyeball" method is used to estimate the relaxation frequency from $(\alpha/f)[f]$. The eye makes judgments based on both the relative[76] magnitude and the derivative of the curve of $(\alpha/f)[f]$ at each point. Let it further be assumed that only the oxygen relaxation frequency is involved, then[77]:

$$(\alpha/f)[f] = (\alpha/f)_{max,0}*(2ff_{r,0})/(f^2 + f_{r,0}^2) \quad , \qquad (6\text{-}4)$$

so that $S_{f_{r,0}}/S_{(\alpha/f)} = (F^2+1)/(F-1)^2$ (6-5)

where $F \equiv f/f_{r,0}$ and $S_{(\alpha/f)} = S_\alpha$,

also $(\alpha/f)' \equiv d(\alpha/f)[f]/df = (\alpha/f)_{max,0}*2f_{r,0}(f_{r,0}^2+f^2)/(f_{r,0}^2-f^2)$,

(6-6)

so that $S_{f_{r,0}}/S_{(\alpha/f)'} = \left|(F^4-1)/(F^4-6F^2+1)\right|$. (6-7)

The autocorrelation function of $(\alpha/f)[f]$ must be known before $S_{(\alpha/f)'}$ can be determined precisely.[78] But since "the eye" is aware of the shape of the curve $(\alpha/f)[f]$, it in effect "smooths" the actual derivative, so that it can reasonably be assumed that the average value of $S_{(\alpha/f)'}$ is of the same order of magnitude as the average value of $S_{(\alpha/f)}$. Alternately, (5-5) and (5-7) can be evaluated for many values of F; the results of such evaluations suggest that $\langle S_{f_{r,0}}\rangle \approx \langle S_\alpha\rangle$, for the "eyeball" method. For example, at the inflection points $F = \sqrt{s} \pm 1$, $(\alpha/f)'$ provides no information about $f_{r,0}$, whereas $(\alpha/f)'$ is a maximum, so that any error in (α/f) will cause a relatively smaller error in $f_{r,0}$; correspondingly, (α/f) yields no information (infinite error) about $f_{r,0}$ when F = 1, whereas the error in $f_{r,0}$ is quite insensitive to error in $(\alpha/f)'$ since the rate of change of $(\alpha/f)'$ is greatest. Therefore, the following rough estimate of the average error in $f_{r,0}$ of the prediction by the attenuation curve will be adopted for the rest of this discussion:

$$\langle S_{f_{r,0}}\rangle = \langle S_\alpha\rangle \text{ , (for the "average" data point) ,} \qquad (6\text{-}8)$$

Now since $H \propto f_{r,0}^{1.8}$, as presented in Chapter IV, it follows that on the average:

$$\langle S_H\rangle = 0.6\langle S_{f_{r,0}}\rangle \text{ ,} \qquad (6\text{-}9)$$

where it has been assumed that P is known exactly. Then combining (6-9), (5-8), and (5-3) gives

$$\langle S_H \rangle = \langle 22./x\alpha \rangle \ \% \tag{6-10}$$

For T = 20°, P = 1 atm, and a relative humidity of 10%, the attenuation is on the order of $\alpha = 10^{-3}$ nepers/meter so that if x = 500 meters, then $\langle S_H \rangle \approx 44\%$. Now if n_D is the number of independent data taken per sweep, n_S is the number of sweeps, n_R is the number of independent receivers, and N is defined as the total number of independent data, then $N = n_R n_S n_D$, and:

$$S_H \approx 44/\sqrt{N} \ \% \tag{6-11}$$

It can be seen that N need only be about 100 for S_H to be less than 5%. Assuming an altitude of 1700 meters for the second sampling volume (meaning a sweep period of 10 seconds), a data rate per speaker of 100 data/sec (a conservative figure), four independent receivers, and a 5 minute test time (i.e., 30 sweeps), gives N = 120000, or $S_H \ll 1\%$. The last estimate of S_H is not justified by this crude "propagation of error" analysis; however, it should be clear that the RFM is far superior to the JGM. Indeed, it seems probable, based on the "overkill" available from N, that the RFM can be the basis of a practical hygrometric sodar.

Statistical Advantages of the RFM

The great statistical improvement realized by the RFM can be traced to several sources: First, and most importantly, the use of FM-CW and several independent receivers greatly increases the amount of data available. Secondly, errors caused by fluctuations encountered during propagation (which are unknown and tremendously variable), and by changes in transducer characteristics have been traded for fluctuations[79] due to the backscattering process, which have a fixed and well-known probability distribution; consequently, no calibration of the transmitter is required. Thirdly, observation of the shape of $(\alpha/f)[f]$ permits identification of any additional errors and permits "tailor-made" corrections. Also the oxygen relaxation frequency provides a sensitive indication of H which is not[80] dependent on the temperature. Finally, the RFM is not highly sensitive to errors in the amplitude of α (as is the JGM), especially if a good curve-fitting technique is used, because the humidity is revealed by the shape or derivative of the curve.

Modification

In the above analysis, it was tacitly assumed that an acceptable signal-to-noise ratio (SNR) existed; as shown in Chapter VIII, this is a critical assumption. Typically an acceptable SNR will exist for some portions of the frequency range and some altitudes and conditions, but not for others. It may be advisable to modify the RFM to construct integrated profiles of humidity by utilizing the sampling scheme of the JGM; this could be advantageous at lower altitudes under cool, dry, and calm conditions. Under these conditions, propagation errors will be smaller and the value of α so diminished as to be difficult to detect over a small range by the regular RFM scheme.

CHAPTER VII

STATISTICAL ANALYSIS

In this chapter, the effects on the RFM estimation of H caused by the sources of error mentioned in the preceeding chapter are investigated. The probability distributions of several intermediate results and the first two moments of these results are derived. In the following discussions it is assumed that the design parameters of the sodar and the prevailing atmospheric conditions are such as to yield an acceptable[81] signal-to-noise ratio; these points are discussed in the next chapter.

Effect of Pressure Variations

The estimate of H given by the RFM is proportional to P^m where $.5 < m \leq 1$, and P is the pressure of the sampling region, as is derived from equations (4-7) and (4-8). Therefore, the percent rms error in H must be greater than or equal to that caused by error in P alone; i.e., $S_H \geq S_P/m$. As indicated by the following discussion, this restriction imposes a negligible limitation on S_H (i.e., $S_P < 1\%$).

As indicated in Chapter 2, the pressure at any given altitude usually varies by less than 5% from its mean value. A better estimate than the mean value can be obtained by using equation (2-1), the Hydrostatic Equation, which requires an estimate of T as a function of altitude from the ground to the sampling region and a ground-level measurement of P.[82] Reference to standard tables[83] which relate pressure to altitude and temperature, supports the conclusion that an estimate of the absolute temperature accurate to about 0.7% (i.e. $\pm$ 20°C), is sufficient to give $S_P \leq 1\%$ for altitudes of up to at least 2 km; knowledge of the temperature to within 4°C permits determination of P with $S_P \leq 0.05\%$. Therefore, a ground-based measurement of T, corrected for altitude, should be sufficient to justify ignoring the pressure contribution to error in H.

Note that an error in estimated height of the sampling volume will show up as an error in P. If the error in height is within $\pm$ 50 meters, then $S_P \leq 1\%$. Also, if the sampling volume is too large, the variation in pressure over the volume will result in a broadening of the absorption peaks in the function $(\alpha/f)[f]$; a 5% change in P would occur for a separation distance of x = 500 meters. A correction for this effect might be desirable for a curve-fitting scheme of estimating H, although a broadened peak's relaxation frequency would still give the correct value of H for the volume, provided that the average value of pressure was used in the calculation.

As shown in equation (4-6), the classical and rotational absorption also depend on the pressure.

Effect of Temperature Variations

Uncertainty in T as a function of height affects the estimate of H in two ways: its direct effect on the estimate of P has already been considered; its other effect is on the estimation of the height of the scattering volume. The height is determined from the time lapse between the start of the transmitter frequency sweep and the start of a given band-pass filter's frequency sweep. This time is, of course, divided by two and then multiplied by the speed of sound to give the height of the scattering volume associated with the given filter. The speed of sound varies as the square root of the absolute temperature, as in equation (4-6), and so the estimate of height will also. But since a 6°C change in T represents only about a 2% change in absolute temperature, it also represents only a 1% change in the estimate of height (an estimate of T which is accurate to within 6°C should be easily obtained).

In addition, uncertainty in T at the scattering volume affects the estimate of H in three ways: 1) the magnitude of the attenuation spectrum is dependent on T, as shown in equations (4-11), (4-12), and (4-13); 2) the difference in absorption between the values at the nitrogen and oxygen relaxation frequencies is solely temperature dependent; and 3) the nitrogen relaxation frequency is a function of the temperature as indicated by equations (4-8) and (4-12). The following relations can be derived from the equations mentioned above:

$$S_{\alpha_{cr}} \approx S_T/2.; \qquad S_{\alpha_{v,O}} \approx 5.*S_T; \qquad S_{\alpha_{v,N}} \approx 9.*S_T \ .$$

The change in α_{cr} will be opposite in sign to the change in the other two absorption components (which will normally overshadow the change in α_{cr}). Therefore, a 6°C change in T will cause a 10% to 18% change in α, as in partially shown in figures (4:5) and (4:6). The second dependence listed above is really just another manifestation of the first dependence and is displayed by equation (4-5). The eyeball method of determining the relaxation frequencies, and thus the humidity, is not influenced by these first two temperature dependencies. A curve-fitting scheme which would also be independent would be to fit the normalized frequency derivative of the attenuation spectrum. If conditions are such that only the oxygen relaxation frequency is of interest these two humidity predicting schemes will be independent of temperature.

For the third temperature dependence mentioned above, equation (4-8) can be used to derive the following approximate result: $S_{f_{r,N}} \approx 2.6\ S_T$. Therefore, a 6°C error in temperature would cause a 5% error in H since $S_H \approx S_{f_{r,N}}$, as seen from equation (4-8). Consequently, either an estimate of T accurate to within about 1°C would be needed to give $S_H < 1\%$, or else the curves must be fit simultaneously with respect to the two variables T and H (which in effect gives the desired $\pm$ 1°C estimate). As will be discussed later, the desired estimate of T is readily obtained by curve-fitting. Alternately there exist several remote sensing schemes capable of determining T to within 1.0°C.[84] Also, of course, T must be accurately known if the relative humidity is required.

Effect of Wind

Wind can also affect the estimate of the location of the sampling volume.[85] The horizontal displacement of the sampling volume by V_h, the horizontal component of the wind is unimportant, given a relatively large sampling volume diameter compared to $V_h{*}t$, where t is the time for the acoustic round-trip to the sampling volume, since the value of H averaged over several cubic meters is fairly constant for a given altitude and approximate location. The angle of bending is less than 2° for a typical horizontal wind of 10 m/s. The decrease in altitude resulting from acoustic-ray bending by V_h is also negligible.

For vertical wind,[86] $c = c_0 + V_v$, so that the ratio of actual height of the sampling volume to the estimated height is $\rho = 1-(V_v/c_0)^2$. Typical values of c_0 and V_v give $\rho = .9999$ or a height error of less than 0.01%.

Effect of Turbulence

The turbulence in the velocity field, as measured by C_V, should have no bearing on backscattered signals, as indicated by equation (4-21). However, there is an effect due to turbulence-induced fluctuations in the propagating wave, as described by equation (4-18). These fluctuations cancel out as discussed in the preceding chapter, except for fluctuations induced between the first and second scattering volumes. To be noticeable, the fluctuations would have to cause a percent rms error of at least[87] 23%, because of the large fluctuation contribution of the backscattering process. Data taken by Kasper, et al. under a wide variety of weather conditions of the rms error induced by turbulence over a distance from the sound source of up to 150 meters and for frequencies of up to 8 kHz, show that the error for the RFM due to turbulence in the scattering volume will be less than 10% (usually much less) provided that the first scattering volume is at a height of at least 40 meters.[88] Since most of the fluctuation-inducing turbulence is within 200 meters of the surface,[89] it seems reasonable to conclude that turbulence-induced fluctuations will be almost totally obscured by fluctuations due to backscattering. Alternately, this conclusion can be reached by examining equation (4-18). For a significant error in received amplitude, $\overline{\chi}^2 \gtrsim 0.1$. Equation (4-18) is approximately represented by:

$$\overline{\chi}^2 = 1.2 \times 10^{-3} f^{1.16} L^{1.8} \langle C_n^2 \rangle \qquad (7\text{-}1)$$

If it is assumed that L < 1000 meters and that the sampling volume is above the surface layer so that the low turbulence condition can be used[90], $<C_n^2> \approx 10^{-8}$, $m^{-2/3}$, then the above condition becomes, with the aid of (7-1):

$$f^{1.16} \gtrsim 0.1 * L^{-1.8}/(1.2 + 10^{-3}<C_n^2>) \text{ , or}$$

$$f \gtrsim 8 \text{ kHz.}$$

The turbulence-induced fluctuations, since the above figure increases sharply as L decreases, will not be important for frequencies of interest.

The temperature turbulence at the first and second scattering volumes, $C_T[r]$ and $C_T[r + x]$, contribute the addend, $LN[C_T[r+x]/C_T[r]]$, to the attenuation spectrum. Under certain conditions, this value will be constant with respect to frequency; then the effect of C_T can be eliminated by fitting the derivative of the received attenuation spectrum, otherwise, this constant must become another independent variable of the curve-fitting process. The conditions under which this value will be a constant are[91]: 1) C_T must be proportional to a power of the frequency (for a Kolmogorov turbulence spectrum, the power is 1/3, --see equation (4-12)); 2) the sampling time must be short compared with the time required for significant change in the average value of C_T in the region of interest (this time is a few seconds if the scattering volume has a diameter of at least a few tens of meters); and 3) the average value of C_T over the scattering volume must not change as the frequency (and thus the beam diameter and therefore the volume over which the averaging takes place) is changed. Design considerations based on these conditions are considered in the next chapter. It is not vital that these conditions be satisfied; any change in $LN[C_T[r+x]/C_T[r]]$ should be a mild function of frequency which can be detected by observing the shape of the received attenuation spectrum.[92]

Doppler Effects

Vertical motion of the scattering volume will cause a Doppler shift in the reflected frequency; however, for the typical value of $V_v = 3.$ m/s, the resultant error in H is less than 1%.

Spectral broadening can also occur due to turbulence and backscattering. Brown[93] has stated that for typical circumstances, "the [spectrum] broadening effects of mean wind during the scattering process outweigh the broadening effects of mean wind during propagation to the scattering layer." The broadening occurring during the scattering process is only a few Hz change.[94] In addition, an energy loss at one frequency due to broadening will be fairly well compensated for by energy added due to broadening for neighboring frequencies. So that if the frequency is swept, as in the RFM, then broadening is of little consequence.

In conclusion, none of errors described above constitutes a serious limitation on the RFM's ability to measure humidity; although, the sodar must be designed with the effects of T and C_T in mind. Otherwise, the effects of these two quantities must be known before H can be determined. Conveniently, the data received in the RFM is such that T and $(C_T[r+x]/C_T[r])$ can be estimated simultaneously from it alone, along with H.

Statistics for A and Q

There is a finite limit to the backscattered amplitude received by the sodar; this is not the case described by the Rayleigh Distribution.

If the Rayleigh Distribution is not truncated to better represent the actual received amplitude distribution, then the means and variances of quantities derived from the received amplitudes will become infinite.

The standard Rayleigh Distribution is:

$$p[A] = (2A/\sigma^2)\ \mathrm{EXP}[-A^2/\sigma^2] \tag{7-2}$$

where σ is root-mean-square error, and the "mean radial error" or simply the mean value is $\langle A\rangle = \sqrt{\pi}\,\sigma/2$. Also the percent rms error is:

$$S_A = 100*\sqrt{-1 + \langle A^2\rangle/\langle A\rangle^2} = 52\% \tag{7-3}$$

For a 12% truncation[95] of (7-2), $S_A \approx 43\%$.

It is mathematically more convenient, and it also is more easily interpreted physically, to derive the distribution of $Q \equiv A_2/A_1$ by assuming A_1 and A_2 to be Rayleigh distributed and then to truncate the resulting distribution[96]:

$$p_Q[q] = \mathrm{INT}[x*p_{A_2}[x]*p_{A_1}[x/q];\ x:\ 0,\infty]/q^2$$

$$= 2*\mathrm{INT}[x^2*\mathrm{EXP}[-\beta x^2];\ x^2:\ 0,\infty]/(\sigma_1^2\sigma_2^2\ q^3\beta^2)$$

$$= -2*\left\{(\beta x-1)\mathrm{EXP}[-\beta x^2]\right\}\Big|_0^\infty*\left(\sigma_1^2\sigma_2^2 q^3\beta^2\right)^{-1} = 2/\left(\sigma_1^2\sigma_2^2 q^3\beta^2\right)$$

where $\beta = \sigma_2^{-2} + \sigma_1^{-2}\ q^{-2}$, or if $\gamma \equiv \sigma_2/\sigma_1$,

$$p_Q[q] = 2q\gamma^2/(\gamma^2+q^2)^2 \tag{7-4}$$

If (7-4) is truncated so that $\gamma/10 < q < 10\gamma$, then (7-4) must be multiplied by k_Q, where

$$k_Q^{-1} = \mathrm{INT}[2\gamma^2 q/(\gamma^2+q^2)^2;\ q:\ 0.1\gamma\ ,\ 10\gamma\ ]\ ,\ \text{or}$$

$$k_Q = 1.02$$

Therefore, only a 2% truncation has been performed, but this is sufficient to keep the means and variances of quantites which are of interest from becoming infinite. The first and second moments of Q are:

$$<q> = 2k_Q\gamma^2 \ \mathrm{INT}[q^2/\gamma^2+q^2)^2;\ q:\gamma/10,\ 10\gamma]$$

$$= 2k_Q\gamma^2\{\mathrm{INT}[(\gamma^2+q^2)^{-1};\ q:\gamma/10,10\gamma]-\gamma^2\mathrm{INT}[(\gamma^2+q^2)^{-2};\ q:\gamma/10,10\gamma]\}$$

$$= k_Q\left(\gamma\ \mathrm{TAN}^{-1}[q/\gamma] - \gamma^2 q/(\gamma^2+ q^2)\right)\Big|_{\gamma/10}^{10\gamma}$$

$$<q> = (1.02)\ \gamma(1.37) = 1.4\gamma \qquad (7\text{-}5)$$

$$<q^2>= k_Q\gamma^2 \ \mathrm{INT}[2q^3/(\gamma^2+q^2)^2;\ q:\gamma/10,10\gamma]$$

$$= k_Q\gamma^2\{\mathrm{INT}[(q^2+\gamma^2)^{-1};\ (q^2+\gamma^2):\ q=\gamma/10,\ q=10\gamma]$$

$$-\gamma^2 \ \mathrm{INT}[(\gamma^2+q^2)^{-2};\ (q^2+\gamma^2):\ q=\gamma/10,\ q=10\gamma]$$

$$= k_Q\gamma^2 \ \left(\mathrm{LN}[\gamma^2+q^2] + \gamma^2/(\gamma^2+q^2)\right)\Big|_{\gamma/10}^{10\gamma}$$

$$<q^2>= 3.66\gamma^2 \qquad (7\text{-}6)$$

From (7-5) and (7-6), S_Q is found to be:

$$S_Q = 100*\sqrt{(3.66\gamma^2/(1.4\gamma)^2)-1} \approx 92\% \qquad (7\text{-}7)$$

This is a considerable departure from the 73% figure derived in Chapter VI because the propagation of error technique is based on a first-order Taylor's Series expansion and assumes that the errors involved are quite small (<5%).

The probability density function of the intensity of the received signal whose amplitude is Rayleigh distributed will be the Exponential Distribution:

$$p_I[z] = \mathrm{EXP}[-z/m]/m \qquad (7\text{-}8)$$

where $m = <z> = \sigma^2$ and $<z^2> = 2m^2$, so that $S_I \approx 100\%$. The ratio $D=I_2/I_1$, has the distribution:

$p_D[d] = \gamma^2/(d + \gamma^2)^2$, where $\gamma^2 = m_2/m_1$ also.

However, there is no reason to convert the received signal, which is in amplitude form to an intensity, since data processing adds no additional information.

Statistics for α

An expression relating q and α can be derived from equations (4-1) and (4-21):

$$q[f] = \frac{A_2[f]}{A_1[f]} = K[x,r]*EXP[-2\alpha[f]x] \tag{7-9}$$

where $K[x,r] \equiv (C_T[r+x]*T[r]/(C_T[r]*T[r+x])$, (7-10)

and where it has been assumed that the thicknesses of both scattering volumes are the same, that α is a constant in the sampling volume (or at least can be replaced by the mean value, $\langle\alpha\rangle$), and that turbulence is homogeneous and Kolmogorov. The probability density function is derived from $p_Q[q]$ as follows:

$$p_\alpha[\alpha] = p_Q[q[\alpha]] * |dq/d\alpha| \tag{7-11}$$

Substituting (7-9) into (7-4) then multiplying by the absolute value of the derivative of (7-9) yields for (7-11):

$$p_\alpha[\alpha] = 4x\gamma^2 K[x,r]^2 *EXP[-4\alpha x]/(\gamma^2 + K[x,r]^2 *EXP[-4\alpha x])^2, \text{ or}$$

$$p_\alpha[\alpha] = x\ \{2\eta\ EXP[-2\alpha x]/(\eta^2 + EXP[-4\alpha x])\}^2\ , \tag{7-12}$$

where $\eta \equiv \gamma/K[x,r]$.

Note that since the range of Q has been defined as $0 < q < \infty$, the range of α is $-\infty < \alpha < \infty$. The negative values can occur because of the fluctuations in received amplitude or because $C_T[r+x] > C_T[r]$, for example. The mean of α is given by:

$$\langle\alpha\rangle = \text{INT}[\alpha * p_\alpha[\alpha];\ \alpha: -\infty,\infty\ ] \qquad (7\text{-}13)$$

$$= -(4x)^{-1}\ \text{INT}[\text{LN}[y]\ \eta^2(\eta^2+y)^{-2};\ y=\text{EXP}[-4x\alpha]:\ 0,\infty]$$

This integral is infinite, therefore a truncation is again needed. Assume $\gamma/10 < q < 10\gamma$, as before, then $\text{LN}[\eta/10] < -2x\alpha < \text{LN}[10\eta]$. So that (7-13) becomes:

$$\langle\alpha\rangle = k_Q(\eta^2/4x) * \text{INT}[\text{LN}[y] * (\eta^2+y)^2;\ y:\eta^2/100,\ 100\eta^2]$$

$$= k_Q(\eta^2/4x)\ \left\{-\text{LN}[y]/(\eta^2+y)\ +\ \text{LN}[y/(\eta^2+y)]/\eta^2\right\}\Big|_{\eta^2/100}^{100\eta^2}$$

$$\langle\alpha\rangle = \text{LN}[\eta^{-1}]/(2x) \qquad (7\text{-}14)$$

Equation (7-14) can be recast into the form: $\eta = \text{EXP}[-2x\langle\alpha\rangle]$, so that equation (7-12) can be rewritten, taking into account the truncation, as:

$$p_\alpha[\alpha] = k_Q x\ \left(2\ \text{EXP}[-2x(\langle\alpha\rangle+\alpha)]/(\text{EXP}[-4x\langle\alpha\rangle] + \text{EXP}[-4x\alpha])\right)^2 \text{ or}$$

$$p_\alpha[\alpha] = 1.02x * \text{SECH}[2x(\alpha - \langle\alpha\rangle)]^2 \qquad (7\text{-}15)$$

The second moment for α is:

$$\langle\alpha^2\rangle = k_Q(\eta/4x)^2\ \text{INT}[\text{LN}[y]^2/(\eta^2+y)^2;\ y:\eta^2/100,\ 100\eta^2]$$

The above integral cannot be evaluated in closed form in terms of a finite number of analytical functions. However, if η^2 is removed from the integral function, the remaining integral can be evaluated numerically. The η^2 can be removed via integration by parts:

$$\langle\alpha^2\rangle = k_Q(4x)^{-2}\ \text{INT}[\text{LN}[\eta^2 z]^2/(1+z)^2;z=y/\eta^2:\ 0.01,100.]$$

$$= k_Q(4x)^{-2}\{-\text{LN}[\eta^2 z]^2/(1+z)\Big|_{0.01}^{100.}$$

$$+\ 2*\text{INT}[\text{LN}[\eta^2 z]/(z+z^2);\ z:\ 0.01,100.]\}$$

The last integral above can be evaluated as:

$$\text{INT} = \text{LN}[\eta^2]*\text{LN}[z/(1+z)]\Big|_{0.01}^{100.} + \text{INT}[\text{LN}[z]/(z+z^2);\ z{:}0.01,\ 100.]$$

Since the immediately last integral doesn't involve η, it is an exact number, which has been numerically evaluated as (-8.98). Consequently, $<\alpha^2>$ can be evaluated:

$$<\alpha^2> = x^{-2}(0.25*\text{LN}[\eta]^2 + 0.181) \tag{7-16}$$

Now S_α can be determined:

$$S_\alpha = 100\left((<\alpha^2> - <\alpha>^2)/<\alpha>^2\right)^{1/2}$$

$$= 100\left((4(0.25*\text{LN}[\eta]^2 + 0.181 - 0.25\ \text{LN}[\eta]^2)/\text{LN}[\eta]^2\right)^{1/2}$$

$$= 200\ \sqrt{0.181}/|\text{LN}[\eta]| = 85/|\text{LN}[\eta]|\ \%$$

Since $<\alpha> = -(2x)^{-1}*\text{LN}[\eta]$, S_α can be written as:

$$S_\alpha = 43/(x<\alpha>)\ \% \tag{7-17}$$

Possible values of x could be from 10 to 500 meters and typical values for α would be $10^{-4} < \alpha < 10^{-1}$, nepers/meter. These values and equation (7-17) demonstrate the critical nature of the selection of the separation distance, x.

Simulation Equation

The cumulative probability, $\mathbb{P}[\alpha]$, can be found by integrating (7-12), with trunction accounted for by the factor $k_Q = 1.02$:

$$\mathbb{P}[\alpha] = 1.02\eta^2\ \text{INT}\left[-(y+\eta^2)^{-2};\ y{=}\text{EXP}[-4x\alpha]:\ \eta^2/100,\ 100\eta^2\right]$$

$$= 1.02\ (1 + \text{EXP}[-4x\alpha]/\eta^2)^{-1} - .01$$

And since $\eta^2 = \text{EXP}[-4x<\alpha>]$, from equation (7-14):

$$\mathbb{P}[\alpha] = 1.02\left(1 + \text{EXP}[-4x(\alpha - <\alpha>)]\right)^{-1} - .01$$

Solving for α yields:

$$\alpha = (4x)^{-1} \mathrm{LN}[(.01 + \mathbb{P}[\alpha])/(1.01 - \mathbb{P}[\alpha])] + \langle\alpha\rangle \qquad (7\text{-}18)$$

The following form is also of interest:

$$(\alpha/f)[f] = (4xf\sqrt{N})^{-1} \mathrm{LN}\left[(.01 + \mathbb{P}[\alpha])/(1.01 - \mathbb{P}[\alpha])\right] + \langle(\alpha/f)\rangle[f] \qquad (7\text{-}19)$$

where the factor $\sqrt{N}$ has been added assuming that N independent observations were made and suitably averaged to give the value $(\alpha/f)[f]$. Equation (7-19) is a very useful representation of the distribution of α for the following reasons: 1) (α/f) has been decomposed into a strictly constant term (the average value) and a term representing only the fluctuations in (α/f); 2) the fluctuation term can be divided into two factors: the "LN" factor contains all the "randomness", and the $(4xf\sqrt{N})^{-1}$ factor includes the parameters of a particular experiment which will affect the magnitude of the fluctuations, but which are not random; 3) the random factor, LN[...], is the same for all experimental situations; it is dependent solely on $\mathbb{P}[\alpha]$ which is uniformly distributed from 0 to 1; 4) the effect of truncation is clearly apparent as the (.01) addend in the numerator and denominator of the argument of the logarithm; the addend bounds the numerator and denominator away from zero and thus keeps the fluctuations finite; and 5) since $\mathbb{P}[\alpha]$ is uniformly distributed, equations (7-18) and (7-19) are ideal for simulating α and (α/f) using a computer.

Curve-fitting

The use of curve-fitting to determine the values of H and T requires an estimator to quantitatively measure the error between the experimental and fitted curves. The "maximum-likelihood-estimator," which will cause selection of the H and T most likely to have caused the observed curve, is normally very well approximated by the "method-of-least-squares" estimator, however, the fluctuations in the present case are such that "least-squares" will yield noticeably different results. The exact maximum-likelihood estimator is derived below: The probability that the observed and actual (or predicted) values of α will differ by an amount $\delta \equiv \alpha - \langle\alpha\rangle$ is, from (7-15):

$$p[\delta] = 1.02x{*}\mathrm{SECH}[2x\delta]^2 \tag{7-20}$$

Therefore, the probability (density) that T and H are correct is given by:

$$p[T,H] = \prod_i (1.02x)\ \mathrm{SECH}[2x\delta_i[T,H]]^2 \tag{7-21}$$

where δ_i represents the difference between observed and predicted values of α for the i th data point. It is desired to pick T and H such that p[T,H] is maximized, which is equivalent to minimizing the following function:

$$M[T,H] = \prod_i \mathrm{COSH}[2x\delta_i] \tag{7-22}$$

or to minimizing:

$$m[T,H] = \sum_i \mathrm{LN}[\mathrm{COSH}[2x\delta_i]] \tag{7-23}$$

Estimates of the error in the chosen T and H can be obtained simultaneously to calculating (7-22) or (7-23).[97] The value of p[T,H], M, or m provides a measure of the "goodness of fit", which can indicate the "skewness" or "broadening" of relaxation peaks mentioned previously.

Simulation

Theoretically, S_H and S_T are functions of each other, of the frequency sweep and estimation method used, and of $S_{\alpha[f]}$. Ideally, formulae could be derived for S_H and S_T, but even if the derivation were analytically possible, it would still depend on the particular estimation method used. A much easier (and more general) alternative is to simulate the received $\alpha[f]$ using equation (7-18), and then to test a given estimation method. Figure (7:1) shows the results of a simulation of $\alpha[f]$, which used the standard IBM-FORTRAN scientific subroutine program "RANDU". The data were then fitted using the estimator given in equation (7-23), which was minimized using another standard IBM-FORTRAN-SSP program, "FMFP". This program uses a gradient search method, but since good[98] initial estimates of T and H are possible and since very accurate (less than 1% error) predictions of T and H are desired, a grid-search method[99], which is simpler, would be more appropriate.[100] Two examples of the sodar simulation are described below: The conditions for the first simulation were: T=10°C; H=.4%; four receivers; 100 Hz to 20 kHz frequency range; one sweep (log-linear); 100 data points (a very conservative number, requiring less than 0.2 seconds); and x=1000 meters. For the given conditions, $f_{r,0} \approx$ 10 kHz. The "FMFP" rapidly converged to the minimum of m, with a resulting absolute error in T of 0.04°C and a percentage error in the numerical value of H of 0.4% (i.e. an absolute error of $1.6*10^{-3}$%); the minimum value of (m/100) was 0.32.

The conditions for the second simulation (which are more likely to be encountered in practice) were: T=10°C; H=.2%; four receivers; 100 Hz to 10 kHz frequency range; 400 data points; x=500 meters; and one sweep. For these conditions, $f_{r,0} \approx$ 3.5 kHz. The resulting error in T was 1°C, and the percentage error in H was 3% (i.e., an absolute error of 0.06%); the minimum value of (m/400) was 0.27. Of course, the percentage error is reduced by a factor of $n_s^{-1/2}$ if n_s sweeps are taken. For the above conditions, n_s could easily be 100.

These simulations suggest that the RFM can be used as the basis for a practical hygrometric sodar, but since the conditions listed are unusual, and since the SNR problem is not addressed, no such conclusion can be reached (at least if just one sweep is allowed).

The answer to the question of practicability of the RFM depends on design limitations (SNR and hardware) which will be considered in the next chapter, and on the question of how many independent data can be collected before the atmospheric variables of interest can change significantly; this last question will now be considered.

Independent Data

If the returns from the scattering volumes were indeed Rayleigh distributed, then a single measurement would give absolutely no information about the mean amplitude of the backscattered signals (and therefore no information about the strength of the signal passing through the scattering volume). Of course, for the actual situation even the one measurement will give an estimate of the mean with some finite error S_A. The error for an estimate based on n measurements is $S_A/\sqrt{n}$, provided that the measurements are independent[101] of one another. The independence condition is met if the aspect (e.g. the relative positions of the effective[102] scattering turbulence within the scattering volume) which the scattering volume presents to the receiver has had the opportunity to change completely[103] between measurements.

The "error-reducing ability" of a continuous[104] signal may be described by the "effective" number of independent data, in other words, the number of independent data, n, which would result the same reduction in S_A as does the continuous signal. The situation can be conceptually approximated by dividing the continuous signal into contiguous, discrete data units of the minimum size necessary for independence. According to Marshall, Hitschfeld, and Wallace,[105] the effective number of independent data for a continuous signal is about 1.5 times the number of discrete independent data, corresponding to a reduction of S_A by a factor of 0.82. For convenience, the discrete data model of the received signal is used for discussion of the RFM.

In order to determine the number of discrete independent data which characterizes a signal, it is necessary to know the minimum datum "size" necessary for independence. The change required for two measurements to be independent can take place in any one of three parameters: 1) time, 2) space, and 3) frequency. Tatarskii[106] has considered the changes necessary which are presented below:

The time required for the vortices[107] in the scattering volume to move enough (by wind action, for example) to generate independent returns is on the order of a few seconds. This is much too long for it to do much good during one sweep of the RFM, but it does mean that data from subsequent sweeps can be treated as independent.

A change in the spacial orientation of the scattering volume, transmitter, and receiver can also produce independent returns. Physical motion of the equipment (or even changing the beam direction slightly[108]) is probably impractical. However, two or more receivers can gather independent data simultaneously if the distance, d, between them is:

$$d \geq cr/(Lf) \tag{7-24}$$

where d is the transverse separation distance, in meters,
c is the speed of sound, in meters per second,
r is the distance between scattering volume and receiver, in meters,
L is the thickness of the scattering volume (Δr or Δx) in meters, and
f is the frequency of the scattered wave.

For distances not satisfying (7-24), the data will still be independent if:[109]

$$d = Jc/(f\phi) \approx J * \Xi \qquad (7\text{-}25)$$

where ϕ is the beam width
J is an arbitrary positive integer, and
Ξ is the diameter of the beam at the transmitter, in meters.

Values of d other than specified in (7-25) can still result in partially independent data. The use of multiple receivers will also reduce error due to background noise.

A change in frequency can also cause independent data since different sets of vortices act as the scatterers at different frequencies. The required change, Δf, for backscattered signals is:

$$\Delta f \approx c/(2L), \text{ Hz.} \qquad (7\text{-}26)$$

Independent data can also be gathered if two or more sweeps with completely different frequency ranges are transmitted (and received from the same scattering volume) simultaneously. The restriction, on the closeness of frequencies of simultaneously propagating waves, which is a result of the relaxation process (discussed in Chapter IV) must be observed with this technique, of course. A reasonable expression of this requirement would be: $f_2[t] \gtrsim 5f_1[t]$; consequently, only two or three simultaneous sweeps would be possible in the range of frequencies available to a practical sodar (even if this condition were satisfied, the equations for $\alpha[f]$ might have to be modified).

For sake of completeness, it should be mentioned that there is no limitation (other than size and cost) on the number of independent sodars which can be used.

Required SNR

A sufficiently high SNR at the receiver is required for the conclusions in this chapter to be fully applicable. Marshall, Hitschfeld, and Wallace[110] have shown that, contrary to most measurement situations, an SNR of 10 decibels is all that is required, and that an improvement in SNR to above 10 dB results in virtually no improvement[111] in S_A and therefore is not helpful in estimating T and H. The available information decreases rapidly as SNR is decreased below 1 dB. The requirement of 10 dB can be reduced for data from two or more receivers separated by more than a wavelength (so that the noise component of the received signals is independent). For n_R receivers and n_S sweeps, the maximum required signal to noise ratio, SNR_{max}, is:

$$SNR_{max} = 10*(1-LOG_{10}[n_R n_S]), \text{ decibels} \tag{7-27}$$

The number of independent data taken per sweep, n_D, will also reduce SNR_{max}, but probably not as strongly as n_R or n_S because the noise at different frequencies can be strongly correlated over periods of time less than a few seconds.

The effect of noise is also reduced if A_1 and A_2 are received close enough together in time that the background noise is correlated; the correlated noise will cancel out when the ratio $Q = A_2/A_1$ is formed.

For the purposes of determining design limitations in the next chapter, a minimum value, SNR_{min} = 4 dB, will be adopted for a sodar with four independent receivers and for one sweep.

CHAPTER VIII

DESIGN CONSIDERATIONS

The physical limitations on the applicability of the RFM and the consequent considerations for RFM sodar design are presented in this chapter. Hardware specifications are not given since no standard sodar components exist; indeed, the economic attractions of acoustic remote-sensing systems include the wide variety of ways in which the sodar can be designed and the resultant ability to build an experimental sodar with "off-the-shelf" components.[112] In addition, any mass-produced sodar would warrant specially designed, state-of-the-art equipment.

Two sets of limitations will be derived; one will be based partly on the sodar capabilities predicted by Little[113] for a "third-generation" sodar; the other will be based on specifications of working sodars and other devices which have actually been built.[114] The former set will furnish an estimate of the ultimate capabilities of the RFM; the latter will provide a minimum capability estimate. The limitations will be examined in terms of altitudes or of conditions of T and H for which a sodar can obtain most of the required meteorological data using the RFM.

Meteorological Requirements

A sodar will provide the required meteorological data most of the time if it can sense H and T to a height of at least 1500 meters[115] for $-10°C < T < 30°C$, for relative humidity greater than 10%, and, correspondingly, for $0.05\% < H < 4\%$. Sodars are not affected very much by reflections from precipitation, fog, or clouds.[116] Vertical resolution should be on the order of a few tens of meters, depending on the altitude.[117]

Design Parameters

Assuming a backscatter, vertically-aimed sodar, the RFM sodar would have the following related design parameters: 1) r, the distance from the transmitter to the center of the first scattering volume; 2) x, the vertical thickness of the sampling volume, i.e., the distance between the scattering volume centers; 3) Δr and Δx, the total thicknesses of the first and second scattering volumes; 4) $f_X[t]$, the frequency transmitted at time t; 5) $f_{R1}[t]$ and $f_{R2}[t]$, the receiver filters' center frequencies for the first and second scattering volumes; 6) $b_1[f]$ and $b_2[f]$ receiver filter bandwidth for the first and second scattering volumes; 7) t_p, the period of the sweep; 8) Ξ, the effective diameter of the transducer; and 9) $A_X[f_X]$, the amplitude of the transmitted frequency. These parameters are not all independent; indeed, the following relationships hold: The time delay between transmission and reception is directly related to the heights of the scattering volumes:

$$f_{R1}[t] = f_X[t - 2r/c] \tag{8-1}$$

$$f_{R2}[t] = f_X[t - 2(r+x)/c]$$

The scattering volume thickness is related to the rate at which the transmission frequency is swept and to the corresponding bandwidth:

$$\Delta r[f_{R1}] = c\left\{f_X^{-1}\ [f_{R1}+ b_1[f_{R1}]/2] - f_X^{-1}\ [f_{R1}- b_1[f_{R1}]/2]\right\} , \tag{8-2}$$

$$\Delta x[f_{R2}] = c\left\{f_X^{-1}\ [f_{R2}+ b_2[f_{R2}]/2] - f_X^{-1}\ [f_{R1}- b_2[f_{R1}]/2]\right\} ,$$

where $f^{-1}[f_1]$ indicates the inverse function of $f[t]$.
For the above equations, it has been assumed that f_X is a monotonically increasing function during each sweep period, t_p.

Design Objectives and Constraints

It is desirable to maximize the product $x\alpha$ in order to reduce the signal fluctuations as shown in equations (6-10) and (7-18). Since the values of $\alpha[f]$ will be determined by the experimental conditions, only x can be maximized. However, if x is too large H may vary significantly over the sampling volume (which can be detected by checking for absorption peak "broadening" or, for curve-fitting methods, by noting that the value of m, the likelihood estimator of equation (7-23), is too large). In addition, an excessive value of x will decrease the correlation between the fluctuations induced by turbulence in the two returning signals as they propagate between the first scattering volume and the receiver. Also, the fluctuations induced by turbulence in the sampling volume may become significant.[118] The analysis associated with equation (7-1) and the two-second time constant for turbulence[119] suggest that x be limited to at least 500 meters and probably to 300 meters (unless the SNR is such that the additional errors can be tolerated). The pressure will also vary significantly over the sampling volume if x is large, causing a similar variation in the relaxation frequencies (if x=500 meters then $\Delta P=5\%$).

The scattering volume thicknesses, Δx and Δr, should be maximized in order to give a stronger backscattered signal (it is more important that Δx be maximized since it is at a greater distance from the transducer and since at higher altitudes C_T is generally smaller). Also, the required Δf for independence is decreased as Δx and Δr increase.[120] The following constraints apply, however, as Δx and Δr are increased: 1) resolution decreases; consequently, 2) the uncertainty in x, thus in α, H and T, is increased; 3) the maximum allowable x for a given resultant error is decreased; and 4) the allowable range of receiver bandwidths and choice of $f_X[t]$ is unfavorably restricted. The second and third constraints listed above suggest that $(\Delta x + \Delta r)$ should be less than, say, 10% of (2x) in order that its effect may be disregarded.

The period of the sweep should be the minimum necessary for unambiguous returns, i.e., $t_p = 2(r+x)/c$, since under most conditions more independent (and therefore "better") data can be obtained during a repeat sweep (this is particularly important at low frequencies for which Δf may be inconveniently large.) The period of the sweep, however, places a restriction on $f_X[t]$, on Δx and Δr, or on b_1 and b_2, as expressed in relations (8-2).

The bandwidths, b_1 and b_2 should be less than the frequency change necessary for independence (otherwise there might be a partial cancellation in the received signal). Unlike the SNR of a pulsed sodar, the SNR of an FM-CW sodar cannot be improved by decreasing the bandwidth[121], since the received signal intensity will be decreased by the same factor as the noise intensity. The Brownian motion which causes thermal noise has a much shorter coherence time than does the motion of the backscattering vortices; consequently, the bandwidth should be just small enough to insure coherence of the backscattered signal if thermal noise is the main noise-source present.[122] If the frequency sweep rates, f'_{R1} and f'_{R2}, are relatively constant over the times associated with the corresponding bandwidths then equations (8-2) can be written as:

$$\Delta r/c = b_1/f'_{R1} \text{ , and } \Delta x/c = b_2/f'_{R2} \tag{8-3}$$

Using (7-26) to express the above recommendation for beamwidth gives:

$$2\Delta r b_1 < c \quad \text{and } 2\Delta x b_2 < c \tag{8-4}$$

Using (8-3) to eliminate Δr and Δx produces for $i = 1,2$:

$$f'_{Ri}[t] > 2b_i\left[f_{Ri}[t]\right]^2 \tag{8-5}$$

If $b[f]$ is the larger of $b_1[f]$ and $b_2[f]$, then (8-5) can be written more conveniently as:

$$f'_X[t] > 2b\left[f_X[t]\right]^2 \tag{8-6}$$

This restriction is of concern only at low frequencies. If it is assumed that $\Delta x \geq \Delta r$ then the other constraint on f'_X which can be derived from (8-3) and (8-4) can be expressed as:

$$f'_X[t] < \left(c/(\Delta x)\left[f_X[t]\right]\right)^2/2 \tag{8-6}$$

This constraint primarily affects higher frequencies which because of their greater attenuation, require that Δx be maximized, and which require a larger $f'_X[t]$.

The diameter of the transducer, Ξ, should be maximized in order to reduce the amount of spherical spreading of the acoustic beam, and to decrease the relative contribution of internal receiver noise, subject to the constraints that the scattering volumes be within the far-field region of the transducer[123], and that the phase of the returning waves be relatively constant over the surface of the transducer. Brown and Keeler have shown that this last constraint is not likely to be important for audible frequencies.[124] Of course, the diameter also affects the sodar resolution.

Naturally, the greatest possible amplitude should be transmitted, subject to consideration of environmental noise pollution[125], and to the rapidly diminishing returns from increasing the SNR above 4 dB (for four receivers and one sweep).[126] Nonlinear effects will be limiting for an output sound power level of greater than 160 dB.

The simulations presented in Chapter VII suggest that doubling the range of the frequency sweep is more important[127] than quadrupling the number of independent data. Intuitively, the larger range greatly aids the curve-fitting process. Consequently, increasing the sweep range is a high-priority design objective. The beginning frequency f_B is bounded below by physical equipment considerations (e.g. an excessively large transducer diameter may be necessary to yield the required resolution), and by the requirement that $x\alpha[f_B]$ not be so small that S_α as given in equation (7-17) becomes intolerably large. The end frequency f_E is bounded above by the requirement that $\alpha[f_E]$ be small enough to permit the returned signals to be received with an acceptable SNR.

Much of the statistical advantage of the RFM would be lost if the frequency sweep range did not include an attenuation peak, or at least halves of two peaks. Figure (8:1) may be used to determine what frequency ranges will provide full coverage (always contain at least one relaxation frequency) under most weather conditions. The required values of f_B are plotted against the upper limit, f_E. The values of H for which $f_B \approx f_{r,N}$ and $f_E = f_{r,0}$ (i.e. the H above which the nitrogen peak is used and below which the oxygen peak is used), are marked along the curve. The "valley" between the two absorption peaks (which exists for H $\gtrsim$ .2%) can be used in place of $f_{r,N}$ as an extremum of $(\alpha/f)_{max}$. The corresponding frequency range curve is also presented in figure (8:1). The particular frequency range used will depend on T, H, and the altitude sampled. It may be advantageous to have two transducers, one designed for low frequency work, and one for high frequency work.

The remaining problem with f_X is to determine that sweep (as a function of time) which will maximize the amount of information gathered concerning H and T. If (α/f) for one absorption process is plotted versus LN[f], then the peak will be symmetrical. This indicates that if an estimate of T and H is not available then a log-linear sweep might be the best function. The information gained about T and H could then be used to improve the sweep function.

The log-linear sweep is of interest for low altitude work when there might not be enough time to collect the available independent data in one sweep. If enough time is available, then a "discrete, independent-data sweep", which changes frequency every cycle by just enough (Δf) to achieve independence, will be more useful. The time, τ, required for such a sweep is approximately:

$$\tau = f_B^{-1} + LN[f_E/f_B]/(\Delta f)_Q, \text{ seconds.} \tag{8-7}$$

Here $(\Delta f)_Q$ is the frequency change in received amplitude signal intensity required to produce independent values of Q; if Δf for the first and second scattering volumes is the same, then[128] $(\Delta f)_Q \approx \Delta f/\sqrt{2}$. The number of independent data gathered in one sweep, n_D, is

$$n_D = (f_E - f_B)/(\Delta f)_Q \tag{8-8}$$

Under many conditions τ will be considerably less than the sweep period t_p. In order to better utilize the time, the step size should be decreased. Even though consecutive data will become partially dependent, more information will be available, especially if substantial noise is present in the received signal. As mentioned in Chapter VII, the effective n_D is increased by a factor approaching 1.5 as the step size is progressively decreased. The factor 1.5 is a good approximation if the step size is decreased by a factor of 4 (or more).[129] The resultant τ will, of course, be four times larger. Should this larger value of τ still be less than t_p, then extra (dependent) data should be taken at the lower frequencies, where the background noise level will almost certainly be higher, in hopes that some noise cancellation will occur. For conditions under which τ as given by equation (8-7), is less than t_p, it would appear that little would be gained by two simultaneous sweeps of portions of the frequency range as opposed to just a single sweep.

Background Noise

The amount of acoustic background noise detected by a receiver varies considerably depending on the amount of "side lobe suppression" present in the receiver and on the location of the receiver. Little[130] has analyzed the available data on noise and has concluded that "... the ambient acoustic noise power at a quiet site is of the order 20 dB above [10^{-12} watts/meter^2] for an octave band centered at 1 kHz and decreases by about 5 dB per octave increase in frequency." Little has also stated that "... the expected increase in noise level per hertz of receiver bandwidth is about 14 dB per octave decrease in frequency." Simmons <u>et al.</u>[131] have compiled data on background noise levels for a wide range of environments. Most of the noise represented by these data is not important, provided that the sodar has good (-90 dB) sidelobe suppression; but the data compilation does furnish an idea of how the noise description of Little may have to be adjusted for different environments. The aforementioned observations can be expressed by the following equations for the noise sound power level[132] expressed in decibels:

$$NSPL_{dB}[f] = 143 - 46.5*LOG_{10}[f] + 10\ LOG_{10}[b/n_R] \qquad (8\text{-}9)$$

where b is the receiver bandwidth in hertz, and
n_R is the number of receivers.

Equation (8-9) represents a maximum value (at an "average" location) for the noise received by the sodar since the background noise is highly anisotropic and a sodar (with good sidelobe suppression) collects noise only from the vertical direction, which is "least noisy".

A minimum value (which has been observed only very rarely) for the received noise based on the ineluctable thermal noise of the atmosphere is given by the following equation:

$$NSPL_{dB} = -10*LOG_{10}[\pi n_R \Xi^2/(4b)] - 83.8 \qquad (8\text{-}10)$$

where Ξ is the effective transducer diameter in meters.

Little[133] reports that "The ambient noise level on most acoustic sounders is 10-40 dB above the theoretical limit ..." which is the thermal noise given in equation (8-10) with $n_R = 1$. Little suggests that with careful design of the sodar, the noise can be reduced by up to

20 dB. Therefore, an optimum noise figure of 5 dB above that given by (8-10) will be used in the remainder of this chapter; the average noise for presently-operating sodars is taken to be 25 dB larger than (8-10). The improvements suggested by Little include using quiet field sites for the sodar and locating the receiver below ground in order to decrease the wind noise (it is probably more important to locate the sodar above the surface layer; the wind noise can be reduced in an elevated receiver as well, however).

Values of Sodar Parameters

Sodars which have actually been constructed have had bandwidths ranging from 6 Hz to 100 Hz. Little has estimated that the smallest realizable bandwidth is 3 Hz, which is limited by "the random fluctuations of acoustic propagation".

Current sodars transmit intensities of up to 140 dB, but 110 dB is a more representative figure. Little estimates that an improvement in transmitted power of 20 dB can be realized. Papers have been published on several devices[134] (some of which are mechanical) which have intensities up to 166 dB. In general, the output intensity is a function of frequency, tending to be much lower for higher frequencies in the case of electro-acoustic transducers.

The frequencies used by present-day sodars range from 800 Hz to 11 kHz[135], and some RASS and EMAC units have been operated at from 80 Hz to 22 kHz (the maximum range usually decreases strongly as the frequency increases).

Transducer diameters have usually been on the order of 1 or 2 meters, although at least one 15 meter diameter sodar has been constructed.[136] Little reports one case where an effective diameter of 100 meters could be obtained. Little notes that the benefits of increasing Ξ are greatly diminished for $\Xi > 20\lambda$.

Feasibility of the RFM

Using the optimum and "average" figures for the design parameters noted above, the feasibility of building an RFM hygrometric sodar will now be investigated. If it is possible to build a system which will give input data equivalent to that used in the simulations of Chapter VII for the "worst case" of the conditions presented at the beginning of this chapter, then it will be concluded that the RFM is a viable technique for measuring water vapor concentration and temperature sufficiently well for most meteorological purposes. The "worst case" used will be for an upper scattering volume altitude of 1500 meters, a ground temperature of 30°C (corresponding to T = 20°C at 1500 meters), and 10% to 100% relative humidity . The analysis will consist of: 1) determining the total allowable round-trip attenuation, ψ in decibels, using the given conditions and the optimum sodar design; 2) finding the maximum frequency which can be used, given ψ, for the range of humidity; and 3) deciding if the maximum frequency is high enough to permit sufficient data to be gathered.

The total allowable attenuation, ψ, will be the transmitted intensity minus the noise level at the receiver and minus the following items (all expressed in decibels): 1) attenuation due to spherical spreading; 2) excess attenuation; 3) the classical and rotational attenuation (which is negligible at the frequencies which will be of interest here); 4) the reduction in intensity resulting from the scattering process; and 5) the required SNR given in Chapter VII, 4 dB for one sweep and four receivers.

The effects of spherical spreading and excess attenuation can be combined using equation (4-17) into a single term representing total beam spreading; but beam spreading between the transmitter and the scattering volume exactly cancels out when the scattering process is considered since the reflected power is proportional to the volume of the scattering region, and therefore is proportional to the beam area. Spherical spreading after the scattering is accounted for by the scattering equation, (4-21), which expresses the reflected power in terms of the power per unit solid angle. Thus the scattering equation treats the scattering region as a collection of single point scatterers for which excess attenuation exists only because the scattering is anisotropic. However, scattering at angles close to 180° should be higher than for complete backscattering so that any broadening due to excess attenuation would mean an intensity increase.[137] Therefore, the beam broadening effects will be neglected, along with classical and rotational attenuation. More study of (4-21) is needed, especially with regard to the single point scatterer approximation; the actual scattering volume can be quite large and will be shaped like a part of a spherical shell. Experimental investigations of backscatter have found returns 10 to 15 decibels higher than that predicted by (4-21). The explanation was suggested that energy is also reflected by temperature gradients which are not represented in (4-21). The strong subsidence which usually marks the top of the boundary layer can be used to give much stronger returns than would normally be available at a particular altitude. The 1500 meter figure mentioned earlier was adopted as a mean upper limit to the boundary layer; for most meteorological purposes, just the boundary layer is important, so that the second scattering volume could normally be placed in the subsidence layer.

From Chapter II, a typical value for C_T^2 at 1500 meters would be $5*10^{-3}{}^\circ K\ m^{-1/3}$; a possible value for Δx would be 75 meters, corresponding to a maximum bandwidth of 4.5 Hz, and requiring an x of greater than 400 meters (which restricts Δr to about 20 meters). For convenience let $\zeta_T = (\pi\Xi^2/4)$ be the effective transmitter area and let ζ_R be the effective receiver area; then substitute $\zeta_T*\Delta x$ for V in equation (4-21)[138], multiply by the solid angle subtended by the receiver, convert to decibels, add 4 dB for the required SNR, and subtract 15 dB to correct the scattering prediction to get the correction term, ξ, whose components were listed above:

$$\xi = 4-15-10*\mathrm{LOG}_{10}[.004(2\pi f/c)^{1/3}\zeta_T*75.*(5*10^{-3})*(293)^{-2}*\zeta_R/(4\pi*1500^2)]$$

$$= -11-10*\mathrm{LOG}_{10}[.01*\zeta_T*(5.5*10^{-6})\zeta_R/(5.66\mathrm{x}10^7)]$$

$$\xi = 139 - 10*\mathrm{LOG}_{10}[\zeta_T*\zeta_R] \quad , \tag{8-11}$$

where it has been assumed that the maximum frequency is about 2 kHz. If $\zeta_T = 100$ square meters and $\zeta_R = 5$ square meters then $\xi = 140-27=113$ dB.

The noise figure is given by equation (8-10); for $b = 3/\sqrt{2}$ hertz and $\zeta_R = 5\ m^2$, where b is the bandwidth of the receiver, the noise figure, corrected 5 dB for minimum background noise, is: 5-88 = -83 dB. Therefore,

$$(\Delta dB)_m = 160-(-83)-113 \cong 130 \text{ dB} \quad .$$

Now the maximum relaxation frequency, based on oxygen absorption alone[139], which can be tolerated is:

$$(f_{r,0})_{max} = .115*(\Delta dB)_m/\{(2*1500)*(\alpha/f)_{max,0}\} \tag{8-12}$$

From figure (4:5), $(\alpha/f)_{max,0}$ for T = 25°C (the average temperature along the propagation path) is $3.3*10^{-6}$ neper-seconds. Therefore, the maximum oxygen relaxation frequency which can be observed is 1500 Hz. This corresponds to $H \approx 0.1\%$ which is about 3% relative humidity; therefore, the oxygen relaxation frequency can only be used below 3% relative humidity, which is outside the normal range of interest. The 1500 Hz figure is the "minimum maximum-frequency"; as H is decreased the maximum frequency, f_m, rises to over 12 kHz, and as H is increased to 100%, f_m increases rapidly to 6.9 kHz. (See figure (8:2).)

The "valley" has a characteristic frequency, f_{val}, of about 250 Hz for a relative humidity of 10%, corresponding to $H = .31\%$. For $H = .31\%$ the maximum frequency which can be used is about 2350 Hz. For 100% relative humidity, $f_{val} \approx 3.8$ kHz and $f_{r,N} \approx 1$ kHz, so that complete coverage of the normal range of H is possible, provided that an $f_B \leq 250$ Hz is possible (which is presumed to be the case since there have been several proposals[140] to use 200 Hz and even 100 Hz to sample to altitudes of up to 10 km). The amount of data available for one sweep for the "worst-case" of $f_B = 250$ and $f_E = 2350$ is given by equation (8-8), with the 1.5 correction factor for a "continuous" sweep:

$$n_D = 1.5(2350-250)/(3/\sqrt{2}) = 1620;$$

with a collection time given by equation (8-7), modified by the 4.0 correction factor for a "continuous" sweep, as:

$$\tau = 4.0\{(250)^{-1} + \mathrm{LN}[2350/250]/(3/\sqrt{2})\} \approx 4.25 \text{ seconds},$$

which leaves about 5 seconds to take additional data at the low frequency end or to take data at higher frequencies than $f_E = f_m$ by means of coherent integration.

Comparing this case study to the second simulation of the previous chapter, it is noted that, although the frequency range is not as great, the range still includes an (α/f) extremum, and n_D is over four times greater; but, most importantly, the error in α as given by equation (7-17) is greatly reduced: for $f = 2350$ and $x = 400$, $S_\alpha \approx 22.\%$ (or 11% for 4 receivers). Consequently, the curve-fit should be excellent and the resulting error in H and T should be less than in the second simulation (errors due to variations in C_T, P, and T excepted). For higher values of humidity, the situation is further improved: for 100% relative humidity and $f_B = 250$ Hz, $f_E = 6.9$ Hz and $n_D = 5100$.

Of course, the design conditions necessary for $(\Delta dB)_m = 130$ dB are difficult and costly to satisfy; fortunately, f_m is proportional to a low power of $(\Delta dB)_m$, between 0.5 and 1. So that for a tremendous decrease to $(\Delta dB)_m = 65$ dB the f_m decreases only from 2350 Hz to 1600 Hz for a relative humidity of 10% at T = 25°C. This decrease is sufficient to allow a sodar to be constructed with parameters within those limits given previously for sodars already built, with the exception of the required $f_B \leq 250$ Hz, and with the caveat that n_D has decreased to 1040 for the case described above. The lower limit on f_B mentioned above can be replaced with $f_B \leq 800$ (the current sodar limit) for $H \gtrsim 0.7\%$, which would be the case more than half the time at 1500 meters and below (the limit is not a crucial restriction on the RFM anyway -- only a guideline so that comparison can be made with the results of the Chapter VII simulations).

On the basis of the case studies above it seems reasonable to conclude that the RFM can be used to measure water vapor concentration and temperature sufficiently well for routine meteorological purposes, using optimum equipment, and that such measurements can be made under most conditions for equipment having parameters consistent with previously built devices -- subject to the following provisions: 1) variations in C_T have not been accounted for;[141] 2) for very low altitudes, the product $x\alpha$ may not be large enough to keep S_α within reason; and 3) the sampling volume and Δx are assumed to be small enough that no objectionable error in H and T results, i.e., that the resolution of the sodar is sufficient for most meteorological purposes.

The first provision is discussed in the next section. The second problem can be solved by using a single scattering volume and estimating the errors such as those due to excess attenuation, or by directly observing the variables, which should be feasible at the low altitudes (this problem arises only for relative humidities of less than 10%, or temperatures below -10°C, which are not very frequently encountered).

The third problem, which is partially associated with the second problem, is assumed not to be significant for the limits already placed on x and Δx (and Δr) because the humidity, averaged over several cubic meters, varies only gradually with changes in altitude and even more slowly for changes in horizontal location (except near weather fronts and shorelines, for example). Also, the sampling volume can be changed to provide an integrated humidity profile which can then be differentiated to give better resolution.

Variations in C_T

The value of q calculated from the amplitudes of the signals received by the sodar from the second and first scattering volumes is directly proportional to the ratio of the temperature turbulence coefficient, C_T, of the two volumes: $q \propto C_{T2}/C_{T1}$. The average[142] value of this ratio does not depend on the frequency for a uniform spectrum of turbulence[143] (such as in the Kolmogorov Theory), and so $LN[C_{T2}/C_{T1}]$ should appear as a constant addend to the absorption spectrum, $\alpha[f]$. It can be eliminated by taking the derivative of $\alpha[f]$ and then applying curve-fitting techniques to find H and T, or it can be treated as an additional variable in the curve-fitting process. Errors will occur, however, if the sweep takes too long (on the order of several seconds), or if the sampling volume changes dimensions or location during the sweep so that the values of C_T are effectively altered. (Such errors can be detected, of course, by observing the shape of the absorption spectrum.) For a normal acoustic transducer, the beam area is inversely proportional to the square of the frequency; so that as the frequency is swept the scattering volume can shrink enough that the average over the volume can significantly change.

Neff[144] has presented data showing the variations of C_T with time and altitude, which can be extended to include spacial variations by invoking Taylor's Frozen Turbulence Hypothesis[145] and assuming an average wind-speed of 10 m/s. Neff's data, extended, shows that the most severe variations in C_T occur below 250 meters[146], and that above 300 meters the changes are much milder, with extreme variations contained within 40-meter-diameter volumes, with a doubling in C_T requiring a change of about 50 meters (or about 5 seconds), and with substantial vertical correlation between values of C_T.

The error caused by C_T is or can be mitigated by several factors: 1) the vertical correlation of C_T means that some of the error will be cancelled when the ratio, C_{T2}/C_{T1}, is formed; 2) multiple sweeps will reduce the error by $(n_S)^{-1/2}$, which is particularly useful below 250 meters where many more sweeps can be taken per unit time; 3) the percentage error in $LN[C_{T2}/C_{T1}]$ is obscured partially by the other terms in the sum which is equal to α (i.e., it is not directly proportional to α); and 4) the sodar can be designed to minimize the effects of variations in C_T by insuring that the scattering volume at the highest frequency is still large enough to give a good spatial average of C_T, by installing collimating "cuffs" around the transducer to limit the size of the beam at low frequencies and therefore keep the scattering volume average more uniform, and, possibly, by using two transmitters, one for high and one for low frequencies designed to keep the scattering volume more nearly the same size as the frequency is swept. Conventional echo-sounding methods could be used to avoid regions of extreme variations in C_T.

Although these mitigating factors are likely to be of considerable importance, the variance of C_T cannot be ruled out as a major source of error for the RFM. The data now available, which is insufficient, would indicate that the problem is manageable.

CHAPTER IX

SUGGESTIONS FOR FUTURE STUDY

Contained in this chapter are suggestions for continuing the present investigation, suggestions for related investigations, and additional information which may be useful in such studies.

Practical Test

The ultimate "future investigation" for a theoretical study is, of course, the building of a practical device. But because of the widely varying conditions over which a hygrometric sodar should operate, it is not necessary to build a completely new system to test the concept; relatively inexpensive modifications to existing sodars should suffice to allow the RFM to be tested for favorable sets of conditions (particularly lower altitudes). The minimum additional equipment which would be required would be a sweep generator, two filters which can be swept, a delay mechanism, and a divider, filter, and logarithmic converter to form α (assuming that the display device can be suitably modified to display $\alpha[f]$, although such a device would not be necessary in order to check the statistical distributions developed in Chapter VII). Possible problems with the sodar include: 1) using the same transducer as both transmitter and receiver which will necessitate a premature end to the transmitted-frequency sweep; 2) possible error due to variations in C_T averaged over the sampling volume; 3) development of a suitable delay device, since a delay of several seconds can be involved; and 4) maintaining a reasonable transducer efficiency (which was not included in the analysis of Chapter VIII) over the range of the frequency sweep. If at all possible, at least one other receiver should be included (velocity-transformer-type transducers are good for 10 Hz to 1500 Hz while acceleration transducers are better for 1.5 to 20 kHz); the effectiveness of spacial independence could then be observed. Also the equations for $\alpha[f,H,T,P]$ which are for pure tones in a calm air (and which do not exactly account for all of the attenuation mechanisms) may have to be adjusted slightly for a practical sodar.

With a working hygrometric sodar various ways of fitting the absorption curve, other than the presumably expensive use of a general-use, high-speed computer, can be evaluated. For example, the relationships between simple functions of the points of the attenuation curve to the variables T and H could be approximated (hopefully in a simple manner); the effect of a constant C_T can be eliminated by subtracting the mean value of the curve from the curve:

$$\mu_i \equiv \alpha_i - \sum_{j=1}^{N} \alpha_j/N \quad ,$$

where the subscript denotes the value of the curve for the i th discrete frequency, f_i (of course the summations will be integrals and the μ_i and α_i will be functions if a "continuous" sweep is considered). Then H and T should be related to the constants:

$$\varepsilon = \sum_{i=1}^{N} \mu_i^2 \quad \text{and}$$

$$\nu = \sum_{i=1}^{N} \mu_i^3$$

Also the point where $\mu = 0$ might be used.

Theoretical Developments

Of considerable interest would be the development of a direct relation between S_α and S_H, S_T, and $S_{C_{T2}/C_{T1}}$; the relationship would depend on the sodar parameters and on the estimation method used. The relation could be empirically derived using a computer simulation rather than analytically which could be accomplished by means of the formulae:

$$S_H^2 = \sum_i \left\{ S_{\omega_i}^2 \left(\frac{\partial H}{\partial \omega_i} \right)^2 \left(\frac{\omega_i}{H[\omega_i]} \right)^2 \right\}$$

along with the analogous formulae for the other derived variables instead of H; and where ω_i is the i-th independent variable such as the attenuation, α. Some intermediate results might also prove useful. For example, $\langle M_0 \rangle^{1/n}$, the geometric mean average of the expected value of the minimum of the maximum likelihood estimator, M, given in equation (7-22) and averaged over the n data samples, could be compared to the experimentally determined values of $\langle M_0 \rangle^{1/n}$ to determine the "goodness-of-fit" and, thereby, to detect systematic error. Since the expected value of a product of independent variables is the product of the expected values, use of (7-22) gives:

$$\langle M_0 \rangle^{1/n} = \langle COSH[2x\delta_i] \rangle$$

Therefore, using (7-20) yields:

$$\begin{aligned}\langle M_0 \rangle^{1/n} &= 1.02 \times *INT\left[SECH[2x\delta_i]^2 * [COSH[2x\delta_i]] ;\delta_i : - LN[10]/2x,\ LN[10]/2x\right] \\ &= 0.51 * INT\left[SECH[z];\ z=2x\delta_i : -LN[10],\ LN[10]\right] \\ &= 0.51 * \left(TAN^{-1}\left[SINH[z]\right]\right)\Big|_{-LN[10]}^{LN[10]} \\ &= 0.51 * 2.74 \simeq 1.4\end{aligned}$$

So that for $n = 10$, for example, the minimum value of M should be about 29; any large deviation from this value would indicate a bad fit.

The equation for scattering cross-section, (4-20), has been successfully checked at low altitudes and relatively small scattering volumes (especially with respect to the dependence on θ, the scattering angle). It has been checked for intermediate altitudes with sodars and the backscattered signals were found to be 10 dB to 15 dB greater than expected (refraction by temperature gradient was named as the cause). However, such a situation as considered in Chapter VIII, namely a relatively large scattering volume at 1500 meters altitude has not been investigated. It is suggested that expression of σ as an intensity ratio per unit solid angle may not be correct for this situation; the received intensity may not be so severely dependent on the altitude, R, as the solid angle concept dictates, i.e., as R^{-2}. At least it would seem that the shape of a large scattering volume (part of a spherical shell in the aforementioned case) would be a factor.

Also, the equations developed by Tatarksii describing the conditions on time, space, or frequency changes necessary for the independence of backscattered returns are quite simple and appear to be just superficial analyses for the special case of Kolmogorov turbulence in an otherwise calm, homogeneous atmosphere. Further investigation in this area is needed, particularly with regards to the correlation effects of simultaneous changes in time, space, and frequency.

Equipment and Techniques

Of great potential aid would be the development of a mechano-acoustic, gas-powered horn whose frequency could be swept with the speed required by the RFM hygrometric sodar; such a horn would probably be more efficient than the present electro-acoustic transducers, and could be an advantage in remote locations.

The RFM is not really applicable to line-of-sight devices. A possible line-of-sight acoustic hygrometer could operate on the humidity dependence of the phase change with frequency for acoustic waves, as described in equation (4-22). Two signals could be transmitted simultaneously with $f_2 >> f_1$ and with f_2 modulated by f_1 so that the difference in phase between the envelope of f_2 and f_1 would be an indication of the humidity. The frequencies would have to be swept in order to get a good estimate, but since wind and temperature variations would affect both beams equally, there should be little error in the method.

Another area which needs more study is the possible use of a "Fast Fourier Transform" with the return signals of an RFM sodar so that returns from all altitudes could be monitored simultaneously.

CHAPTER X

CONCLUSIONS

The new results or highlights of the present sodar investigation include: 1) a compilation of information concerning the atmosphere and containing descriptions of the variations of atmospheric parameters so that the information necessary to satisfy most meteorological requirements could be determined, and so that atmospheric acoustics could be properly interpreted; 2) a study and analysis of previous hygrometric sodar proposals as well as a study of other proposals and devices for the remote-sensing of water vapor; 3) a very detailed study of atmospheric acoustics, including theoretically-, and experimentally-based formulae for the major sources of attenuation and for turbulence induced fluctuations, and including a detailed consideration of the relaxation process which resulted in important restrictions on the operation of FM-CW sodars; 4) proposal of the RFM and favorable analysis of it; 5) derivation of statistics important to the RFM, particularly the development of a "maximum-likelihood estimator"; and 6) the presentation of suggestions for future study on the subjects of hygrometric sodar and atmospheric acoustics.

The relaxation frequency method which was proposed as part of the above studies considered several phenomena not addressed by previous sodar investigators, including: 1) the effects of changes in temperature, pressure, wind, and turbulence; 2) the strongly characteristic attenuation spectrum and the relation of the relaxation frequencies to water vapor concentration; and 3) independence of acoustic returns as a method of increasing the information gathered per unit time by a sodar.

Conclusions of the study of previous proposals for the remote-sensing of water vapor are that although Raman lidars offer the best long-term promise for detecting water vapor, present lidar equipment is too costly and difficult to operate, and it can only be used at night; lacking a suitable lidar system, a sodar system appears to be the only practical alternative. In addition, the development of technique to measure water vapor by sodar would furnish the "keystone" for the entire collection of sodar devices which are currently limited by a lack of knowledge of the amount of acoustic attenuation which in turn depends on a precise knowledge of H and T; therefore an "acoustic meteorograph" could be built capable of sensing T, H, wind, and turbulence in the boundary layer. Supplemented with a central radar which could detect liquid water, it would constitute a remote sensing system capable of furnishing the type of information required to satisfy the weather forecasting needs cited by Little. Knowledge of the temperature and humidity, and therefore, the acoustic attenuation should aid the investigations of wind-shear, vortex-wakes, and noise pollution now being conducted for aeronautics. For environment protection purposes, some means of remotely sensing the concentration of specific pollutants is still needed.

As a result of the present study, it has been concluded that the Relaxation Frequency Method should permit the determination of temperature and humidity accurately to an altitude sufficient for most meteorological purposes if the state-of-the-art sodar parameters proposed by Little can be realized, and that even present devices with minor modifications should be capable of using the RFM to detect water vapor concentration and temperature over a wide range of conditions of meteorological interest.

NOTES

1. As general references for this section, see Derr, Chapter 1 (written by R. L. Grossman), or Tennekes.

2. See Sutherland.

3. See Derr, Chapter 4 (written by W. C. Meechan); or Tatarskii, Chapter 1.

4. See Brown (1976).

5. See Tennekes, p. 59.

6. See Beran and Hall (1974).

7. See Beran (1971).

8. See Little (1972), and Chapter 30 in Derr.

9. A line-of-sight device is bistatic with a transmitter and a receiver at the ends of a straight path.

10. The acoustic estimate comes from Beran (1971); that for optical is based on a system employing Raman scattering; and the figure for radar varies widely -- doppler systems will be most expensive.

11. See Marshall, Peterson, and Barnes.

12. See Little (1969).

13. See Derr and Little or Chapter 30 in Derr or Little (Oct. 1972); also see papers on devices listed in the bibliography.

14. See Derr, Chapter 15.

15. Ibid.

16. See Strauch, Derr, and Cupp.

17. Contained in Derr and Little.

18. See Little (1973).

19. The operation is valid only for the "far field" of the source; i.e. R and R_0 must be such that $R \geq R_0 \geq R_f = 2D^2/\lambda$ where R_f is the distance from source to "far field", D is the diameter of the source and λ is the wavelength of the emitted acoustic radiation (all units are meters).

20. A similar equation could be written for the intensity of the wave; there would be an additional factor of 2 multiplying α. This factor is often omitted (e.g., see Gething and Jenssen), which is incorrect if α is expressed in nepers/meter. Frequently, α is given in terms of decibels (i.e., dB/1000 ft., or dB/100 m.), in which case it automatically applies to intensity.

21. The general mechanism, however, was understood, but not well enough to predict α_m over ranges of T and H. See Kneser.

22. Gething and Jenssen uses an unusual definition for α_{cl} and α_m; judging from the frequency given for these terms in the paper, the definition used was $\alpha_{cl} = \alpha_{cr}$, and $\alpha_m = \alpha_v$ only. This same convention is used in Harris.

23. This equation is slightly modified from that given by Sutherland,et al.

24. Evans compares the predictions of this two parameter model with the more general, 24-reaction model of Evans, et al.

25. See Kneser and Knudsen.

26. A more exact "rule of thumb" would be: $0.5 < f_1/f_2 < 2$.

27. Argon causes no effect because it is a single atom and has neither rotational nor vibrational energy levels.

28. This is slightly modified from material made available by Dr. H. E. Bass, University of Mississippi (private communication); see Sutherland, et al. or Evans, et al. For alternate forms of these equations see DeLoach.

29. This variable is not used in the literature.

30. DeLoach discounts dust, fog, some other possibly-existent relaxation processes, and refraction as possible causes of excess attenuation.

31. See DeLoach for analysis of past investigations of excess attenuation; for theory, however, consult Brown and Clifford (1976). The most careful (and recent) experimental observations are contained in Kasper, et al. Additional information on ground turbulence, shadow zones, and other, non-turbulence, sources of excess attenuation can be found in Ingard.

32. The observations in DeLoach suggest a $r^{-2/3}$ dependence, where r is the altitude, and also suggest that α_s is important mainly below 200 meters.

33. See Ingard, figure 4.

34. When attenuation is measured in decibels, it automatically refers to intensity.

35. These forces are controlling only for extremely loud sounds in air; otherwise, attenuation affects the wave-shape first.

36. See Beyer or various papers by Blackstock in J. Acoust. Soc. Am.

37. See Brown and Keeler; the test was conducted with the source atop a 150 meter tower, and a microphone at ground-level, 333 meters, obliquely, from the source, mean winds were from 3 to 23 m/s.

38. See Kasper, et al.; frequencies used were 500 to 8000 Hz, with a range of 150 m, and elevated sound source. Data was taken with a 0.5 Hz high-pass filter.

39. See Tatarskii or Brown and Keeler (there are several typographical errors in this last paper). Brown (Dec. 1974) states that a "saturation" phenomenon for χ occurs for $c_n^2 \gtrsim (k^7 L^{11})^{-1/6}$, which would apply to the examples given. Brown (Dec. 1974) also presents a historical overview of work on this topic.

40. See Monin or Tatarskii. Brown (Dec. 1974) presents a history of the study of scattering. McAllister, et al. present a discussion of scattering from the sodar point-of-view.

41. See Brown (Dec. 1971).

42. See Baerg or McAllister, et al.

43. See Brown, (Nov. 1974). Brown also shows that the most effective turbulence has characteristic lengths of from $\lambda/2$ to $\lambda/\sqrt{2}$, where λ is the acoustic wavelength.

44. See Harris (1971).

45. See Little (1969).

46. See Harris (1966).

47. This oversight was probably due to experiments and remarks made by Kneser and Knudsen, who measured absorption due to water vapor in otherwise pure oxygen gas and then in nitrogen gas. They found that absorption in nitrogen was much smaller than in oxygen (under the specific conditions chosen) and so gave the impression that vibrational absorption in air was due almost exclusively to a water vapor-oxygen relaxation process. See Kneser or Knudsen.

48. See Tatarskii, p. 452.

49. This distribution will apply, e.g., if the sampling volume contains a temperature inversion layer which would contribute a major portion of the backscattered signal.

50. See Parry and Sanders (1972).

51. If the distribution is Rice-Nakagami, this statement will have to be weakened accordingly.

52. The graph is apparently mislabelled, since no distance is specified, and the vertical axis is labelled "absorption ratio $(-1 + I_1/I_2)$". The graph also incorrectly shows combinations of temperature and absolute humidity for which the relative humidity is greater than 100%.

53. See Gething and Jenssen (1971). This paper was submitted only a couple of months ahead of Parry and Sanders so that Parry and Sanders were probably not aware of it.

54. See DeLoach for references to this dependence.

55. If S is the standard deviation for one sample and S_n if the standard deviation for n samples, then $S_n = S/\sqrt{n}$, assuming that each observation is independent.

56. U. Radok, private communication.

57. See Chapter 19, section 19.5.3, in Derr (1972).

58. See Little (1973).

59. This could be the case if the pulse length were 0.01 seconds and the pulse repetion rate were one pulse per second which corresponds to a sampling height of about 170 meters.

60. Using the figures given for a 17 meter sample height in Chapter V, a hundred-fold increase in the data rate would mean a sampling time of about 2.2 hours rather than 22 hours, i.e.: $22/\sqrt{100} = 2.2$.

61. This cancellation is especially strong when the transmitter is located within 10 meters of earth's surface, since C_T can become quite large in the surface layer (thus meaning that a major portion of the excess attenuation will occur here).

62. The "two second" figure comes from analyzing the oscillograms of Kasper, et al.; Kasper, et al. also state that most of the energy of the fluctuation spectrum of an acoustic wave is contained below 10 Hz (corresponding to a fluctuation time constant of greater than 0.1 seconds).

63. For the JGM, error in amplitude information is sensitive to uncertainty in temperature and pressure, and in tranducer characteristics, excess attenuation, and C_T at the scattering volume, as functions of frequency; the RFM amplitude information may contain errors due primarily to the change from minute to minute of C_T at the two scattering volumes.

64. See equations (4-8) and (4-10).

65. See Tatarksii, p. 452.

66. By "aspect" is meant the distances to various parts of the scattering volume and the value of the resultant addition in phases performed by the receiver.

67. A fast-Fourier-transform could be taken of the received signal so that returns from all heights would be continuously available.

68. Parameters could include scattering volume separation distance, frequency range and sweep rate, and receiver bandwidths (which determine the resolution of the sampled volume).

69. Preferably, T should be measured above the surface layer, say at a height of 10 meters. Then T can be assumed to decrease at a rate of 6.5°K/km.

70. This can be speeded up by using the fast-Fourier-transform scheme as noted above.

71. It should be completely masked by the backscatter fluctuations.

72. This is the same quantity as the standard deviation expressed in percent.

73. See, for example, Bevington, Ch. 4.

74. Actually, these fluctuations are not "errors", but are due to factors which cause the received signal to vary no matter how precisely it is measured; see Bevington, Ch. 1.

75. Notice that the inequality has been dropped.

76. Since only the relative magnitude is important, error in $(\alpha/f)_{max,0}$ can be neglected.

77. In the following derivation it is tacitly assumed that several data points are available so that it is indeed possible to form the derivative, to roughly evaluate $(\alpha/f)_{max,0}$ and to determine the approximate location of $f_{r,0}$ (i.e., to the right or left of the data point).

78. See Beckmann, Ch. 6.

79. These errors are really present in the JGM anyway.

80. It is dependent on the pressure estimate, of course.

81. If "acceptable" is taken to mean a SNR for which the background noise contributes less than 10% to the total received fluctuations, then the signal to noise ratio need only be greater than about 7 dB. The last figure was derived as follows: The total percent rms error in the received amplitude $S = (S_B^2 + S_N^2)^{1/2}$, where the subscripts B and N refer to backscatter and noise fluctuations, respectively. Since $S_B \cong 50\%$, s_N must be such that $S = 55\%$ to make a 10% change. Thus, $S_N^2 = (55)^2 - (50)^2$, or $S_N = \sqrt{525} \approx 23\%$, which corresponds to a signal-to-noise ratio of $20 \log_{10}[1/.23] \approx 7$ dB.

82. It may be advisable to make the ground-based measurements of T and P at a point above the surface layer, <u>i.e.</u>, at a height of 10 to 30 meters, because of the large variations in temperature and wind which occur in the layer.

83. See "Reduction of Barometric Pressure to Sea Level", <u>CRC Handbook of Chemistry and Physics</u>.

84. See <u>Derr</u>, Chapter 30.

85. See <u>Georges and Clifford</u>.

86. The c_0 is the speed of sound without the wind.

87. The argument for this figure is analogous to that given in note 81.

88. See <u>Kasper, et al.</u>

89. The 200 meter figure is reported for excess attenuation in <u>DeLoach</u>.

90. See <u>Brown and Keeler</u>.

91. These conditions are sufficient but not necessary, in the mathematical sense.

92. The "received attenuation spectrum" is defined as $LN[A_2/A_1]$, which is the attenuation spectrum plus various errors. The spectrum will be "skewed" if there is a variation due to temperature turbulence change.

93. See <u>Brown</u> (1973).

94. See <u>Beran and Clifford</u>.

95. In other words, 12% of the area under the curve p[A] has been deleted (corresponding to the extreme values of A) and p has been multiplied by 1.12 so that the total area will still be unity, as is required

for a probability density distribution. The retained values in this case are $.166\sigma < A < 1.66\sigma$.

96. The q represents a member of the total population of Q. See Beckmann, p. 78, for equation (7-3); note that A_1 and A_2 can be treated as though they were independent (for the present purpose).

97. See Bevington.

98. T can be estimated within 2% and from this estimate, H can normally be guessed within a factor of 3.

99. See Bevington.

100. See Marshall and Hitschfeld as a general reference and specifically page 968, for the explanation of the "no information situation".

101. Two measurements are independent if the probability of any possible outcome of one measurement does not depend on the outcome of the other measurement.

102. The diameter of the vortices most effective in the scattering process is $\lambda/2$ where λ is the wavelength of the scattered signal.

103. This condition is satisfied if the backscattered signal for each effective scattering vortex could have changed phase (relative to the receiver) by at least 2π radians.

104. The meaning of the term "continuous" here is not limited to time; it may also refer to space and frequency.

105. See Marshall and Hitschfeld, p. 979, and Wallace, pp. 1000-1001.

106. See Tatarskii, pp. 134 and 452.

107. Temperature vortices are responsible for backscattering.

108. The beam might be moved electronically by means of an antenna array; the results would depend on the correctness of the assumption that the average turbulence (and humidity) remain the same at the same altitude for small displacements.

109. See Marshall and Hitschfeld, p. 982.

110. See Marshall and Hitschfeld, and Wallace, p. 990.

111. The reason for this result is treated in note 81; it is concluded there that an SNR of 7 dB is sufficient to keep the increase (caused by noise) in S_A under 10%.

112. Commercially available transducers, for example, are not usually described well enough by the manufacturer to satisfy the needs of a sodar designer. See Simmons, Wescott, and Hall.

113. See Derr, Chapter 19.

114. For hardware design considerations see especially: Parry and Sanders; Derr, Chapter 18; Hall and Wescott; and Simmons, Wescott, and Hall.

115. See Brown and Keeler.

116. See Little (May 1972).

117. It is assumed here, of course, that H averaged over, say, a cubic meter varies slowly in space, and that the humidity turbulence is not of practical importance.

118. See the analysis in note 81.

119. See note 62.

120. See equation (7-26).

121. This statement applies to broad band noise such as thermal noise; however, if there is some background noise of a specific frequency, the signal to noise ratio might be increased by increasing the receiver filters' bandwidths.

122. For a given frequency sweep rate, the time during which a frequency band is interrogated will increase with the bandwidth.

123. This restriction is a real problem if a fast-Fourier-transform sampling shceme is used.

124. See Brown and Keeler (1975).

125. See Simmons, Wescott, and Hall. Since low frequencies have less attenuation (and therefore are more of a noise problem) they can be transmitted at lower amplitudes than high frequencies.

126. See Chapter VII.

127. There is, of course, no conflict between these two improvements.

128. Achieving complete independence is not really possible; implied is the adoption of a convention that independence has been achieved if the variable has had the opportunity to change by so many percent of its value. Since $Q = A_2/A_1$, it will have the opportunity to change by $\sqrt{2}$ more percent than the possible percentage change in A_1 or A_2 (if the change possible in both these variables is the same).

129. Inequalities (8-6) and (8-7) can be changed to reflect these points. The restrictions on the bandwidth remain the same since A, not Q, is the variable which is physically sensed.

130. See Little (1969) and Derr, Chapter 19.

131. See Simmons, Wescott, and Hall.

132. A zero-decibel sound-power-level corresponds to a signal intensity of 10^{-12} watts/meter^2.

133. See Derr, Chapter 19.

134. See Allen and Rudnick, Jones, or "The Electroacoustic Horn," by Baucher and Kreuter, J. Acoust. Soc. Am., 1969; vol. 46, no. 6 (part 1). Also see Perry's Handbook of Chemical Engineering, "Solid-gas separators," the Handbook of Physics, Acoustics, or Ingard (40 horsepower siren).

135. See the following paper by Kelton and Bricout, who use a "powerful Levavasseru whistle": "Wind velocity measurements using sonic techniques," Bull. Amer. Meteor. Soc., Sept. 1961; vol. 45, no. 91.

136. See Fukushima, Okita, and Janaka in J. of Radio Research Laboratories, 1975,; vol. 22, no. 108.

137. See Brown and Clifford for an example which suggests that even for a speaker transmitting from 1500 meters altitude to the ground that the excess attenuation would be less than 2 dB.

138. The ζ_T is substituted to cancel the aforementioned effects of beam spreading.

139. The nitrogen absorption is negligible at the oxygen relaxation frequency.

140. See, for example, McAllister, et al. (1969).

141. It is assumed that variations in P and T with height can be corrected for.

142. The average is to be taken over the time necessary for several sweeps.

143. Brown and Keeler among others have found this to be a reasonable assumption.

144. See Derr, Chapter 18; the data is believed to be for f = 2 kHz.

145. See Derr, Section 1.7.3.

146. This activity is usually contained in "thermal plumes".

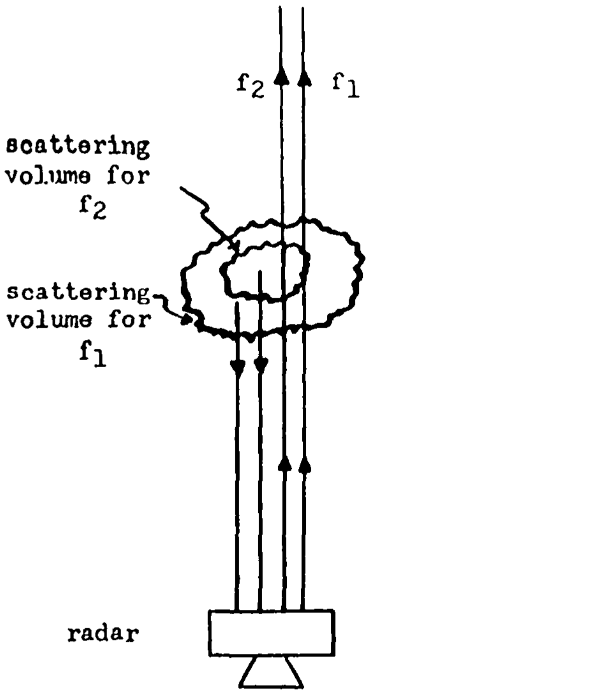

Figure (1:1): Jenssen-Gething Method
(only two of four frequencies are shown.)

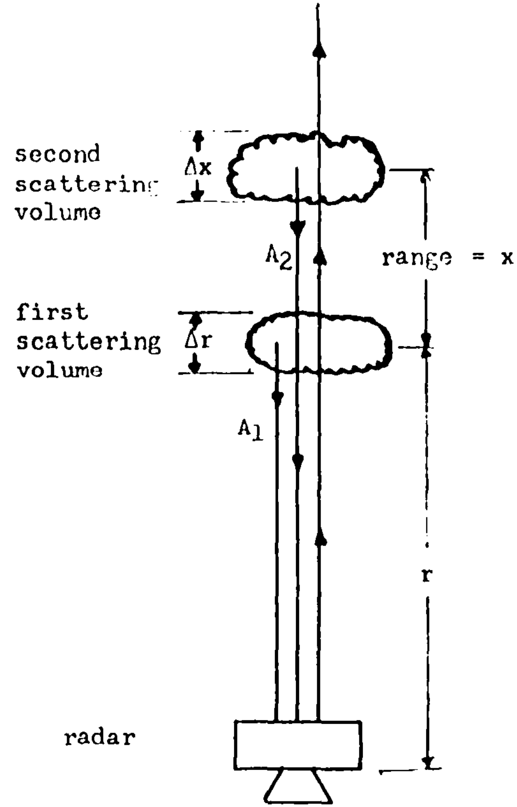

Figure (1:2): Relaxation Frequency Method

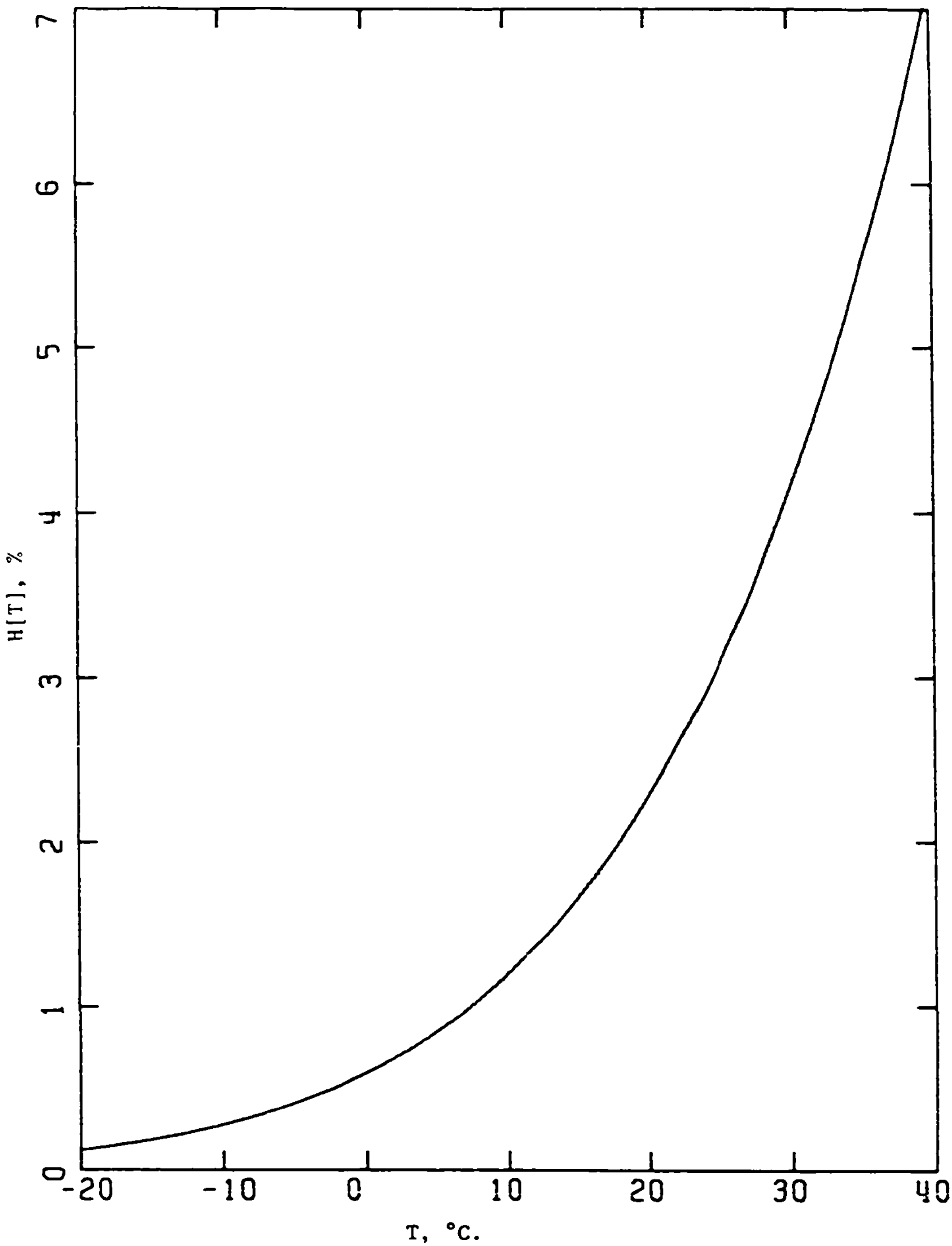

Figure (2:1): Percent molar concentration of water vapor, H[T], as a function of temperature, T, for a pressure of one atmosphere, at saturation.[a]

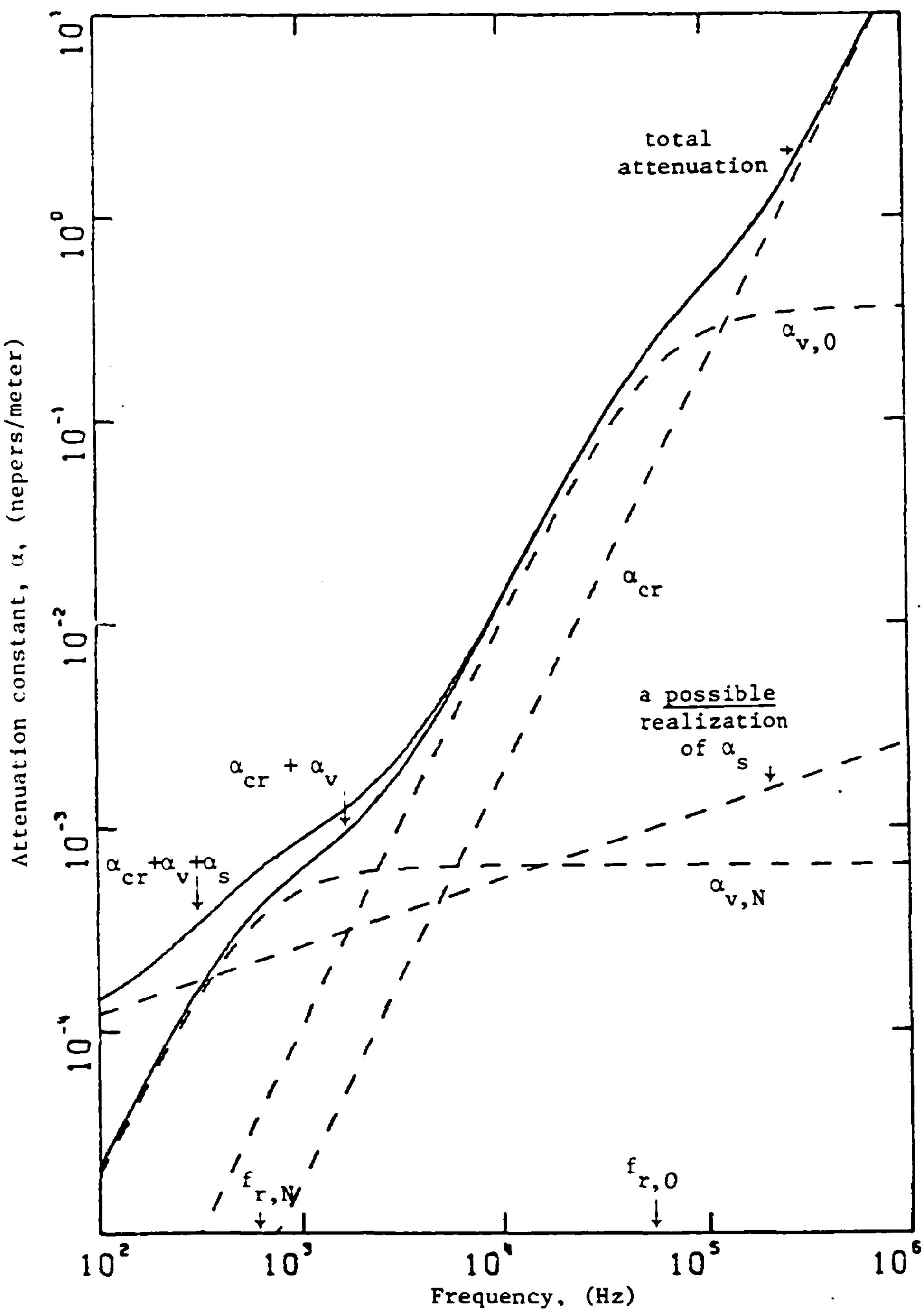

Figure (4:1): Spectra of absorption components for temperature, T=20°C.; pressure, P=1 atm.; relative humidity, H_r=70%. (after Bass, et al.)

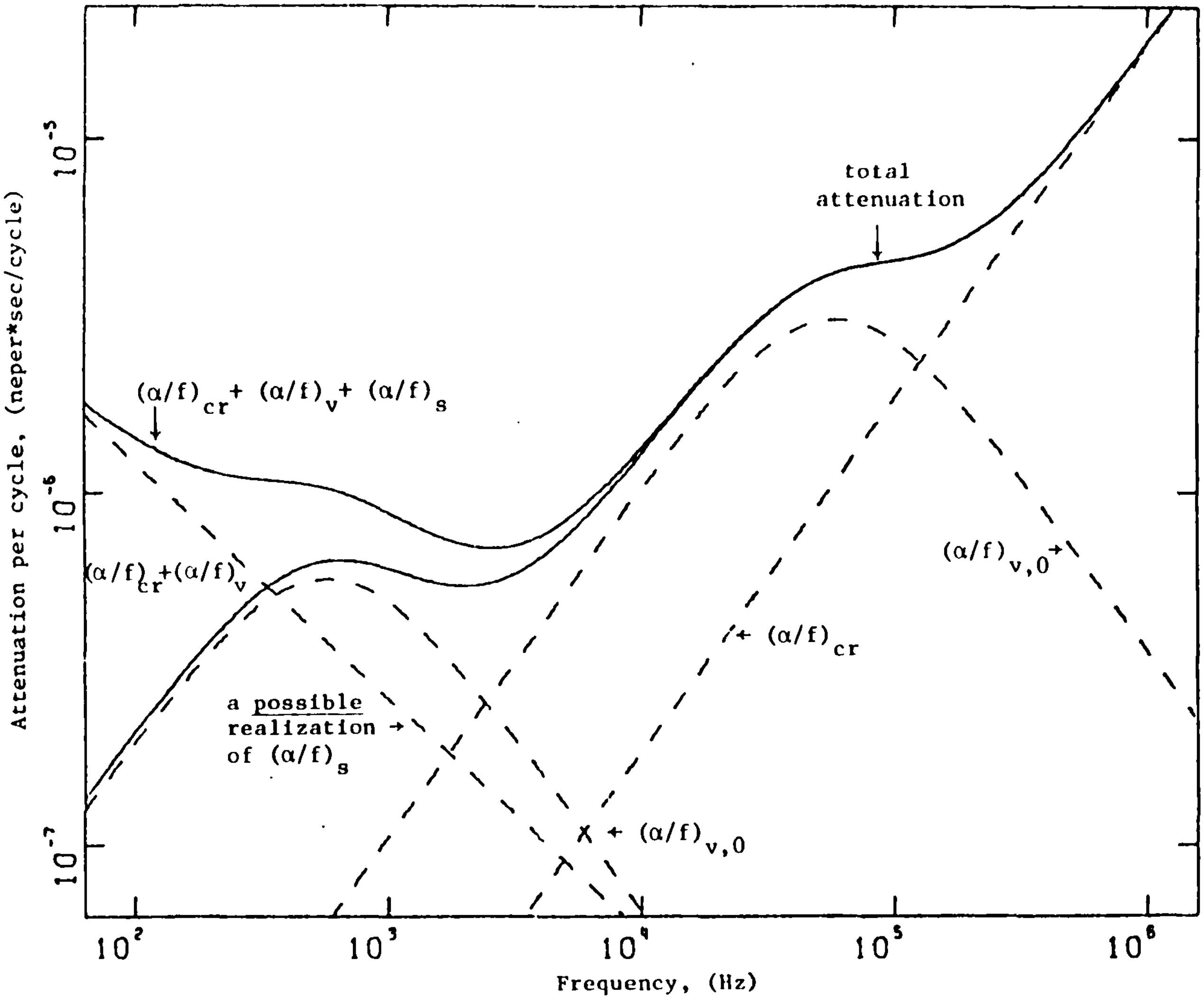

Figure (4:2): Spectra for components of absorption per cycle for a temperature of T=20°C., a pressure of P=1 atm., and a relative humidity of H_r=70%. (after Bass, et al.)

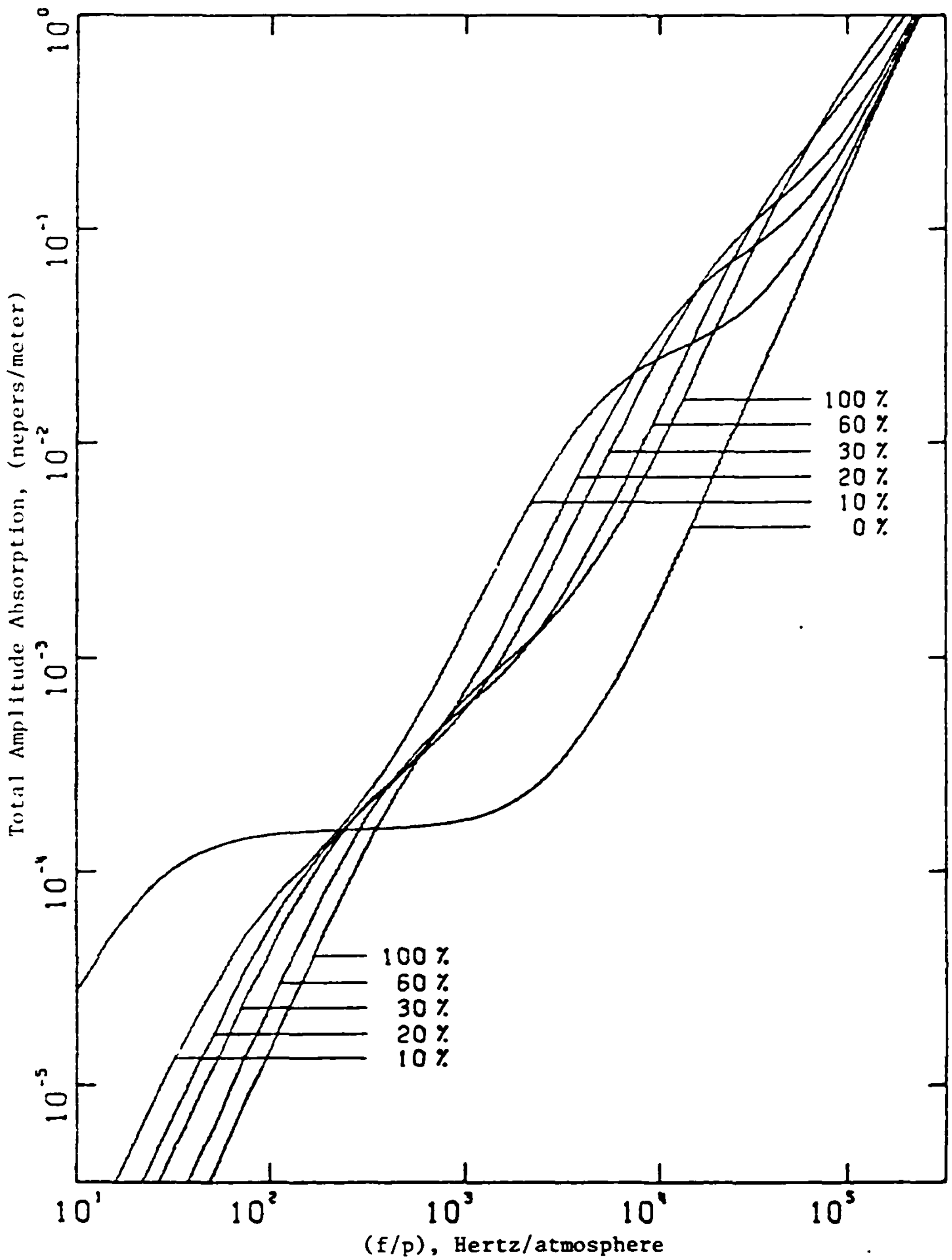

Figure (4:3): Frequency dependence of the sum, $(\alpha_{cr} + \alpha_v)$ at 20°C. for various relative humidities, as indicated. (after Evans, et al.)

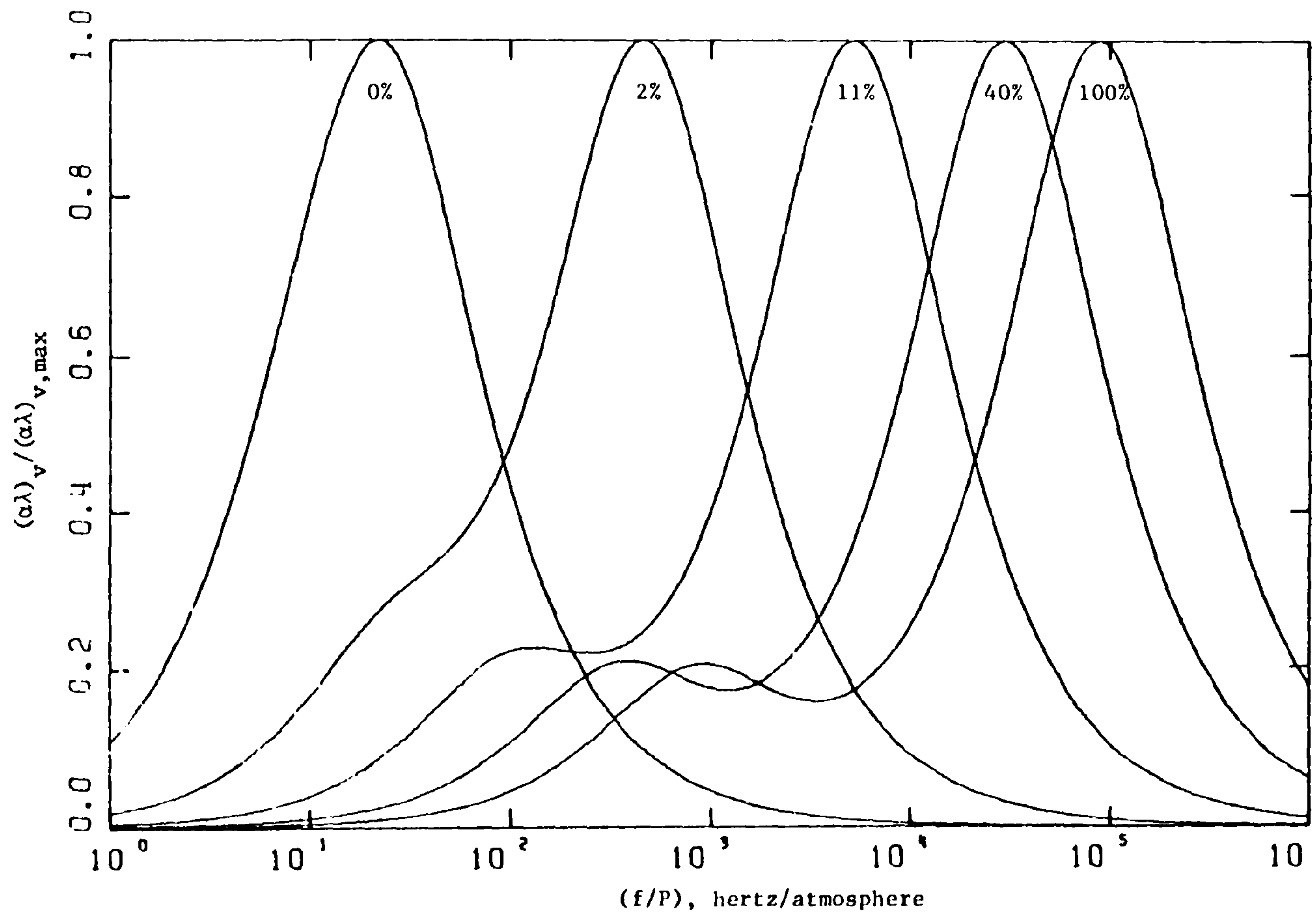

Figure (4:4): Normalized molecular absorption per unit wavelength at 25°C, for relative humidities of 0%, 2%, 11%, 40%, and 100%, as indicated.

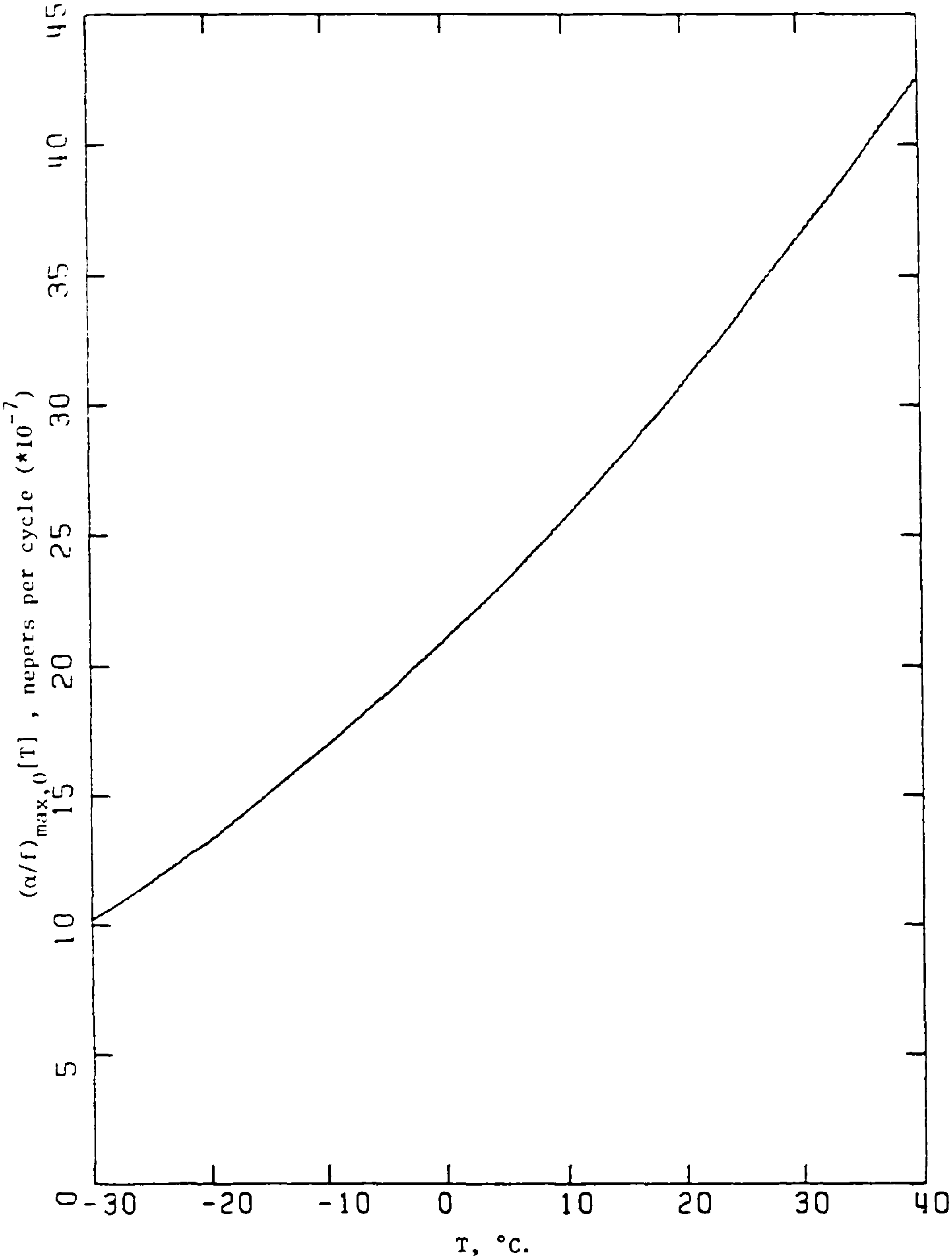

Figure (4:5): The maximum absorption per cycle for oxygen $(\alpha/f)_{max,0}[T]$, as a function of temperature, T. Multiplication by $2f^2 f_{r,0}/(f^2 + f_{r,0}^2)$ gives $\alpha_{v,0}$.

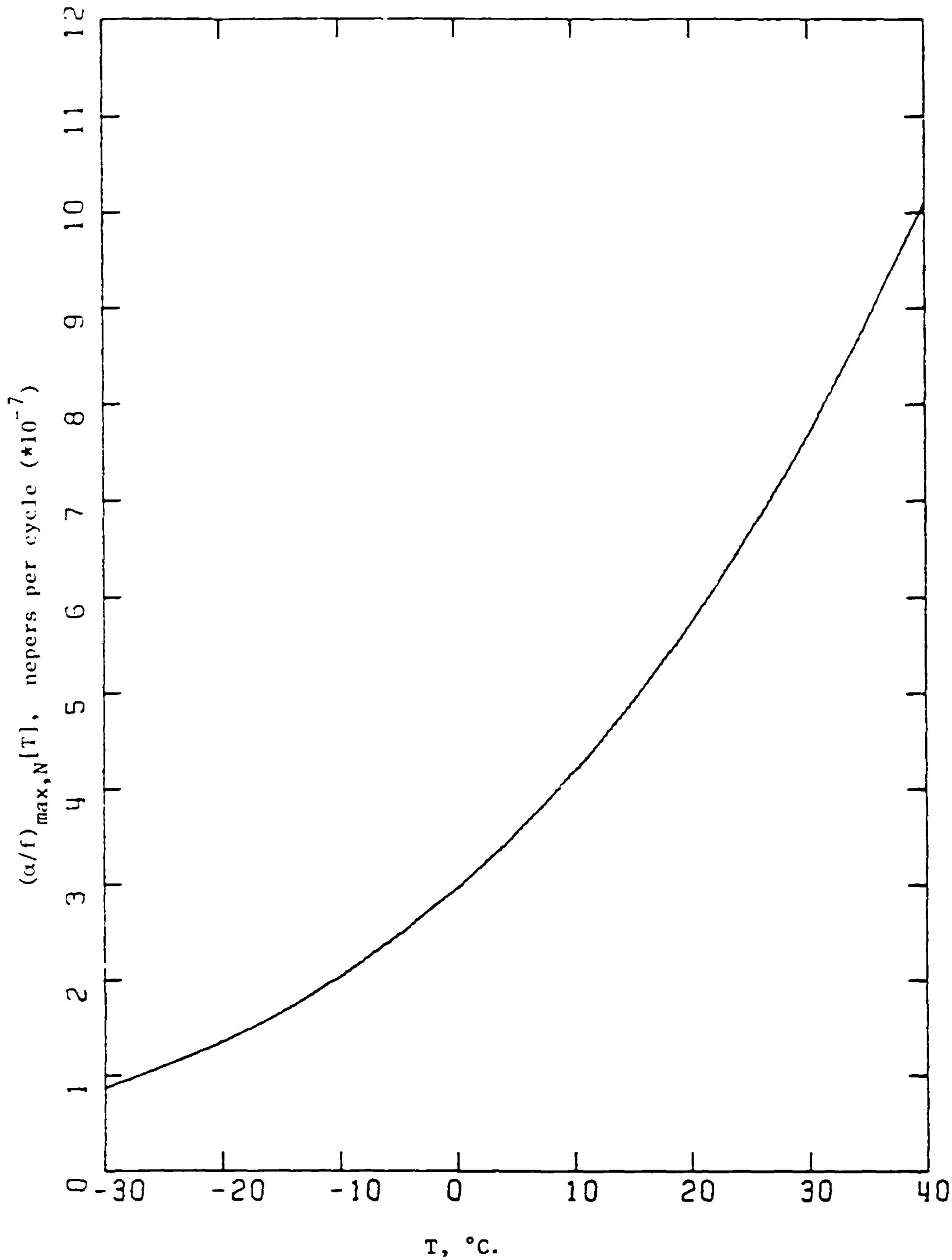

Figure (4:6): The maximum absorption per cycle for nitrogen, $(\alpha/f)_{max,N}[T]$, as a function of temperature, T. Multiplication by $2f^2 f_{r,N}/(f^2 + f_{r,N}^2)$ gives $\alpha_{v,N}$.

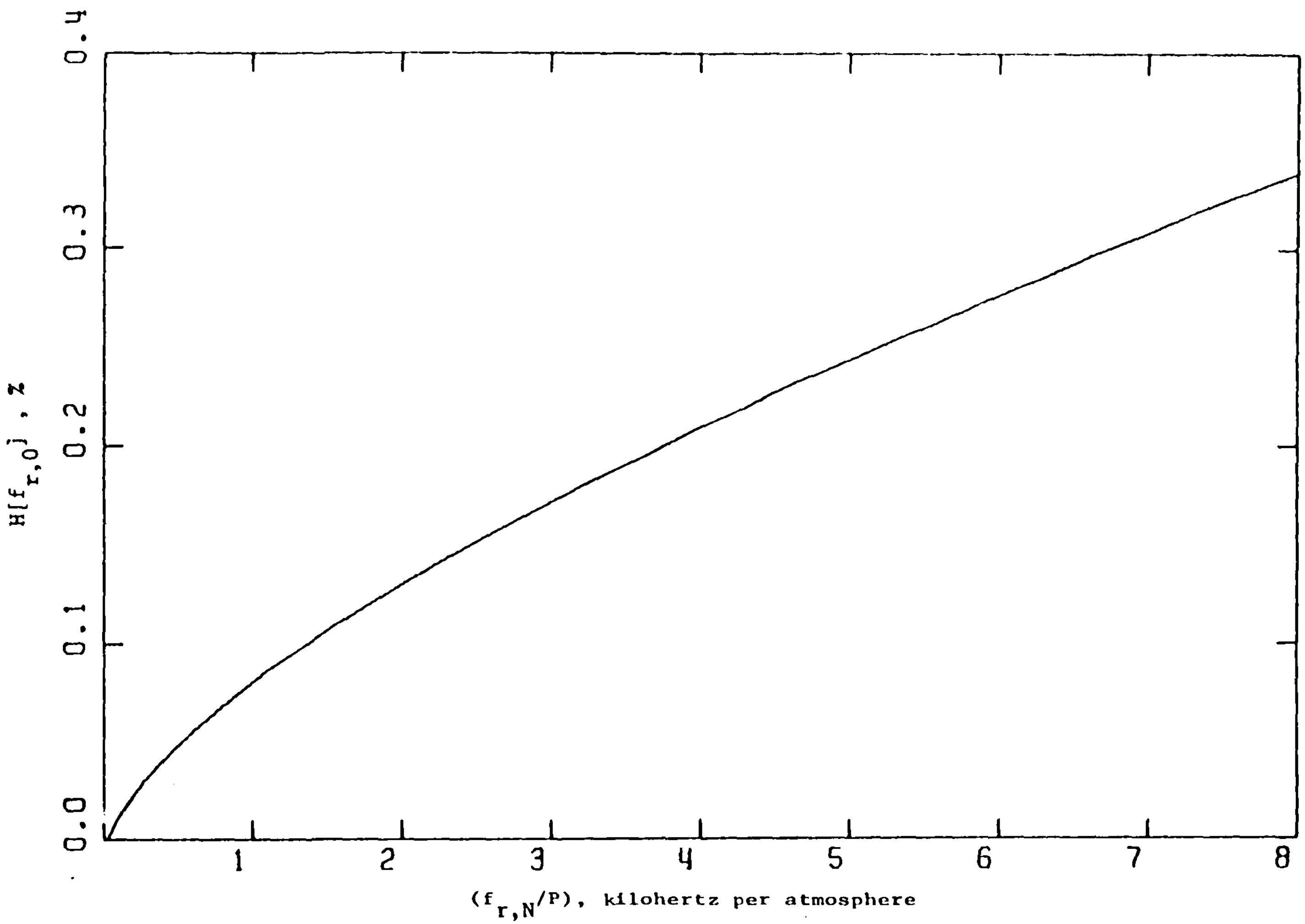

Figure (4:7): The percent molar concentration of water vapor, $H[f_{r,0}]$, as a function of the relaxation frequency of oxygen per unit of atmospheric pressure.

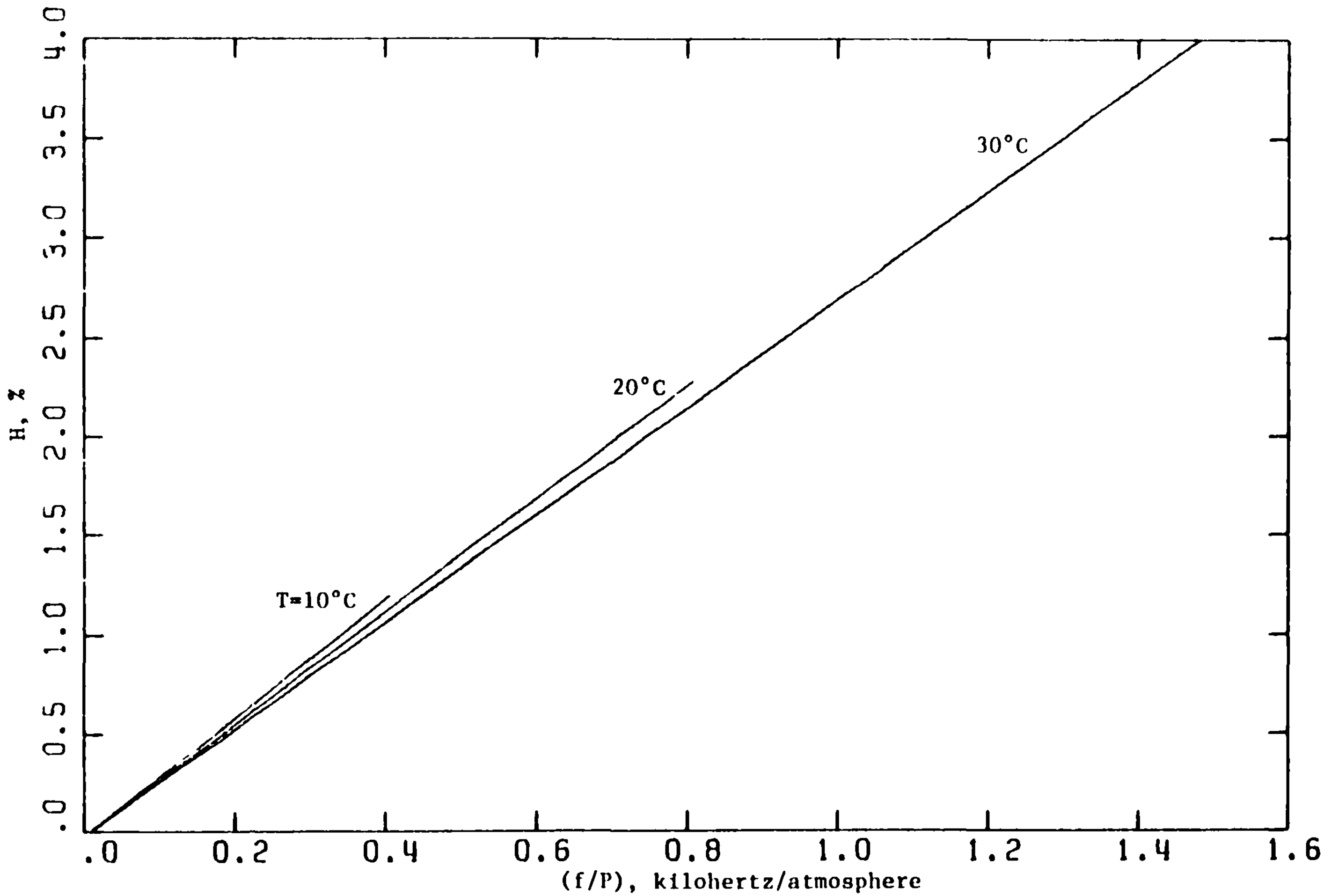

Figure (4:8): Relation between the relaxation frequency of nitrogen at one atmosphere pressure and the percent molar concentration of water vapor for the indicated temperatures. (Lines end at 100% relative humidity.)[b]

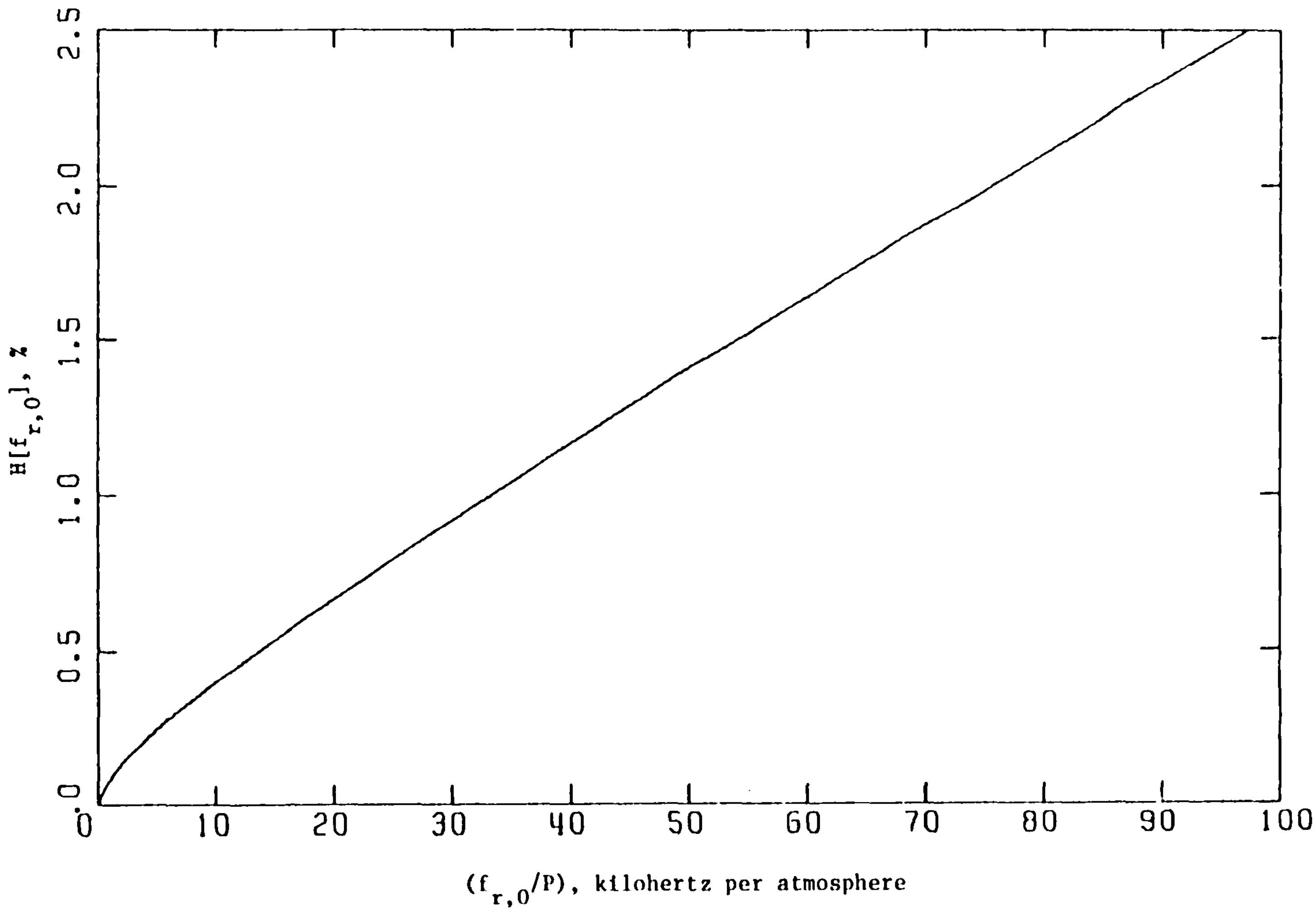

Figure (4:9): The percent molar concentration of water vapor, $H[f_{r,0}]$, as a function of the relaxation frequency of oxygen, per unit of atmospheric pressure, for higher frequencies.[c]

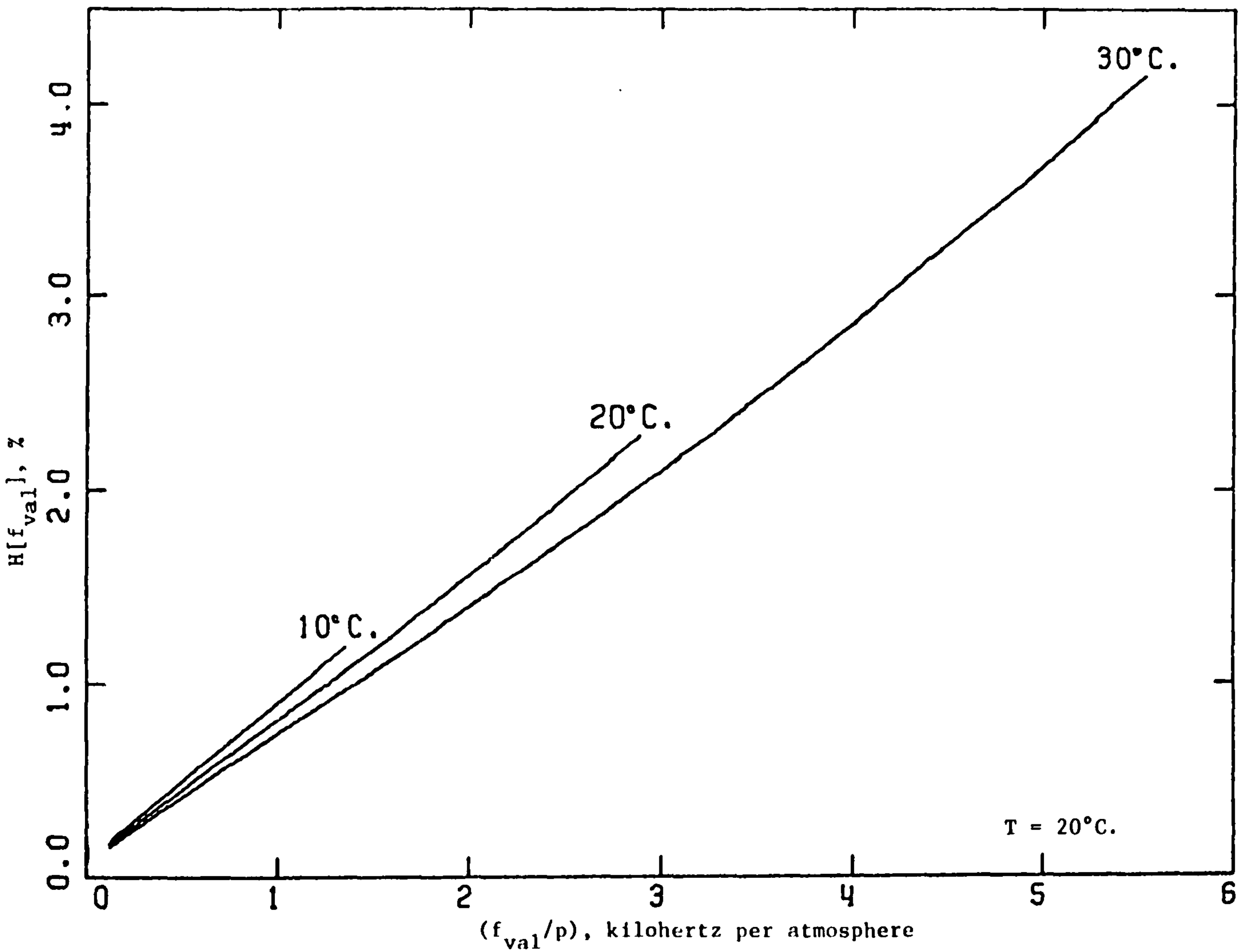

Figure (4:10): The percent molar concentration of water vapor, $H[f_{val}]$, as a function of the frequency, per unit of atmosphere pressure, of the minimum of the absorption per cycle curve, which occurs between the two absorption peaks, for T=20°C. There is no valley for $H \lesssim .2\%$.[d]

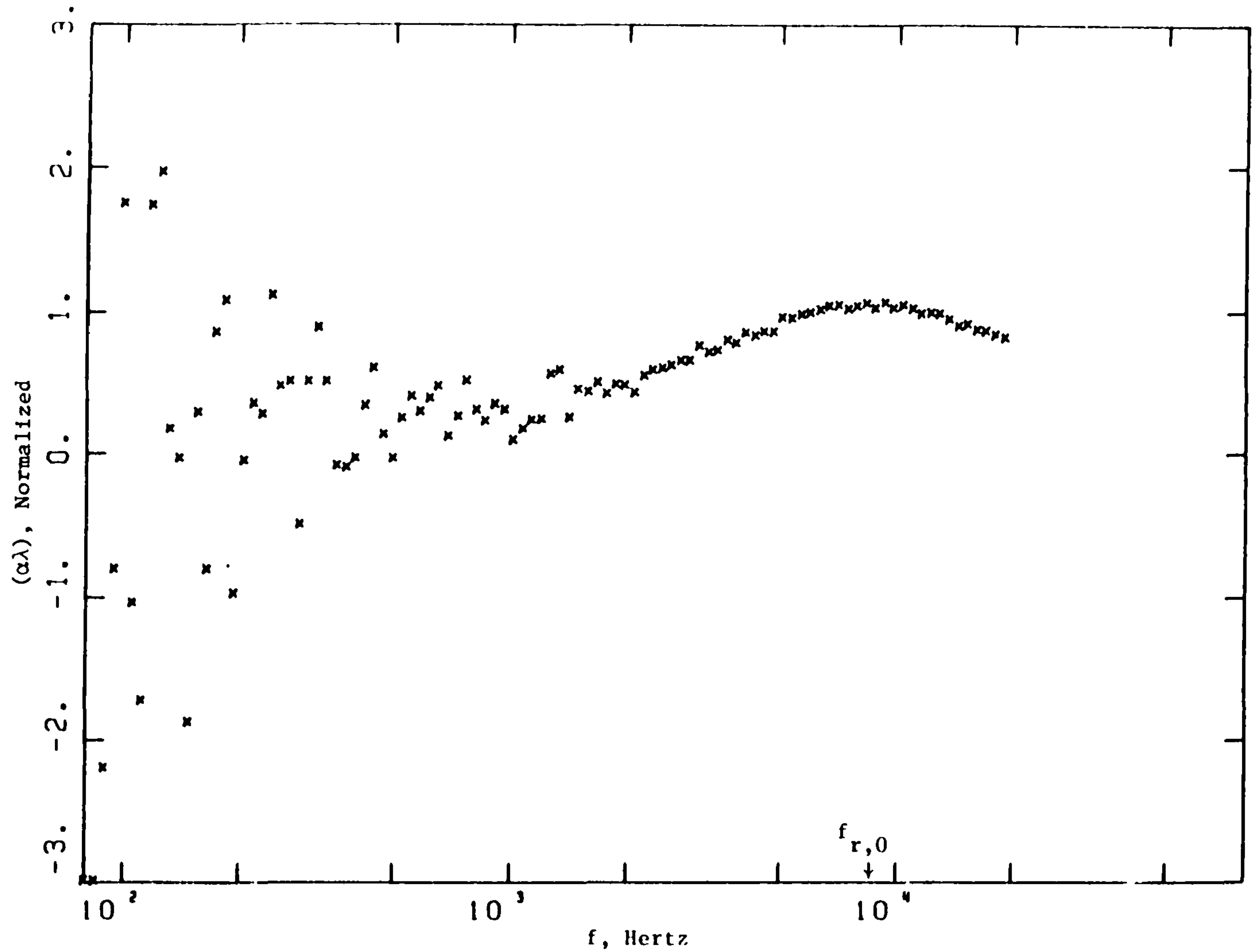

Figure (7:1): Simulated measurements of (αλ), normalized by $(\alpha\lambda)_{max,0}$ for T = 20°C, H = .34% (which is about 15% relative humidity), P = 1 atm., and 100 data points, with the frequency swept logarithmically. The relaxation frequency of oxygen is indicated.

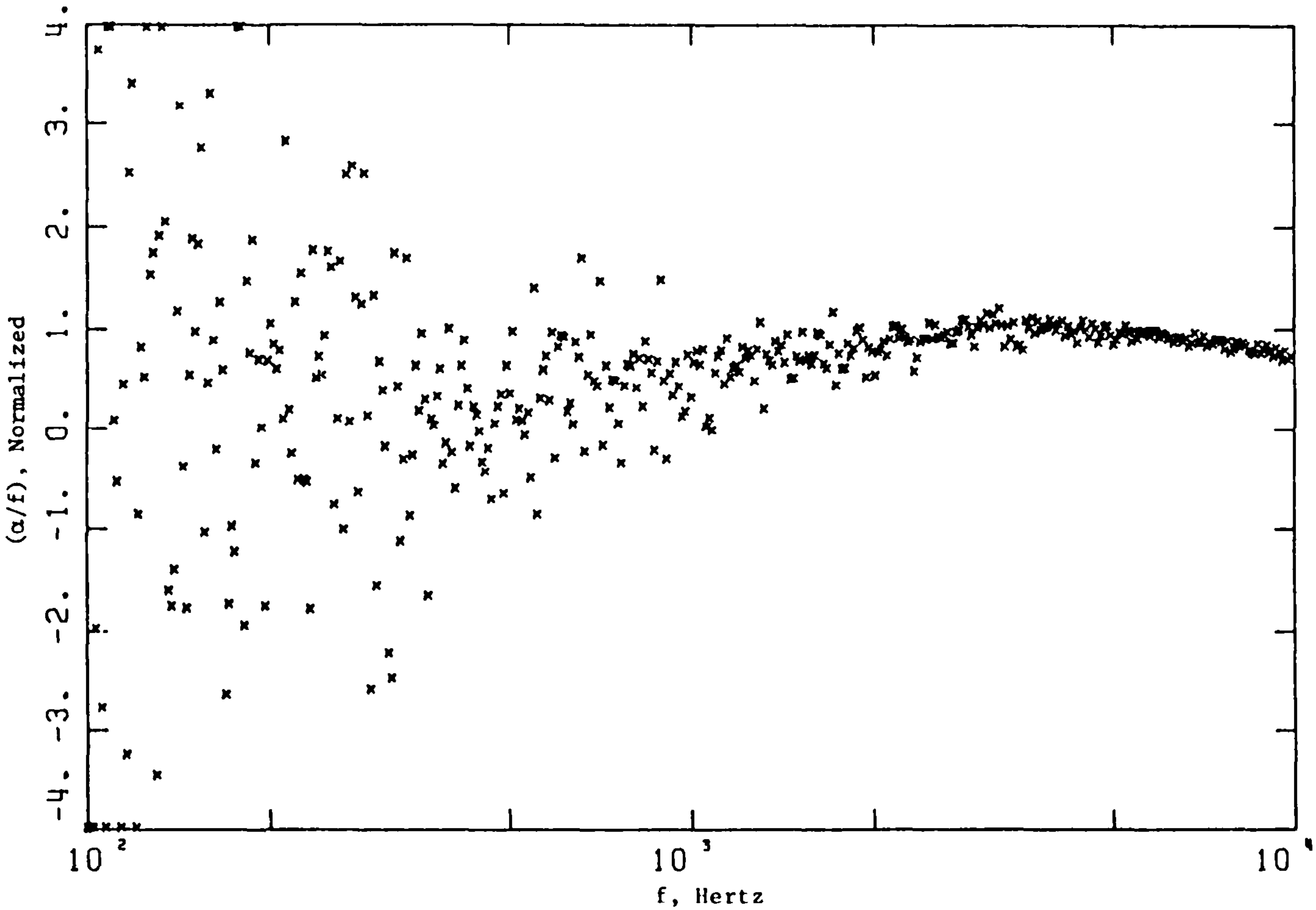

Figure (7:2): Simulated measurements of (α/f), normalized by $(\alpha/f)_{max,0}$, for T=10°C; P=1 atmosphere; H=0.2%; a separation distance, x, of 500 meters; four receivers; and 400 data points; with the frequency was swept logarithmically.

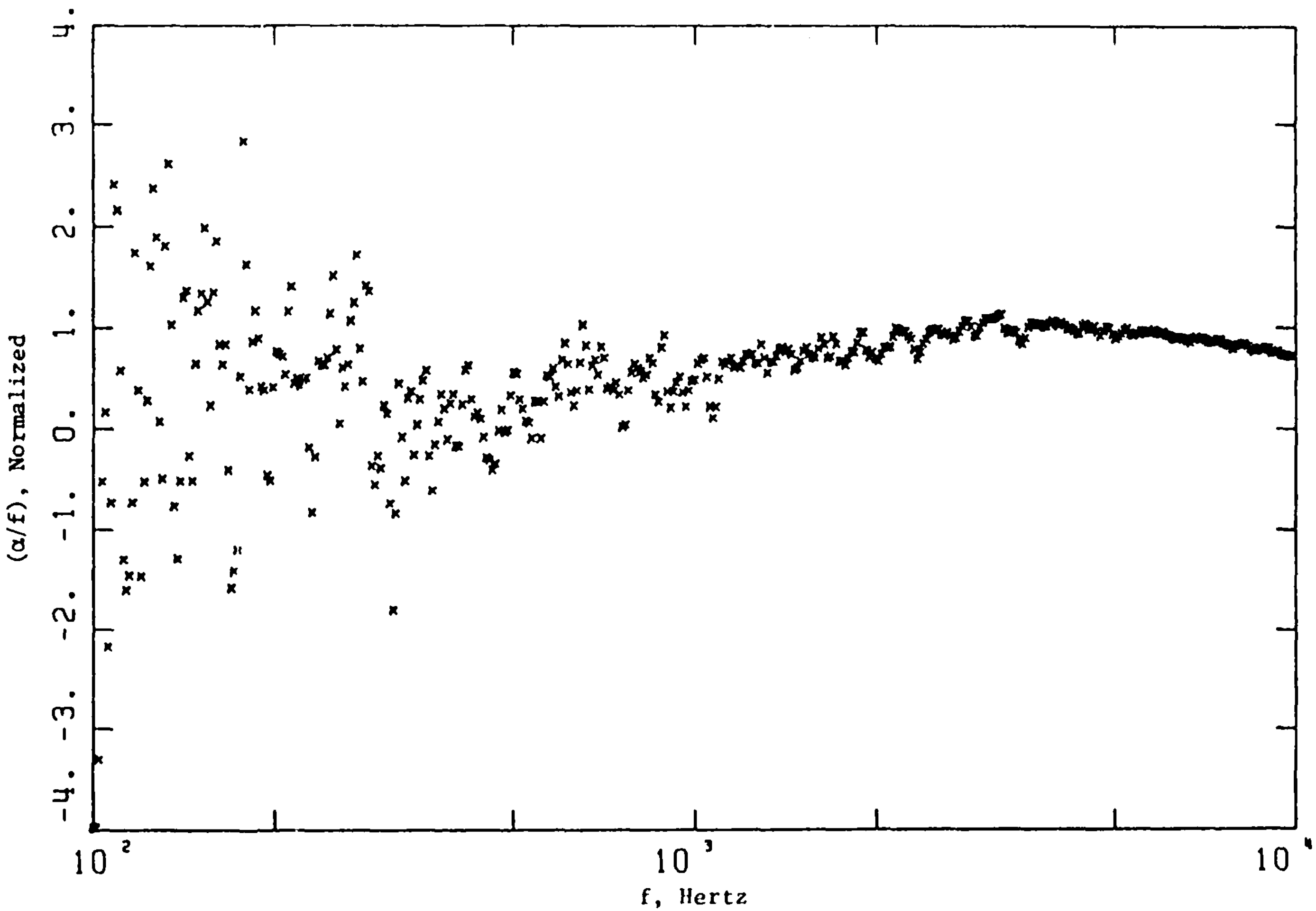

Figure (7:3): The simulated data of Figure (7:2), with each datum averaged with the immediately succeeding and preceding data.

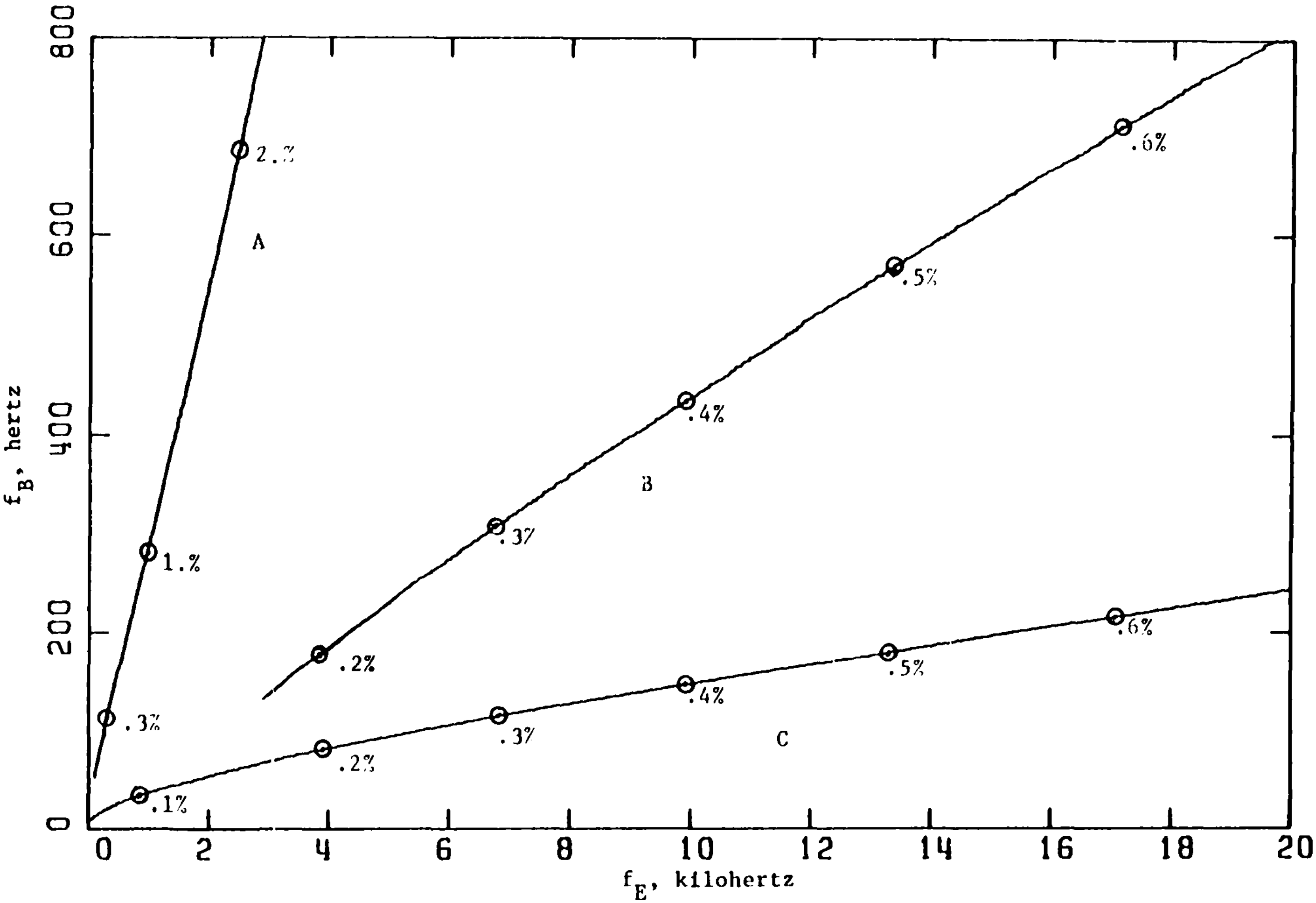

Figure (8:1): Nomogram for determining the frequency range (f_B to f_E) for inclusion of an extremum of the absorption per cycle curve, at 20°C. Curve A is for the nitrogen peak or the "valley", curve B is for the valley or the oxygen peak, and curve C is for the nitrogen or oxygen peaks. Corresponding values of H, the percent molar concentration of water vapor are indicated for one atmosphere pressure.[e]

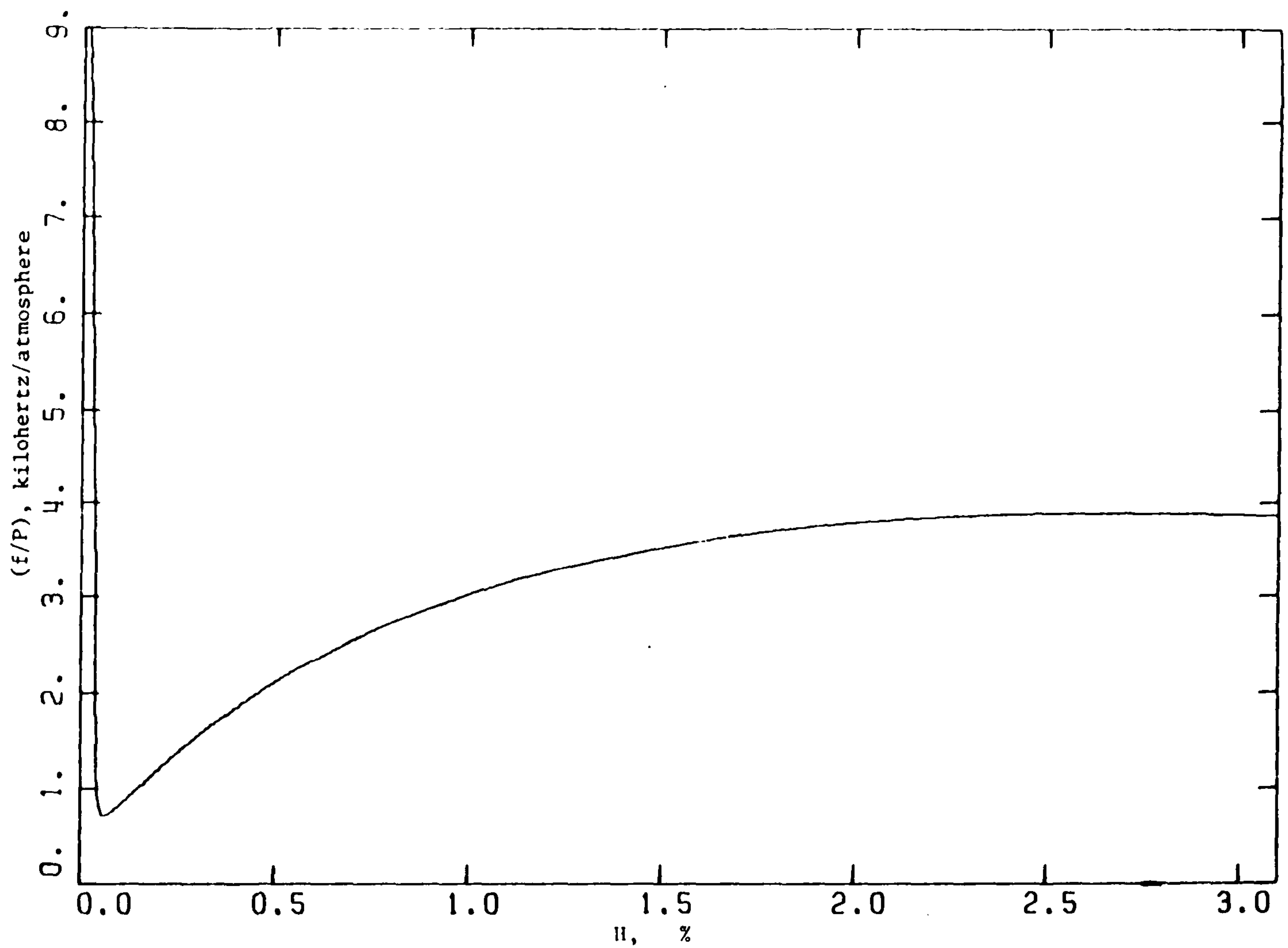

Figure (8:2): Maximum transmittable frequency for one atmosphere pressure at 25°C as a function of humidity, H, for $(\Delta dB/(2x)) = 0.022$, e.g. a one-way trip of 1500 meters and an allowed attenuation of $\Delta dB = 65$ dB. (Pressure variations and excess attenuation have been ignored.)

NOTES FOR FIGURES

[a] Figure (2:1) can be used to convert between relative humidity and absolute humidity since the curve corresponds to 100% relative humidity.

[b] The temperature dependence of the curves in figure (4:8) is small enough to be overlooked, especially if the temperature is known within 5°C.

[c] The absorption is so great for the frequencies displayed in figure (4:9) that the curve is of interest only for an _in situ_ device.

[d] The "valley" described in figure (4:10) is present in the curves of figure (4:4); it does not exist beyond the endpoints of the curves shown in (4:10).

[e] Figure (8:1) is a condensation of figures (4:7), (4:8), and (4:9) for design purposes. The necessary sweep range for continuous coverage of H by one or more of the extremum of the absorption per cycle curve, and the corresponding range of absolute humidities (H) can be determined as follows: Select one curve and enter as f_B the lowest frequency at which the sodar is capable of operating. The corresponding f_E is the minimum upper limit of the sweep, as is necessary for continuous coverage. Using the same curve; if the previously determined f_E is entered on the f_B axis and f_B entered on the f_E axis; then the two corresponding values of H read off the curve are the limits of the range of H covered by the sweep. Any pair of sweep endpoints can be utilized in this manner to determine the corresponding range of H. Usually, curve B will be most favorable; although it should be noted that a combination of curves can be used. For example, curve C and f_B= 100 Hz yields f_E= 7kHz with corresponding H range of $.01\% \leq H$, with no practical upper limit.

BIBLIOGRAPHY

Allen and Rudnick. "A Powerful High Frequency Siren," J. Acoust. Soc. Am., 1947; vol. 19, no. 5, p. 857.

Alekseev. "Equations for the statistical moments of a wave field in a randomly inhomogeneous medium," Soviet Physics-Acoustics, April-June 1973; vol. 18, no. 4, pp. 427-431.

Baerg, W., and Schwarz, W. H. "Measurements of the Scattering of Sound from Turbulence," J. Acoust. Soc. Am., 1966; vol. 39, no. 6, pp. 1125-1132.

Balser, M., McNary, Nagy, Loveland, and Dickson. Remote Wind Sensing by Acoustic Radars, April 1975; Research and Development Technical Report ECOM-5560, U. S. Army.

Beckmann, P. Probability in Communication Engineering. New York: Harcourt, Brace & World, 1967.

Beran, D. W. "Acoustics: A New Approach for Monitoring the Environment near Airports," AIAA, Journal of Aircraft, 1971; vol. 8, no. 11, pp. 934-936.

Beran, D. W. "Acoustic Radar Detection Techniques," presented at the FAA Turbulence Symposium, March 22, 1971.

Beran, D. W., and Clifford, S. F. "Acoustic Doppler Measurements of the Total Wind Vector," AMS Second Symposium on Meteorological Observations and Instrumentation, San Diego, California, March 27-30, 1972.

Beran, D. W., and Hall, F. F. "Remote Sensing for Air Pollution Meteorology," Bull. of the Amer. Meteor. Soc., Sept. 1974; vol. 55, no. 9, pp. 1097-1105.

Beran, D. W., Hall, Wescott, and Neff. "Application of an Acoustic Sounder to Air Pollution Monitoring," Proc. of Symposium in Air Pollution, Turbulence and Diffusion, Dec. 7-10, 1971, March 1972, pp. 66-72.

Beran, D. W., Hall, Willmarth, Keeler, and Hunter. "Operational Test Results of Acoustic Doppler Wind Shear Detector," Preprint Volume, 6th Conference on Aerospace & Aeronautical Meteorology, Nov. 12-15, 1974, El Paso, Texas, Boston: Amer. Meteor. Soc., pp. 412-417.

Beran, D. W., Hooke, W. H., Clifford, S. F. "Acoustic Echo-Sounding Techniques and Their Application to Gravity-Wave, Turbulence, and Stability Studies," Boundary Layer Meteorology, 1973; vol. 4, pp. 133-153.

Beran, D. W., Little, C. G., Willmarth, B. C. "Acoustic Doppler Measurements of Vertical Velocities in the Atmosphere," Nature, March 19, 1971; vol. 230, no. 5290, pp. 160-162.

Beran, D. W., and Willmarth, B. C. "Doppler Winds from a Bistatic Acoustic Sounder," Proc. 7th International Symposium on Remote Sensing of the Environment, May 17-21, 1971, 1971; vol. 1, no. 10259-1-X, pp. 1699-1714.

Bevington, P. R. Data Reduction and Error Analysis for the Physical Sciences. New York: McGraw-Hill, 1969.

Beyer, R. T. "Nonlinear Acoustics," in Physical Acoustics, Vol. II, Part B. New York: Academic Press, 1965; Mason, W. P., ed.

Bode, J. D., and Carrico, J. P. "Remote Optical Sensing for Air-Pollution Monitoring," Bendix Technical Journal, Winter 1971; pp. 14-28.

Brown, E. H. "Turbulent spectral broadening of backscattered acoustic pulses," J. Acoust. Soc. Am., November 1974; vol. 56, no. 5, p. 1398.

Brown, E. H. "Some Recent Theoretical Work on Echo Sounding in the Atmosphere," Journal of Geophysical Research, Dec. 20, 1974; vol. 79, no. 36, pp. 5567-5571.

Brown, E. H., and Clifford, S. F. "Spectral Broadening of an Acoustic Pulse Propagating Through Turbulence," J. Acoust. Soc. Am., 1973; vol. 54, no. 1, pp. 36-38.

Brown, E. H., and Clifford, S. F. "Resolving the Excess Attenuation Controversy," Journal of the Acoustical Society of America, Spring 1976; vol. 59, supplement no. 1, p. 593.

Brown, E. H., and Keeler, R. J. "Applications of Propagation Parameters to Atmospheric Echosondes," Preprint Volume, 16th Radar Meteorology Conference, April 22-24, 1975, Houston, Texas, Boston: Amer. Meteor. Soc., p. 272.

Chadwick, R. B., Little, C. G. "The Comparison of Sensitivities of Atmospheric Echo-Sounders," Remote Sensing of Environment, 1973; vol. 2, pp. 223-234.

Cronenwett, W. T., Walker, G. B., and Inman, R. L. "Acoustic Sounding of Meteorological Phenomena in the Planetary Boundary Layer," J. of Appl. Meteorology, Dec. 1972; vol. 11, no. 8, pp. 1351-1358.

Damkevala, R. J. "Acoustic Echo-Sounding Experiments in an Urban Environment," presented at the Joint Conference on Sensing of Environmental Pollutants, Palo Alto, California; Nov. 8-10, 1971.

DeLoach, R. On the Excess Attenuation of Sound in the Atmosphere, NASA TN D-7823. Washington: NASA, March 1975.

Derr, V. E., ed. Remote Sensing of the Troposphere. Washington: U.S. Government Printing Office, 1972.

Derr, V. E., and Little, C. G. "A Comparison of Remote Sensing of the Clear Atmosphere by Optical, Radio, and Acoustic Radar Techniques," Applied Optics, Sept. 1970; vol. 9, no. 9, pp. 1976-1991.

Dryer, W. ed. "Remote Sensing with Sound Waves," Atmospheric Research, Sept. 1971; no. 18, pp. 2-11.

Evans, L. B. "Atmospheric Absorption of Sound: Validity of a Two Relaxation Parameter Model," presented to the 89th meeting of the Acoustical Society of America; Austin, Texas: April 7-11,1975.

Evans, L. B., Bass, H. E., and Sutherland, L. C. "Atmospheric Absorption of Sound: Theoretical Predictions," J. Acoust. Soc. Am., 1972; vol. 51, no. 5(part 2), pp. 1565-1575.

Foster, et al. "A spectral hygrometer for measuring total precipitable water," in Humidity and Moisture, Vol. 1. New York: Reinhold, 1965, pp. 455-464.

Georges, J. M., and Clifford, S. F. "Acoustic Sounding in a Refracting J. Acoust. Soc. Am., 1972; vol. 52, no. 5 (part 2), pp. 1397-1405.

Gething, J. T., and Jenssen, D. "Measurement of Temperature and Humidity by Acoustic Echo Sounding," Nature, Physical Science, June 28, 1971; vol. 231, pp. 198-200.

Georke, V. H., and Woodward, M. W. "Infrasonic Observation of a Severe Weather System," Monthly Weather Review, June 1966; vol. 94, no. 6, pp. 395-398.

Hall, F. F. "Acoustic Remote Sensing of Temperature and Velocity Structure in the Atmosphere," Proc. NATO Adv. Study Institute, Statistical Methods and Instrumentation in Radio-Meteorology, April 15-22, 1971, 1971; pp. 167-180.

Hall, F. F. Report on the July 1972 Workshop in Atmospheric Acoustics, NOAA Technical Memorandum, ERL WPL-8.

Hall, F. F., and Wescott, J. W. "Acoustic antennas for atmospheric echo sounding," J. Acoust. Soc. Amer., Nov. 1975; vol. 56, no. 5, pp. 1376-1382.

Hall, F. F., Wescott, J. W., and Simmons, W. "Acoustic Echo Sounding of Atmospheric Thermal Wind Structure," Proc. 7th International Symposium on Remote Sensing of Environment, May 17-21, 1971; vol. 1, no. 10259-1-X, pp. 1715-1732.

Harris, C. M. "Absorption of Sound in Air versus Humidity and Temperature," J. Acoust. Soc. Am., no. 1, 1966; vol. 40, p. 148.

Harris, C. M. Absorption of Sound in Air versus Humidity and Temperature, NASA-CR-647. George C. Marshall Space Flight Center; NASA, 1967.

Harris, C. M. "Effects of Humidity on the Velocity of Sound in Air," J. Acoust. Soc. Am., 1971; vol. 49, no. 3 (part 2), pp. 890-893.

Henderson, M. C. and Herzfeld, K. F. "Effect of Water Vapor or the Napier Frequency of Oxygen and Air," J. Acoust. Soc. Am., June, 1965; vol. 37, no. 6, pp. 986-988.

Ingard, U. "A Review of the Influence of Meteorological Conditions on Sound Propagation," J. Acoust. Soc. Am., May, 1953; vol. 25, no. 3, pp. 405-411.

Ingard, U. "On Sound-Transmission Anomalies in the Atmosphere," J. Acoust. Soc. Am., 1969; vol. 45, no. 4.

Jones. "A fifty-horsepower siren," J. Acoust. Soc. Am., 1946; vol. 18, p. 371.

Kasper, Pappa, Keefe, and Sutherland. A Study of Air-to-Ground Sound Propagation Using an Instrumented Meteorological Tower, NASA CR-2617. Washington: NASA, October 1975.

Kneser, H. O. "The Interpretation of the Anomalous Sound-Absorption in Air and Oxygen in Terms of Molecular Collisions," J. Acoust. Soc. Am., October, 1933; vol. V, p. 122.

Knudsen, V. O. "The Absorption of Sound in Air, in Oxygen, and in Nitrogen - Effects of Humidity and Temperature," J. Acoust. Soc. Am., Oct. 1933; vol. V, p. 112.

Little, C. G. "Acoustic Methods for the Remote Probing of the Lower Atmosphere," Proc. of the IEEE, April 1969; vol. 57, no. 4, pp. 572-578.

Little, C. G. "Acoustic Sounding of the Lower Atmosphere," Meteorological Monographs, 1970; vol. 11, no. 33, pp. 397-404.

Little, C. G. "On the Detectability of Fog, Cloud, Rain, and Snow by Acoustic Echo-Sounding Methods," Journal of Atmospheric Sciences, May 1972; vol. 29, no. 4, pp. 748-755.

Little, C. B. "Status of remote sensing of the troposphere," Bull. Amer. Meteor. Soc., Oct. 1972; vol. 53, no. 10, pp. 936-949.

Little, C. G. "Remote Sensing of the Atmosphere," Atmospheric Technology-NCAR, June, 1973; no. 2, pp. 51-56.

Marshall, J. M., Peterson, A. M., and Barnes A. A. "Combined Radar-Acoustic Sounding System," Applied Optics, Jan. 1972; vol. 11, no. 1, pp. 108-112.

Marshall, J. S., and Hitschfeld, W. "Interpretation of the Fluctuating Echo from Randomly Distributed Scatterers, Part I," Canadian Journal of Physics, 1953; vol. 31, pp. 962-994.

McAllister, L. G. "Acoustic sounding of the lower troposphere," J. of Atmospheric and Terrestrial Physics, 1968; vol. 30, pp. 1439-1440.

McAllister, L. G., Pollard, Mahoney, and Shaw. "Acoustic Sounding - A New Approach to the Study of Atmospheric Structure," Proc. of the IEEE, April, 1969; vol. 57, no. 4, pp. 579-587.

Melfi, A. H., Lawrence, J. D., and McCormick, M. P. "Observation of Raman Scattering by Water Vapor in the Atmosphere," Applied Physics Letters, Nov. 1, 1969; vol. 15, no. 9, p. 295.

Monin, A. S. "Characteristics of the Scattering of Sound in a Turbulent Atmosphere," Soviet Physics - Acoustics, April-June, 1962; vol. 7, no. 4, pp. 370-373.

Neff, W. D. "An Investigation of Acoustic Scatter from Small Scale Thermal Fluctuations in the Planetary Boundary Layer," Preprint Volume, 16th Radar Meteorology Conference, April 22-24, 1975, Houston, Texas. Boston: Amer. Meteor. Soc., pp. 263-270.

Ottersten, H., Hardy, K. R., Little, C. G. "Radar and Sodar Probing of Waves and Turbulence in Statically Stable Clear-Air Layers," Boundary Layer Meteorology, April 1973; vol. 4, pp. 47-89.

Papoulis, A. Probability, Random Variables and Stochastic Processes. New York: McGraw-Hill, 1965.

Parry, H. D., Sanders, M. J. "The Design and Operation of an Acoustic Radar," IEEE Transactions on Geoscience Electronics, Jan. 1972; vol. GE-10, no. 1, pp. 58-64.

Russell, P. B., Uthe, E. E., Shaw, N. A. "A comparison of Atmospheric Structure as Observed with Lidar and Acoustic Sounder Techniques," submitted to J. of Geophysical Research - Oceans and Atmosphere in April 1974.

Simmons, W. R., Wescott, J. W., and Hall, F. F. Acoustic Echo Sounding as Related to Air Pollution in Urban Environments, NOAA Technical Report ERL 216-WPL 17. Boulder, Colorado: May, 1971.

Strand, O. N. "Numerical Study of the Gain Pattern of a Shielded Acoustic Antenna," J. Acoust. Soc. Am., 1971; vol. 49, no. 6, pp. 1698-1703.

Strauch, R. G., Derr, V. E., and Cupp, R. E. "Atmospheric Water Vapor Measurement by Raman Lidar," Remote Sensing of Environment, Feb. 1972; vol. 2, no. 2, pp. 101-108.

Sutherland, L. C., Piercy, Bass, and Evans. "Method for Calculating the Absorption of Sound by the Atmosphere," Journal of the Acoustical Society of America, 1974, (program for the 88th Meeting).

Tatarskii, V. I. The Effects of the Turbulent Atmosphere on Wave Propagation. Washington: National Technical Information Service, 1971.

Tennekes, Hendrick. "The Atmospheric Boundary Layer," Physics Today, January, 1974, pp. 52-63.

Wallace, P. R. "Interpretation of the Fluctuating Echo from Randomly Distributed Scatterers, II", Canadian Journal of Physics, 1953; vol. 31, pp. 995-1009.

Willmarth, B. C., Brown, Priestley, and Beran. "Beam Pattern Measurements for Large Acoustic Antennas," Preprint Volume, 16th Radar Meteorology Conference, April 22-24, 1975, Houston Texas. Boston: Amer. Meteor. Soc., p. 278.